AD-A083 374 FOREIGN TECHNOLOGY DIV WRIGHT-PATTERSON AFB OH F/G 1/3
PHYSICAL BASES OF AIRCRAFT ICING,(U)
AUG 79 I P MAZIN
UNCLASSIFIED FTD-ID(RS)T-1161-79 NL

1 OF 3
AD A083374

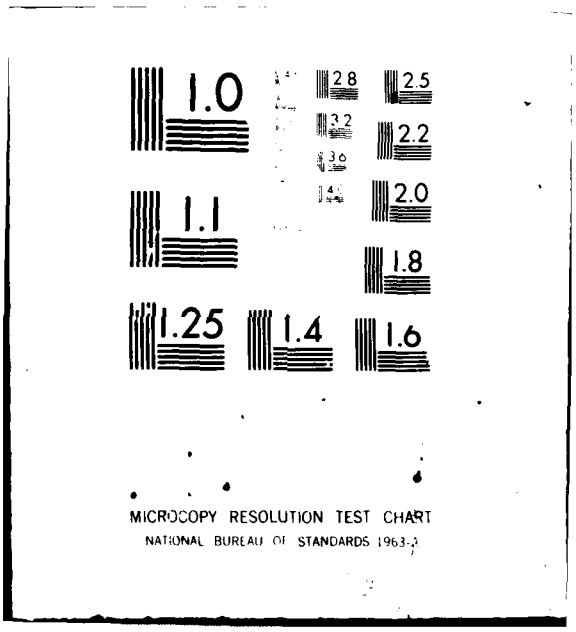
1.0
2.8
2.5
3.2
2.2
3.6
2.0
1.1
1.8
1.25
1.4
1.6
MICROCOPY RESOLUTION TEST CHART
NATIONAL BUREAU OF STANDARDS 1963-A

PHOTOGRAPH THIS SHEET

AD A083374

DTIC ACCESSION NUMBER

LEVEL

1

INVENTORY

FTD-ID(RS)T-1161-79

DOCUMENT IDENTIFICATION

DISTRIBUTION STATEMENT A
Approved for public release;
Distribution Unlimited

DISTRIBUTION STATEMENT

ACCESSION FOR		
NTIS	GRA&I	☑
DTIC	TAB	☐
UNANNOUNCED		☐
JUSTIFICATION		
BY		
DISTRIBUTION /		
AVAILABILITY CODES		
DIST	AVAIL AND/OR SPECIAL	
A		

DISTRIBUTION STAMP

DTIC
ELECTE
S APR 24 1980 D
D

DATE ACCESSIONED

80 4 29 110

DATE RECEIVED IN DTIC

PHOTOGRAPH THIS SHEET AND RETURN TO DTIC-DDA-2

DTIC FORM OCT 79 70A

DOCUMENT PROCESSING SHEET

FTD-ID(RS)T-1161-79

FOREIGN TECHNOLOGY DIVISION

PHYSICAL BASES OF AIRCRAFT ICING

by

I. P. Mazin

Approved for public release;
distribution unlimited.

UNEDITED MACHINE TRANSLATION

FTD-ID(RS)T-1161-79 31 August 1979

MICROFICHE NR. AFD-79-C-001195L

PHYSICAL BASES OF AIRCRAFT ICING

By: I. P. Mazin

English pages: 272

Source: Fizicheskiy Osnovy Obledeneniya Samoletov, Gidrometeoizdat, Moscow, 1957, pp. 1-120.

Country of origin: USSR
This document is a machine translation.
Requester: AEDC/SRFI
Approved for public release; distribution unlimited.

PREPARED BY:

TRANSLATION DIVISION
FOREIGN TECHNOLOGY DIVISION
WP-AFB, OHIO.

Table of Contents

U. S. BOARD ON GEOGRAPHIC NAMES TRANSLITERATION SYSTEM

Block	Italic	Transliteration	Block	Italic	Transliteration
А а	*А а*	A, a	Р р	*Р р*	R, r
Б б	*Б б*	B, b	С с	*С с*	S, s
В в	*В в*	V, v	Т т	*Т т*	T, t
Г г	*Г г*	G, g	У у	*У у*	U, u
Д д	*Д д*	D, d	Ф ф	*Ф ф*	F, f
Е е	*Е е*	Ye, ye; E, e*	Х х	*Х х*	Kh, kh
Ж ж	*Ж ж*	Zh, zh	Ц ц	*Ц ц*	Ts, ts
З з	*З з*	Z, z	Ч ч	*Ч ч*	Ch, ch
И и	*И и*	I, i	Ш ш	*Ш ш*	Sh, sh
Й й	*Й й*	Y, y	Щ щ	*Щ щ*	Shch, shch
К к	*К к*	K, k	Ъ ъ	*Ъ ъ*	"
Л л	*Л л*	L, l	Ы ы	*Ы ы*	Y, y
М м	*М м*	M, m	Ь ь	*Ь ь*	'
Н н	*Н н*	N, n	Э э	*Э э*	E, e
О о	*О о*	O, o	Ю ю	*Ю ю*	Yu, yu
П п	*П п*	P, p	Я я	*Я я*	Ya, ya

*ye initially, after vowels, and after ъ, ь; e elsewhere.
When written as ё in Russian, transliterate as yё or ё.

RUSSIAN AND ENGLISH TRIGONOMETRIC FUNCTIONS

Russian	English	Russian	English	Russian	English
sin	sin	sh	sinh	arc sh	$\sinh^{-1}$
cos	cos	ch	cosh	arc ch	$\cosh^{-1}$
tg	tan	th	tanh	arc th	$\tanh^{-1}$
ctg	cot	cth	coth	arc cth	$\coth^{-1}$
sec	sec	sch	sech	arc sch	sech^{-1}
cosec	csc	csch	csch	arc csch	csch^{-1}

Russian	English
rot	curl
lg	log

Page 1.

PHYSICAL BASES OF AIRCRAFT ICING.

I. P. Mazina.

Edited by A. M. Borovikov.

Page 2.

Abstract.

This work is dedicated to the theoretical and experimental study of the icing of aircraft in flight. Work examines the effect of the microphysical parameters of clouds and flight conditions on icing intensity. Are theoretically studied questions of the flow around different bodies of the flows of the weighed in air water drops and role of the processes of heat exchange, which weaken aircraft icing. Are examined also questions of icing at supersonic flight speeds. The book is of interest for meteorologists, weather forecasters and workers of aviation, who carry out by questions of deicing of aircraft and operations of aircraft.

Page 3. No typing.

Page 4.

Preface.

The problem of aircraft icing during quarter of century already attracts considerable attention of the researchers. To this

contributes the fact that aviation equipment rapidly is improved and are posed all new problems in the region of the protection of aircraft from the danger of the fading: depending on the construction of the aircraft is changed the probability of icing under one or the other atmospheric conditions, it is changed the sensitivity of aircraft to icing, appear new tasks as, for example, about the icing of helicopters or internal icing in jet engines.

Is very close to this series of question and the task about erosion, i.e., the damage of skin/sheathing by the shocks of drops at high rates.

Study of icing gave large jerk/impulse to the science about the structure of the clouds: it stimulated the study of the microstructure of clouds and prompted, for example, some methods of measurement of water content of clouds. Some contemporary meters of liquid-water content are close in construction/design to the monitors of icing. The calculations of the coefficients of capture which occupy the large place in the theory of icing, rapidly found application/appendix in the theory of the formation of residues/settlings, in the theory of the errors for different instruments, etc.

The problem of icing, thus, played in physics of the atmosphere

the large role, emerging beyond the framework of the demands produced by aviation.

The published work of I. P. Mazin gives response/answer to the series/row of questions important for aviation equipment - about the icing intensity, its dependence on the structure of clouds, etc. These calculations are added also to the calculation of the formation/education of ice-covered surface - another dangerous phenomenon, from which strongly suffers the economy of connection/communication. Special interest in work I. P. Mazina are of some obtained simple laws governing the icing at supersonic speeds.

The simultaneously made theoretical calculations are important for studying of clouds, their structure, phase, etc., i.e., for aerological practice. Work of I. P. Mazin makes the large contribution to the development of the aircraft investigations of the atmospheres in region of which the Soviet Union made already much and it goes in front of other countries.

A. Kh. Khrgian.

Introduction.

1. Problem of fight with the icing of aircraft.

At the glow of its existence the aviation was so/such low-power, that it was limited to flights mainly in good, clear weather. Although the phenomenon of icing then was already known, it did not draw considerable attention, since it was enccuntered sufficiently rarely.

With aeronautical development the position changed. Strongly increased the role of aviation as the form cf transport. Escapes began to be conducted according to schedule, in any weather, up to distant distances, in the most diverse climates. Along main routes with large motion strictly is observed the separation - aircraft is forced to adhere to base altitudes. Under these conditions it is not possible to avoid icing virtually. For this very reason fight with the fading of aircraft gradually became the vital problem of aviation. Already since the beginning Thirties appeared different constructions/designs of anti-icings gear and proposition on fight with this phenomenon.

In usual transport aircraft to icing are subjected the most diverse part- propeller and the planes of aircraft, the cook of

fuselage and the cowlings or motors, window of pilot's cabin/compartment and stabilizer, ailerons and radio antenna, air-pressure head and other parts, up to rivets on planes and fuselage. Both the intensity and character icing can be in this case different, different proves to be the effect of icing on flight aircraft quality/fineness ratios. In one case it only insignificantly increases drag and reduces rate of climb and ceiling, in other - renders inoperable the speed indicator, breaks antenna, it causes severe vibration and it so increases drag it makes the generally aerodynamic conditions worse for the flow around aircraft, which can lead to forced landing and even catastrophe.

All contemporary aircraft are provided with one or the other anti-icing (de icing) or deicing (anty icing) system.

During the construction of deicing system arises the question, what aircraft components and to what degree need protection from ice, on which principle most favorable of designing this system.

De-icing systems provide the timely dropping of grown ice either by applying the special pneumatic coverings (Goodrich), or via the wetting of ice with anti-icing liquid (alcohol, mixture of glycerin with alcohol, etc.), or finally preheating.

Deicing systems are based on the principle of preheating the shielded aircraft components with the fact or as another method (electric heating, heated by air or continuous wetting with anti-icing liquid, etc.) and serve for the prevention of possible icing.

Much attention is recently given to the deicing in aeronautical meteorology and aeroclimatology where attempt to find the best methods of passive protection, i.e., to forecast conditions icing and to find the paths of output of them.

In order to have correct representation about the commercial advisability of using anti- or deicers of that or other power and system on one or the other aircraft components, it is necessary to know the possible intensity of the increase of ice on them depending on the conditions of icing and the frequency of the recurrence of the varied conditions of icing. For the calculations of the thermal deicers required power it is necessary to also investigate thermodynamic processes on the icing up surface and to study the questions, connected with its heat emissions. Furthermore, in each case of icing in flight it is necessary clearly to represent, what is more advisable - to continue flight under conditions of the icing (if, of course, this does not threaten flight safety) or to attempt

to find another, more favorable route. For this it is necessary to, first of all, correctly forecast the possible conditions of icing.

The given short enumeration of the questions, which require their resolution during the study of aircraft icing, is the demonstrative illustration of an entire complexity of the general/common/total problem of deicing of aircraft. Already by itself this enumeration makes it possible to break entire problem at least into four independent sections.

To the first of these sections, which it is possible to call physical-meteorological, we relate the investigations, connected with the study of quantitative connections/communications of intensity and form of ice accumulation on separate aircraft components with different meteorological parameters and flight conditions, and also study of the separate factors, which affect these connections/communications.

To the second section, engineering-operational, can be referred the work on the study of the effect of aircraft icing on its flight characteristics in dependence on form and quantity of grown ice.

To the third section, named technical, is related the work on direct development and construction of different systems, which make

it possible to carry on an active struggle with ice accumulation on aircraft.

Finally, to the fourth section, synoptic-meteorological, can be attributed the works of prognostic and statistical character.

Although the given division of an entire problem into 4 sections is not indisputably absolute, since these sections in many respects are mutually connected, nevertheless it in general terms correctly transfers those directions which appeared in science.

This work, as is shown by its name, is dedicated to the study of the first section according to the classification given above. The basic results, presented below, are obtained in the laboratory of the cloud investigations by TsAO - Central Aerological Observatory] during the years 1950-1956. We did not place to ourselves by the target of giving the complete survey/coverage of the works, dedicated to the problem of deicing of aircraft, since their quantity at present has already been counted by thousand and their survey/coverage exceeds the scope of our possibilities, and also they did not approach a strict observance of historical sequence in the presentation of material.

However, the basic achievements of latter/last years both in our

country and abroad they found in the work the appropriate reflection.

Page 8.

2. Formulation of the problem.

the experimental investigations of the processes of icing in free-air conditions were initiated as early as by 1922-1923 Peppler [72] with the aid of kites [1].

FOOTNOTE [1]. In this survey are not examined questions of ice-covered surface, although the mechanism of ice accumulation on the communication lines and on aircraft is actually similar and many results, obtained during the study of icing, can be applied, also, to the phenomena of ice-covered surface. ENDFOOTNOTE.

From 1929-1930 numbers of investigations in icing sharply it grows/rises. Appear thorough theoretical (Blekker 1932 [47]) and experimental (Samuels 1932 [74]) works.

The first large monographs, dedicated to aircraft icing, appeared in the USSR at the end Thirties. They include: the collector/collection edited by V. F. Bonchkovskiy, with the vast theoretical article of Khrgian [21] and N. V. Lebedev's book [10]. In

N. V. Lebedev's monograph was given the sufficiently detailed survey/coverage of all principal works on aircraft icing, made up to 1938. During the subsequent years to the problem of aircraft icing begins to pay ever increasing attention the number of scientific institutions as in the USSR (central institute of predictions/forecasts. Main Geophysical Observatory, central aerological observatory, State or NII - Scientific Research Institute] GVF, etc.), so also abroad (in particular national consultative committee on aeronautics - NACA - in the USA).

As a result of the first investigations it was already explained that the dominant role in aircraft icing plays the freezing of the supercooled cloud drops, which encounter the icing up surface, and that the role of sublimation, even if it occurs, it is insignificant.

It is obvious that in general view the intensity of freezing ice on one or the other aircraft component, which moves with speed u_∞ can be expressed by the formula

$$I = \frac{4}{3}\pi u_\infty \beta \cdot \frac{\rho_в}{\rho_л} \int_0^\infty r^3 n(r) E(r)\, dr. \qquad (0.1)$$

Here $4/3\pi r^3 n(r)dr$ - mass of water, prisoner in the drops of a radius from r to r+dr per unit of volume of air, n (r) - the density of the spectral distribution of drops according to sizes/dimensions, calibrated by liquid-water content, i.e., in such a way that

$$\frac{4}{3}\pi\rho_{в}\int_{0}^{\infty} r^{3} n(r)\,dr = w,$$

E(r) - the coefficient of the capture whose introduction considers the degree of deviation of drops from rectilinear path, namely he indicates, what portion of drops from the volume through which passes the section of the surface of aircraft being investigated, encounters the latter. The coefficient of freezing β is equal to the ratio of the mass of grown ice to the mass of the water, deposited for the same time to the same surface.

From formula (0.1) it is evident that for determining the icing intensity of different parts under different conditions it is necessary to know the form of the function n(r), E(r) and β.

Page 8.

The knowledge of these functions plays the significant role not only for studying the processes of aircraft icing, but also for solving a whole series of other independent tasks. Thus, for instance, with the coefficient of capture we meet during the calculation of corrections to different instruments, based on the principle of the catching of cloud particles [38, 31, etc.]. With the spectra the distributions of cloud drops at present collide in radar

during the study of absorption, reflection and passage of ultrashort radio waves, in the theory of visibility [36], in the theory of residues/settlings [37], etc. Finally, the determination of the coefficient of freezing is connected with the examination of the equations of heat balance, used in psychrometry, calculation of corrections to aircraft thermometers, etc.

For this very reason it is represented by advisable to conduct the detailed investigation by each of these three functions individually (chapter II, III and IV).

The rapid and continuous development of jet aviation led to the need to specially examine questions of aircraft icing at high flight speeds. This is made in V chapter of present monograph.

3. Basic conventional designations, used in work.

r - radius of the drop (see or μ).

$r_{кр}$ - radius of the minimum drop, which still deposits on the obstruction (see or μ).

$r_{ср}$ - mean radius of the cloud drops (see or μ).

R - radius of cylinder (cm).

C - significant dimension of the body (cm) being investigated.

x, y, z - moving coordinates of drop (cm).

$\dot{x}$, $\dot{y}$, $\dot{z}$ - components of the rate of drop (cm/s).

$u_x u_y u_z$ - components of air-stream velocity (cm/s).

$\ddot{x}$, $\ddot{y}$, $\ddot{z}$ - components of the acceleration of drop (cm/s).

ρ - density of substance (g/cm^3).

u_∞ - rate of the undisturbed flow (cm/s.) (rate of aircraft).

Δu - relative rate of drop in airflow (cm/s).

$F_0 = 6\pi r \mu \Delta u$ - resisting force to motion of sphere in viscous fluid according to the law of Stokes ($g \cdot cm/s^2$).

$P = F_0 \phi(Re)$ - real resisting force ($g \cdot cm/s^2$).

$\phi(Re) = 1 + 0{,}17\,Re^{2/3}$ - correction factor to Stokes' law (dimensionless).

$C_x = \frac{24}{Re} \frac{F}{F_0}$ - drag coefficient (dimensionless).

$p = \frac{2}{9} \frac{u_\infty r^2}{\nu C} \rho_*$ - parameter of inertia, equal in the dimensionless coordinates of the stopping distance of the Stokes drop, been cast into flow with an initial velocity of u_∞.

$p_{кр}$ - minimum value of the parameter, at which is possible the collision of drop with body (dimensionless).

Page 9.

λ - real stopping distance of drop (dimensionless).

λ_0 - stopping distance of the drop, which moves but to Stokes' law (dimensionless).

l - real stopping distance of drop (cm).

t_0 - temperature of the undisturbed flow (cloud) (deg).

t_s - temperature of surface (deg.).

$t_{cr} = t_0 + \frac{u_\infty^2}{2Jc_p}$
- static temperature of flow (deg.).

$t_{ad} = t_0 + \frac{r u_\infty^2}{2Jc_p}$ - adiabatic temperature of wall (deg.).

$r = \frac{t_{ad} - t_0}{t_{cr} - t_0}$ - recovery factor (dimensionless).

$c_p = 0{,}241$ - heat capacity of the air at a constant pressure (cal./g. deg.).

$J = 4{,}18 \cdot 10^7$ - mechanical heat equivalent (erg/cal.=g.cm²/s²cal).

λ - heat-transfer coefficient (cal/cm s deg.).

μ - coefficient of dynamic viscosity (g/cm/s)

ν - kinematic viscosity coefficient (cm²/s).

a - coefficient of thermal diffusivity (cm²/s).

w - liquid-water content of the drop part of the cloud (g/cm³) or (g/m³).

w_{kp} - minimum value of the liquid-water content with which the temperature of the icing up surface becomes equal to zero (g/cm³) or

(g/m^3).

w_i - portion of liquid-water content, which compensates for surface evaporation (g/cm^3) or (g/m^3).

m_s - mass of the water, which deposits per unit of surface per unit time $(g/cm^2\ s)$.

m_n - mass of ice, which freezes per unit of surface per unit time $(g/cm^2\ s)$.

m_i - mass of ice, which evaporates per unit time from the unit of surface $(g/cm^2\ s)$.

α - heat-transfer coefficient $(cal/cm^2\ s.\ deg.)$.

$L_2=79.7$ - latent heat of the crystallization of water at 0° (cal/g).

$L_{исп.t}$ - latent heat of vaporization of water with t° (cal/g).

$L_{исп.t=0}=677,1$ - latent heat of vaporization of ice with t=0° (cal/g).

e_t - saturating vapor pressure with t° (mb.).

$\mathrm{Re} = \frac{2\Delta u r}{\nu}$ - Reynolds number for the drop, which moves in flow with relative rate Δu (dimensionless).

Page 10.

$\mathrm{Re}_0 = \frac{2u_\infty r}{\nu}$ - Reynolds number for the drop, which moves in flow with a relative rate of u_∞ (dimensionless).

$\gamma = \frac{\mathrm{Re}}{\mu}$ - scale modulus/module (dimensionless).

ξ, η, ζ - moving coordinates of drop (dimensionless).

ξ', η', ζ' - components of the rate of drop (dimensionless).

u_ξ, u_η, u_ζ - components of air-stream velocity (dimensionless).

ξ'', η'', ζ'' - components of the acceleration of drop (dimensionless).

$\tau = \frac{u_\infty}{C} t$ - time (dimensionless).

$E(P, \mathrm{Re}_0)$ - the complete coefficient of capture (dimensionless).

$E_s(P, \mathrm{Re}_0)$ - local coefficient of capture (dimensionless).

$E_0(P, \mathrm{Re}_n)$ - local coefficient of capture at the singular point of profile/airfoil (dimensionless).

$\tilde{E}$ - integral complete coefficient of capture (dimensionless).

$\tilde{E}_*$ - integral local coefficient of capture (dimensionless).

$\tilde{E}_0$ - integral local coefficient of capture at the singular point of profile/airfoil (dimensionless).

n(r) - the spectral density or distribution of cloud drops according to sizes/dimensions ($1/cm^4$).

β - coefficient of freezing (dimensionless).

I - intensity of freezing ice (cm/s) or (mm/min).

Indices.

a
~~and~~ - the air

C - the water

l - ice

k - drop

kr - critical value

s - surface

isp - evaporation

sub - sublimation

H - freezing

t - at temperature t°C.

Chapter I.

Aerodynamics of the flow around bodies of the flow of monodisperse aerosol [1].

FOOTNOTE [1]. By monodisperse aerosol is understood, in particular, the idealized cloud, which consists of identical drops. ENDFOOTNOTE.

1. Equation of motion of drops.

From the very concept of the coefficient of the capture of drops by any body it is obvious that for its determination it is necessary to study the trajectories or the motion of drops during the flow around by them this body.

The first attempts at the determination of these trajectories are related to Thirties. In 1931 Albrecht [42] it fulfilled some calculations of the coefficient of capture for a circular cylinder

(Fig. 4). However, the calculations of Albrecht were also very rough. From Taylor's works [76] and Glauert [55], that relate to 1940, and then Langmuir and Blodgett [62] in 1945 was begun, actually, new stage in the solution of the problem of the flow around bodies of the particles of aerosol.

Taylor investigated the system of equations, which is determining the motion of water drops in the case when the forces, acting on drops from the side of flow, are described by Stokes' law. In this case it brought together this system of equations to dimensionless form [2]

$$\begin{cases} p\xi'' = u_\xi - \xi' \\ p\eta'' = u_\eta - \eta' \end{cases} \tag{1.1}$$

FOOTNOTE [2]. Here below all designations, used by different authors, if this is not especially stipulated, are given to the single designations, accepted in this work. ENDFOOTNOTE.

Thus, Taylor found that in the case of Stokes motion parameter p is the sole, necessary and sufficient similarity criterion.

Allowing/assuming some assumptions, Taylor succeeded in finding the very important consequences of equation (1.1), namely: if the speed of flow in the vicinity of the point of settling can be

represented in the form $\frac{u_x}{u_y} = \frac{-k_x}{k_y}$ (hyperbolic flow) and at certain moment of time the speed of drop coincides with the speed of flow, then drop can achieve the surface of settling only in such a case, when $\rho > \frac{1}{4\kappa}$. Being based on this important consequence, it is possible to show that under given conditions for flight and form of the body being investigated on the latter (as during the hyperbolic flow, examined by Taylor) can be precipitated out only drops by the radius more than certain critical value.

Page 12.

Glauert [55] according to the formulas, derived by Taylor, it was possible to conduct the series/row of numerical calculations for circular cylinders and some calculations for the wing of aircraft.

The most complete and precise calculations on the study of the flow around of circular cylinders, spheres and infinite flat/plane strips/films were completed by Langmuir and Blodgett in 1945 on differential analyzers [62]. However, with the results of these calculations we took the opportunity of becoming acquainted only on separate extractions of them in the form of the graphs/curves, given in the series/row of works [49, 77].

Let us examine more strictly and consecutively/serially the task

of determining the coefficient of capture, which is actually reduced to the determination of the probability of colliding the body, which moves in the medium of aerosol (in cloud or in the zone of residues/settlings), with the particles of this aerosol (water drops).

To mathematically more simply solve problem in the coordinate system, rigidly connected with body, i.e., to consider body motionless, and medium together with particles - leaking in to it.

Let at infinity the medium together with particles move with the speed u_∞[1].

FOOTNOTE [1]. Here it is below, where this is not especially stipulated, the discussion deals with subsonic speeds.

With approximation/approach to body the speed of medium begins to change, while the particles attempt to preserve uniform and rectilinear motion. As a result of the forces, which appear due to a difference in the speeds of the particle motion and medium, deflect/divert the particles from inertia rectilinear path. If we consider that the particle concentration is small, they do not affect by one another and the character of the flow around body of flow, then the force, which acts on particle, depends only on particle

speed with respect to medium. Considering flow as that being steady, it is possible to write that this force F is equal to

$$\vec{F} = F(\vec{u}_n - \vec{u}_k). \tag{1.2}$$

Here $\vec{u}_k(x,y,z)$ - particle speed, and $\vec{u}_n(x,y,z)$ - speed of the steady airflow, which flows around about the body.

Let us designate through m the mass of particle and will write the equation of motion of particle in projections along the axes of the coordinates

$$\begin{cases} m\ddot{x} = F_x \\ m\ddot{y} = F_y \\ m\ddot{z} = F_z. \end{cases} \tag{1.3}$$

For the determination of the trajectory of drop and, consequently, also capture coefficient E it is necessary to integrate the system of differential equations (1.3). In the problem of icing the discussion deals with the capture of spherical water drops, which considerably simplifies the task of finding the function $\vec{F}$.

In work [14] we in detail examined those conditions under which force $\vec{F}$ obeys the law of Stokes, i.e., $F = F_0 = 6\pi r\mu\Delta u$, where $\Delta\vec{u}$ - particle speed relative to flow. For sufficiently major drops practicability/feasibility conditions of Stokes' law are not observed, in this case the deviation from it by pillar is determined

by the value of Reynolds number (Re).

Page 13.

The theoretical and semi-empirical expressions for resisting force $\vec{F}$, obtained by Oseen, Allen and Rittinger, give a good coincidence with experiment only in comparatively narrow ranges of Reynolds numbers. Utilizing experimental data of Rayleigh about the resistance to motion of spherical particles in viscous fluid (Fig. 1), we succeeded in to find empirical relationship/ratio [14], describing the dependence of resisting forces on Re in the range of change Re from 0 to 10^3, which virtually overlaps entire range of the sizes/dimensions of cloud drops at flight speed to 100 m/s. This formula takes the form [1]

$$\vec{F} = \vec{F}_0(1 + 0{,}17\,\mathrm{Re}^{2/3}). \qquad (1.4)$$

FOOTNOTE [1]. In 1954 analogous relationship/ratio was obtained by the American researcher Serafini [75], on whom the correction factor takes form $1+0.157\ \mathrm{Re}^{2/3}$. In 1955 I. A. Fuks [28] gave relationship/ratio $C_d = \frac{24}{\mathrm{Re}} + \frac{4}{3\sqrt{\mathrm{Re}}}$, undertaken from the work L. Klyachko [8], published in the journal "Heating and ventilation" for 1934. It is easy to see that independently obtained by us relationship/ratio (1.4) virtually on differs from obtained L. Klyachko. ENDFOOTNOTE.

Here $\vec{F}$ - true resisting force, $\vec{F}_0$ - resisting force, designed according to the law of Stokes.

The degree of the coincidence of empirical formula with experimental data can be traced according to rayleigh's the same diagram (Fig. 1), on which along the axis of abscissas are deposited/postponed the logarithms of Re number, and along the axis of ordinates - logarithms of drag coefficient $\varkappa = \frac{F}{\frac{1}{2}u^2 r^2 \rho_a}$ [2].

FOOTNOTE [2]. Drag coefficient $\varkappa$ differs from coefficient C_d accepted in all latter/last works [28, 45, 63] in terms of factor $\pi/8$. ENDFOOTNOTE.

Here u - the relative speed of the motion of spherical particle in flow, r - its radius, ρ_a - the density of air flow.

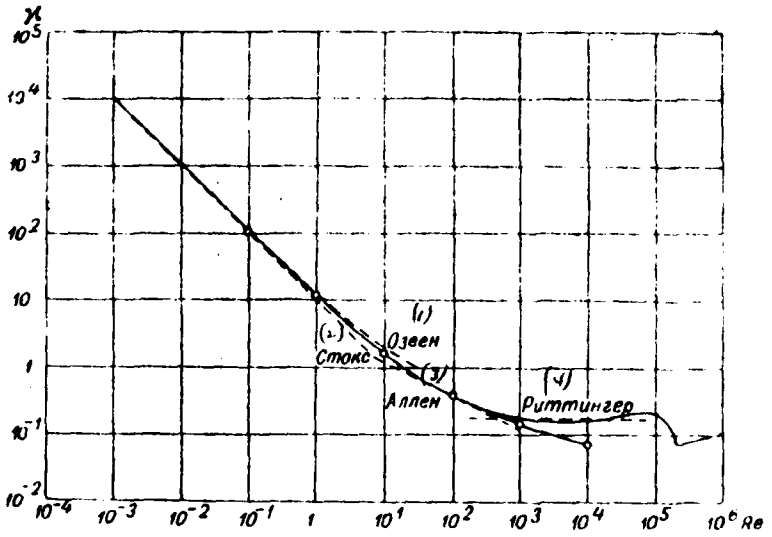

Fig. 1. Rayleigh's diagram (small circles noted values χ calculated on the basis of formula (1.4).

Key: (1). Oseen. (2). Stokes. (3). Allen. (4). Rittinger.

Page 14.

On the diagram of solid curve are plotted/applied the experimental data of Rayleigh, dash - those calculated respectively according to the formulas of Stokes, Oseen, Allen and Rittinger and finally small circles showed the values, calculated by formula (1.4).

In Fig. 2 is given the comparison of relation $\frac{F}{F_0} = \frac{C_d \mathrm{Re}}{24}$, designed

on (1.4) with the data given by Langmuir [63].

Equation (1.3) taking into account (1.4), bearing in mind that the particles are simply spherical drops, i.e., $m = \frac{4}{3}\pi r^3 \rho_в$, signs the form

$$\begin{cases} \ddot{x} = \frac{9}{2}\frac{\mu}{r^2\rho_в}(u_x - \dot{x})\varphi(\mathrm{Re}) \\ \ddot{y} = \frac{9}{2}\frac{\mu}{r^2\rho_в}(u_y - \dot{y})\varphi(\mathrm{Re}) \\ \ddot{z} = \frac{9}{2}\frac{\mu}{r^2\rho_в}(u_z - \dot{z})\varphi(\mathrm{Re}) \end{cases} \qquad (1.5)$$

where

$$\varphi(\mathrm{Re}) = 1 + 0{,}17\left(\frac{2r}{\nu}\right)^{3/4}\left[(u_x - \dot{x})^2 + (u_y - \dot{y})^2 + (u_z - \dot{z})^2\right]^{1/4}.$$

For obtaining the criterial relationships/ratios let us write system (1.5) in dimensionless coordinates, after selecting as the unit of length the significant dimension of body C (cm), as the unit of speed - speed of undisturbed flow u_∞ (cm/s) and as time unit - a transit time of section C with a speed of u_∞, i.e. $\frac{C}{u_\infty}$ (s).

Let us designate dimensionless coordinates respectively after ξ, η, ζ and the dimensionless time through τ. Then equations (1.5) take the form (if we by prime designate differentiation with respect to time τ):

$$\begin{cases} \xi'' = -\frac{1}{\beta}(\xi' - u_\xi)\varphi(\mathrm{Re}) \\ \eta_1'' = -\frac{1}{\beta}(\eta_1' - u_{\eta_1})\varphi(\mathrm{Re}) \\ \zeta'' = -\frac{1}{\beta}(\zeta' - u_\zeta)\varphi(\mathrm{Re}) \end{cases} \tag{1.6}$$

where $\beta = \frac{2r^2 u_\infty}{9\mu C}\rho_0$, $\varphi(\mathrm{Re}) = 1 + 0{,}17\,\mathrm{Re}_0^{2/3}[(\xi' - u_\xi)^2 + (\eta_1' - u_{\eta_1})^2 + (\zeta' - u_\zeta)^2]^{1/3}$,

$$\mathrm{Re}_0 = \frac{2ru_\infty}{\nu}.$$

System of equations (1.6) obtained thus, determining the trajectory of the motion of drop, is very important for our further presentation. Let us enumerate therefore the assumptions which became the basis of the conclusion/output of these equations.

Page 15.

1. Presence of cloud drops does not affect field of circumfluent flow.

2. The heterogeneity of medium is small in comparison with the sizes/dimensions of drops, i.e., on the surface of drop there is no slip.

3. Field of current in the absence of drop is uniform (flow lines are parallel).

4. Drops have spherical form, they smooth, solid and constant/invariable.

5. Drop do not coagulate and do not decompose during process in question settlings.

6. On drop do not act other forces, except force of viscosity of air (in particular, it does not act gravitational force).

7. Temperature is permanent, so that parameters μ, ν, ρ_0 are not changed along trajectory of drops.

In the examined formulation of the problem we do not postulate the validity of Stokes' law, i.e., it is not disregarded by the inertial forces of medium.

Let us estimate the assumptions enumerated above.

1. Overall relative volume, occupied by drops in air, does not exceed several millionth portions (maximum known liquid-water contents are of the order 1 g/m^3) from total volume, concentration of

their order of hundreds to cubic centimeter. Thus, distance from drop to drop is measured by millimeters, i.e., hundreds of times exceeds their transverse sizes/dimensions. This it is completely sufficient in order with the good reason to consider that their mutual effect is excluded, since, as is shown in the monograph of Figurovskiy [26], the mutual effect of drops negligibly already when the distance between them ten times only exceeds the transverse sizes/dimensions of drops.

On the other hand, the sizes/dimensions of drops into hundred are and thousands of times less than the sizes/dimensions of body. Thus, assumption 1 is possible to consider with a high degree of accuracy.

2. Heterogeneity of medium, i.e., the comparability of the intermolecular distance of air with a radius of drops, can exert noticeable influence only on very small drops, by a radius less than 1 μ.

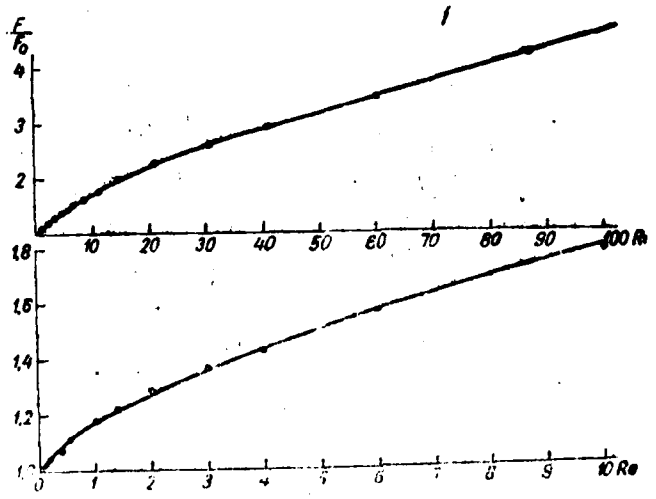

Fig. 2. Curves are calculated by formula (1.4) (points note Langmuir's data).

Page 16.

The greater the intermolecular distance, the more time drop flies as in void, without testing/experiencing resistance, and the less the total resisting force, which acts on drop. So, according to Millikan [16], this effect shows up only when mean free path is compared with a radius of drops r. The force, which acts on drop in this case, can be written in the form $F = F_0 f\left(\frac{l}{r}\right)$, where l - mean free path of molecules. Decomposing/expanding $f\left(\frac{l}{r}\right)$ in series/row according to degrees l/r, in the first approximation, we have

$$f\left(\frac{l}{r}\right) = 1 - A\frac{l}{r}.$$

According to Millikan Aэр. 9, what gives correction to Stokes' law for the drops of a radius 1μ of order 5o/o (with t=0° and p=760 mm Hg), and for drops 10 μ - order 0.5o/o. If necessary, as can easily be seen, these deviations from Stokes' law easily yield to account by the introduction, for example, of the effective value of viscosity/ductility/toughness $\mu_{эф} = \mu \cdot f\left(\frac{l}{r}\right)$. however, the account of this effect becomes necessary for such small drops which do not play any noticeable role in the problem of icing.

3. Heterogeneity of field, i.e., streamline curvature on elongation/extent of drop, has negligible effect, since sizes/dimensions of body in hundred or more times exceed sizes/dimensions of drops [14].

4. Assumption 4 also can be considered virtually carried out, since small deviations from sphericity, as prompted Andreasen [43], they do not play noticeable role, and remaining conditions lead to corrections of order $\mu_в/\mu_ж$, where $\mu_в$ - viscosity/ductility/toughness of air, and $\mu_ж$ - viscosity of water, i.e., they do not exceed 1o/o.

5. Small sizes/dimensions of drops - order 10^{-3}-10^{-4} cm and

their relatively small concentration make assumption 5 with that completely justified.

6. Condition 6, first of all, means that we is disregarded by gravitational force, that does not cause serious fears, since rates of free fall in drops thousands times of less than rates of inertial motion in question. We is disregarded also by the electric forces of interaction of drops with body. On its role were presented different hypotheses; however, Hann [54] experimentally demonstrated that it does not exert appreciable effect. In recent years L. M. Levin [13] demonstrated that also theoretically.

7. For propeller-driven aircraft whose rates do not exceed 100-150 m/s (360-540 km/h), heating even dry air in layer of disturbance does not exceed 5-10°, which has insignificant effect on oscillations/vibrations μ, ν and φ does not affect significantly trajectory of drops.

Thus, it is possible with the large basis/base to consider that the trajectories of the water drops, which flow around together with the flow of air about the one or the other part of aircraft, with large accuracy are described by system of equations (1.6).

the solution of system of equations (1.6) is determined by the

field of the air-stream velocities, i.e., by values u_x, u_y and u_z in each point in the trajectory or drop of radius r, and by two dimensionless parameters p and Re_0, which can be examined as similarity criteria. This solution makes it possible to construct the trajectories of drops and to calculate the series/row of the characteristics of icing.

Page 17.

Let us recall that here we examine subsonic speeds at which $M^2<<1$, i.e., it is possible to consider that such parameters of medium as temperature, density, viscosity - virtually are not changed in motion by the latter. In this case, obviously, the drops do not evaporate and do not increase. However, form and the sizes/dimensions of the streamlined body can partially be changed in the process of icing, which it is necessary to bear in mind during the study of aircraft icing.

2. Analysis of the equations of motion of drops.

As shown in the preceding/previous section, for the determination of the trajectories of the motion of drops it is necessary to solve system of equations (1.6). However before converting/transferring to the solution of this system, let us pause

briefly at its qualitative examination.

Into system of equations (1.6) in contrast to the system, examined by Taylor, organically enter no longer one, but two dimensionless parameters p and Re_0, which, therefore, and are the criteria of similarity of phenomenon. Let us incidentally note that as such criterial parameters they can be accepted and other parameters, which are combinations p and Re_0. Thus, for instance, in the USA widely are utilized parameters Re_0 and so-called scale modulus/module $\psi = \frac{Re_0}{p}$. In the investigations of L. M. Levin are utilized parameters p and Ru, where $Ru = \frac{Cu_\infty}{\nu_0}$ - Reynolds number for a body. It is not difficult to see that $Ru = \frac{\rho_0}{\rho_\infty} \frac{Re_0}{p}$. Thus, during the simulation of the conditions of icing one should proceed from the presence of 2 similarity criteria, in this case, running in forward, it is possible to say that parameter p plays substantially greater role than parameter Re_0.

As has already been mentioned, Taylor into 1940 more [76], investigating a simpler system of equations (1.7), describing particle motion under the action of Stokes force, showed that in the specific field of air-stream velocities there is this critical value of parameter $p = p_{кр}$, that when $p < p_{кр}$ the drops completely do not encounter obstruction, but they flow about the it together with airflow.

$$\begin{cases} \xi'' = -\frac{1}{p}(\xi' - u_\xi) \\ \eta_1'' = -\frac{1}{p}(\eta_1' - u_{\eta_1}). \end{cases} \tag{1.7}$$

Taylor
~~Hoot-R~~ examined the case when the velocity field of flow is assigned by system of equations (1.8) (origin of coordinates combined with the critical point at which $u_\xi = u_{\eta_1} = 0$), it assumed/set flow by the hyperbolic

$$\begin{cases} u_\xi = -a\xi \\ u_{\eta_1} = a\eta_1. \end{cases} \tag{1.8}$$

Equations (1.7) take in this case the form

$$\begin{cases} \xi'' + \frac{1}{p}\xi' + \frac{a}{p}\xi = 0 \\ \eta_1'' + \frac{1}{p}\eta_1' - \frac{a}{p}\eta_1 = 0. \end{cases} \tag{1.9}$$

In system of equations (1.9) the variable/alternating were divided. these linear equations with constant coefficients easily are integrated in final form.

Page 18.

Let us examine the motion of drop along the axis of symmetry for which $\eta_1 = \eta_1' = \eta_1'' = 0$. The solution of the 1st of equations (1.9) takes the form

$$\xi = Ae^{K_1\tau} + Be^{K_2\tau}, \qquad (1.10)$$

where K_1 and K_2 - the solutions of characteristic equation are respectively equal to

$$K_1 = -\frac{1}{2p}(1 - \sqrt{1-4ap}),$$
$$K_2 = -\frac{1}{2p}(1 + \sqrt{1-4ap}).$$

Let us assume that at some moment of time with coordinate $\xi = \xi_0$, the drop had a rate of flow, equal $-a\xi_0$. The zero time reference let us begin from this point on, i.e., will place at this moment/torque $\tau=0$. Then, after finding from initial conditions of the value of coefficients A and B, equation (1.10) can be written in the form

$$\xi = -\frac{a+K_2}{K_1-K_2}\xi_0 e^{K_1\tau} + \frac{a+K_1}{K_1-K_2}\xi_0 e^{K_2\tau}. \qquad (1.11)$$

It is clear that the drop can achieve body, i.e., the situation, when ξ turns into zero, when both members, entering equation (1.11), have different signs. The latter means that expressions $a+K_2$ and $a+K_1$ must have one and the same sign, if roots K_1 and K_2 are real. Let us show that satisfaction of these two conditions is incompatible, i.e., let us show that if roots K_1 and K_2 are real, then $\frac{a+K_2}{a+K_1}<0$ and not with what τ the coordinate of drop ξ will be able to become equal to zero. Actually the reality of the roots of the characteristic equation K_1 and K_2 is equivalent to the condition that $1-4ap>0$, i.e.,

in this case

$$p < \frac{1}{4a} = p_{кр}. \tag{1.12}$$

Now let us assume that $a+K_2$ and $a+K_1>0$, then $a+K_1 = a-\frac{1}{2p}(1+\sqrt{1-4ap})>0$ and, therefore, is those more $a>\frac{1}{2p}$, т. е. $p>\frac{1}{2a}>\frac{1}{4a}$, which contradicts condition (1.12).

Let us assume that $a+K_2$ and $a+K_1<0$, then from (1.11) when $t=0$ and after the substitution of values K_1 and K_2 follows that

$$\frac{a-\frac{1}{2p}+\frac{\sqrt{1-4ap}}{2p}}{a-\frac{1}{2p}-\frac{\sqrt{1-4ap}}{2p}} = e^{\frac{\sqrt{1-4ap}}{p}\tau}. \tag{1.13}$$

Since numerator and denominator on the left side of equation (1.13) are negative, then left side is always less than unity, since in absolute value the denominator of more than numerator on $\frac{\sqrt{1-4ap}}{p}$. However, the right part of equation (1.13) is always more than one. Thus, equality (1.13) occurs only with 1-4ap=0, i.e., with p=1/4a and it is not fulfilled with p<1/4a.

Page 19.

Thus, drops with parameter $p<\frac{1}{4a}=p_{кр}$ do not reach body.

The conclusion, obtained by Taylor, has deeper value, since the

fact of the presence of critical parameter $p_{кр}$ for the hyperbolic flow around body of air flow is a sufficient condition for existence $p_{кр}$ in general. From the point of view of existence $p_{кр}$ hyperbolic flow will be major for real flow.

Actually/really, let us examine the trajectory of drop during hyperbolic and real flow on phase diagram (Fig. 3). The curve AO characterizes the particle motion of air flow during real flow. The curve A'O characterizes the trajectory of drop in this case. the straight line B'O it characterizes hyperbolic flow, while the curve BB'B"⌣O - trajectory of drop in this flow, if at point B' its rate coincides with the rate of flow.

From the analysis of the equations of motion of drop (1.7) it is possible to show (on what paid our attention L. M. Levin) that when $p \leq p_{кр}$ the curves B'B"⌣O and A'O in phase diagram are approached point O at one and the same angle. Actually/really, let us examine the first equation of system (1.7) and let us write it in the form:

$$\frac{d\xi'}{d\xi}\xi' = -\frac{1}{p}(\xi' - u_\xi), \tag{1.14}$$

at point O $u_\xi = 0$, whence we have

$$\left(\frac{d\xi'}{d\xi} + \frac{1}{p}\right)\xi' = 0. \tag{1.15}$$

FOOTNOTE 1. Partially the line of the reasoning given below is presented in the work of Devies [from literature] [49]. ENDFCOTNOTE.

If $\xi' \neq 0$, then the gradient of velocity of drop in the vicinity of critical point 0 is equal to $\frac{d\xi'}{d\xi} = -\frac{1}{p}$ and does not depend on the field gradient of the air-stream velocities in the vicinity of this point.

If in (1.15) $\frac{d\xi'}{d\xi} + \frac{1}{p} \neq 0$, then $\xi' = 0$. For determination in this case of the gradient of velocity of drop in the vicinity of point 0 let us differentiate (1.14) on ξ

$$\xi' \frac{d^2\xi'}{d\xi^2} + \left(\frac{d\xi'}{d\xi}\right)^2 = -\frac{1}{p}\left(\frac{d\xi'}{d\xi} - \frac{du_\xi}{d\xi}\right),$$

by assuming/setting $\xi' = \xi = 0$ and, therefore, $\frac{du_\xi}{d\xi} = -a$, we will obtain

$$\left(\frac{d\xi'}{d\xi}\right)^2 + \frac{1}{p}\frac{d\xi'}{d\xi} + \frac{a}{p} = 0,$$

whence

$$\left(\frac{d\xi'}{d\xi}\right) = -\frac{1}{2p}(1 \pm \sqrt{1 - 4ap})$$

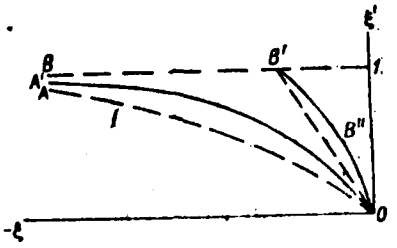

Fig. 3. Schematic of the flow around body of hyperbolic and real air flow and the corresponding particle trajectories of the aerosol on phase diagram.

Page 20.

On the basis of the condition that when $p \to 0$, $\frac{d\xi}{d\xi}$ must approach $\frac{du}{d\xi} = -a$, it is possible to immediately reject/throw one solution as unsuitable, and then we will obtain that

$$\frac{d\xi}{d\xi} = -\frac{1}{2p}(1 - \sqrt{1 - 4ap}) = K_1, \qquad (1.16)$$

Relationship (1.16) shows that when $p < p_{кр}$ the gradient of velocity of drop at point O depends only on parameter p and gradient of the air-stream velocity in the vicinity of singular point. Thus, returning to phase diagram, it is possible to say that curves B'B''O and A'O are approached point O at the identical angle, equal to arctg K_1. Since on phase plane the particle trajectory of air flow during hyperbolic flow of pillar lies/rests the more to the right

corresponding trajectory during real flow, then is obvious that also the trajectory of drop during hyperbolic flow lies/rests by the pillar of the more to the right real trajectory of drop. This means that at each assigned point with coordinate ξ the rate of drop during hyperbolic flow is more than the rate of drop during real flow. From the latter it is obvious that if with what the p less $p_{кр}$, the drop does not reach the body with the hyperbolic streamlining, then it moreover does not reach it during real flow. Consequently $p_{кр}=\frac{1}{4a}$ is the critical parameter, general/common/total for both types of flow.

In the basis of conclusion/output the assumption about the validity of Stokes' law does not limit him, since, the nearer p to $p_{кр}$, the less the relative rate of drop in flow, the less Reynolds number and thereby with larger accuracy it is possible to consider valid Stokes' law. It is possible with confidence to say that when $p<p_{кр}$ the force, which acts on the drop from the side of air flow, with a high degree of accuracy is described by Stokes' law. Thus, it is possible to consider that the gradient or velocity of drop in the vicinity of singular point is actually/really determined by relationship/ratio (1.16) during actual flow and conclusion/output about existence and to its value, obtained above remains in this case valid.

Let us incidentally note that when $p=p_{кр}$ the gradient of velocity of drop at point $\xi=0$ is not defined, since $\frac{d\xi'}{d\xi}$ as function

p_* undergoes gap when $p = p_{кр}$.

Existence $p_{кр}$ independent of Taylor and in the more general case was shown also by L. M. Levin into 1952. In his work Levin gives values $p_{кр}$ for an elliptical cylinder, equal to $p_{кр} = \frac{1}{4(1+A)}$, where A - the relation to the longitudinal axis of cylinder to transverse. In the particular case, for circular cylinders $p_{кр} = \frac{1}{8}$, but for a flat/plane plate (more accurate than the continuous belt, since we we examine two-dimensional task)

$$p_{кр} = \frac{1}{4}.$$

Page 21.

In the literature [45] are encountered the indications about that which and during the flow around asymmetric bodies also exists $p_{кр}$, equal to 1/4a, where a - the first coefficient in the resolution of the rate in terms of normal coordinates in the vicinity of singular point. However, the proof of existence $p_{кр}$ in this most general case to us is unknown.

The analysis of the equations of motion of drop in simplified form (1.7) makes it possible to find one additional important consequence, for the first time obtained by A. M. Yaglom [1] in 1951, and then, independently, by Robinson in 1956 [73].

FOOTNOTE 1. The results of the investigations of A. M. Yaglom were reported by it at seminar in the Geophysical institute of the AS USSR, but they were not published in press/printing. ENDFOOTNOTE.

The authors showed the potentiality of the hypothetical liquid, consisting of cloud drops.

Actually/really, let us write in vector form system (1.7)

$$\frac{d\vec{\rho}'}{d\tau} = -\frac{1}{\rho}(\vec{\rho}' - \vec{u}_\rho). \qquad (1.17)$$

Here $\vec{\rho}$ - dimensionless radius-vector of drop, $\vec{\rho}'$ - dimensionless rate of drop, $\vec{u}_\rho$ - dimensionless air-stream velocity.

For the proof of the potentiality of the flow of true liquid let us examine circulation integral of the vector of the speed of drop G on certain locked duct/contour c

$$\Gamma = \oint_c \vec{\rho}' d\vec{s}. \qquad (1.18)$$

Derivative of circulation integral of the vector of the speed of drop on time is equal to

$$\frac{d\Gamma}{d\tau} = \frac{d}{d\tau}\oint_c \vec{\rho}' d\vec{s} = \oint_c \frac{d\vec{\rho}'}{d\tau} ds + \oint_c \vec{\rho}' d\left(\frac{d\vec{s}}{d\tau}\right). \qquad (1.19)$$

On the basis (1.17) the first integral in the right side of equality (1.19) is converted to the form

$$\oint_c \frac{d\vec{\rho}}{d\tau} d\vec{s} = -\frac{1}{\rho} \oint_c (\vec{v}' - \vec{u}_\rho) d\vec{s} = -\frac{1}{\rho}(\Gamma - \Gamma_0).$$

It is obvious that Γ_0, which represents circulation integral of the vector of air-stream velocity, is equal to zero in view of the potentiality of the latter. Thus,

$$\oint_c \frac{d\vec{\rho}}{d\tau} ds = -\frac{1}{\rho}\Gamma. \qquad (1.20)$$

It is easy to see that the second integral in the right side of equality (1.19) turns into zero, since under integral will cost total differential. Actually/really,

$$\oint_c \vec{v}' d\left(\frac{d\vec{s}}{d\tau}\right) = \oint_c \vec{v}' d\vec{v}' = \frac{1}{2}\oint_c d(\vec{v}^2) = 0. \qquad (1.21)$$

Page 22.

And, therefore, from equality (1.19) taking into account equalities (1.20) and (1.21) we have

$$\frac{d\Gamma}{d\tau} = -\frac{1}{\rho}\Gamma,$$

whence

$$\Gamma = \gamma e^{-\frac{\tau}{\rho}}. \qquad (1.22)$$

Thus, if at some moment of time circulation integral of the vector of the speed of drop was equal to zero, then this means that it remains equal to zero at any other moment of time. From the proved theorem of the retention/preservation/maintaining zero vortex/eddy it follows that the motion of "hypothetical" true liquid potentially, since it is obvious that at sufficient removal/distance from the body where the flow is not disturbed and the trajectory of drops represent straight lines, parallel between themselves, circulation integral of the vector of the speed of drops is equal to zero.

The potentiality of the motion of this liquid and the fact of the absence of sources and flows out of body surface testify about the absence of the intersection of the particle trajectories of the liquid, i.e., the trajectories of the drops of identical size/dimension. Let us note incidentally that thereby is disproved Taylor's assumption [76] about the possibility of similar intersection.

It should be pointed out that the obtained conclusion about the potentiality of the flow of true liquid is based on the use/application of equation (1.7), comprised on the assumption that to drops from the side of flow acts the Stokes viscous force.

Actually the motion of drops is described by more complicated equation (1.23)

$$\frac{d\vec{\rho}'}{d\tau} = -\frac{1}{p}(\vec{\rho}' - \vec{u}_\rho)[1+0{,}17\,\mathrm{Re}_0^{2/3}(\vec{\rho}' - \vec{u}_\rho)^{2/3}]. \qquad (1.23)$$

It is here hardly possible to find circulation integral of the vector of the speed of drop by method presented above, since in this way we come to the complicated integrodifferential equation of the form

$$\frac{d\Gamma}{d\tau} = -\frac{1}{p}\Gamma - \frac{0{,}17\,\mathrm{Re}_0^{2/3}}{p}\oint_c (\vec{\rho}' - \vec{u}_\rho)^{2/3}(\vec{\rho}' - \vec{u}_\rho)\,d\vec{s}.$$

However, also in this more general case the fact of the nonintersection of trajectories is evident by stability strength of task and absence of sources and flows out of body surface.

3. Trajectories of drops and coefficient of capture.

Let us examine the schematic of the flow around of the wing of cloud drops.

The nonintersection of the trajectories of drops of one and the same radius means that:

1) the points of contact of the tangency of extreme trajectories define the zone of the collision of the drops of this radius with body,

2) the distance between the extreme tangential trajectories of drops in their undisturbed region determines the total quantity of drops, which encounter body, and the ratio of this distance to the midship section of body is equal to its complete coefficient of capture E,

3) distance ratio between adjacent trajectories in the undisturbed region to the distance between points of intersection of their with body determines the intensity of settling drops in this section of surface. The limit of this sense during the unlimited approach of trajectory is called the local coefficient of capture E_*

Page 23.

Let us return to the reference system of equation (1.6). While the exact solution of the system of nonlinear differential equations (1.6) is not impossible, their numerical solution does not compose fundamental difficulties. One of such calculation methods in detail have described we in work [14]. There the method of the approximate grapho-analytic integration of system of equations (1.6) indicated was successfully used for the calculations of settling drops to round cylinders [14], spheres and to the center sections of flat/plane

plates [32].

a) the flow around the bodies of simple forms.

Let us illustrate the mentioned method based on the example of the calculation of the collision of drops with cylinder. In this case the task becomes two-dimensional. The velocity field during the flow around round cylinders in dimensionless coordinates is described by the equations

$$\begin{cases} u_\xi = 1 - \dfrac{\xi^2 - \eta^2}{(\xi^2 + \eta^2)^2} \\ u_\eta = \dfrac{2\xi\eta}{(\xi^2 + \eta^2)^2} \end{cases} \tag{1.24}$$

After substitution (1.24) into system of equations (1.6), the latter is converted into the complicated system of the nonlinear differential second order equations.

$$\begin{cases} \xi'' = -\dfrac{1}{p}\left\{\xi' - \left[1 - \dfrac{\xi^2 - \eta^2}{(\xi^2+\eta^2)^2}\right]\right\}\left\{1 + 0{,}17\,\mathrm{Re}_0^{2/3}\left[\left(1 - \dfrac{\xi^2 - \eta^2}{(\xi^2+\eta^2)^2} - \right.\right.\right. \\ \left.\left.\left. - \xi'\right)^2 + \left(\dfrac{2\xi\eta}{(\xi^2+\eta^2)^2} - \eta'\right)^2\right]^{1/3}\right\} \\ \eta'' = -\dfrac{1}{p}\left[\eta' - \dfrac{2\xi\eta}{(\xi^2+\eta^2)^2}\right]\left\{1 + 0{,}17\,\mathrm{Re}_0^{2/3}\left[\left(1 - \dfrac{\xi^2 - \eta^2}{(\xi^2+\eta^2)^2} - \xi'\right)^2 + \right.\right. \\ \left.\left. + \left(\dfrac{2\xi\eta}{(\xi^2+\eta^2)^2} - \eta'\right)^2\right]^{1/3}\right\}. \end{cases} \tag{1.25}$$

The integration of the equations of motion of drops (1.25) was realized step by step, from one section to the next, for each of which the speed of flow (u_ξ, u_η) was considered constant. Constant was

considered Reynolds number in each section, what, let us note incidentally, is less important assumption, than the first. In this case the system of equations (1.25) with two unknowns decomposes into two linear differential ones equation with constant coefficients (1.25') and (1.25") which easily are integrated in the elementary functions

$$\xi'' = -\varkappa_i(\xi' - u_\xi{}^i), \qquad (1.25')$$

$$\eta'' = -\varkappa_i(\eta' - u_\eta{}^i). \qquad (1.25'')$$

Here $\varkappa_i = \frac{3\pi(\mathrm{Re}_i)}{p} = \frac{1+0.17\,\mathrm{Re}_i^{2/3}}{p}$, and $u_\xi{}^i$ and $u_\eta{}^i$ - constants for each i section of velocity of flow along the axes ξ and η The solutions of equations (1.25') and (1.25") take the form

$$\xi = a_1{}^i e^{-\varkappa_i \tau} + u_\xi{}^i \tau + a_2{}^i,$$

$$\eta = b_1{}^i e^{-\varkappa_i \tau} + u_\eta{}^i \tau + b_2{}^i.$$

Coefficients $a_1{}^i$, $a_2{}^i$, $b_1{}^i$ and $b_2{}^i$ are found from the conditions of the cementing of the solutions at the end of the i-th and beginning of (i+1) sections.

Page 24.

Moving in the solution from one section to the next, it is possible to construct the trajectory of drop up to its intersection with the duct/contour of cylinder, if drop deposits on it, or to those pores when trajectory passes knowingly past cylinder.

The dismantled/selected calculation method gives the possibility to solve the unknown task to any degree of accuracy - for this it suffices to select properly the value of intervals (i.e. to make their sufficiently small ones).

Thus, were constructed the tangential trajectories of drops and were found complete coefficients of capture. The comparison of our calculations when $Re_c = 0$ with the results of the calculations of different authors is given in Fig. 4 [1].

FOOTNOTE [1]. Fig. 4 is borrowed from the latter/last work of Davis and Peetz [49]. ENDFOOTNOTE.

From Fig. 4 it is evident that our results virtually coincide with the data of Langmuir and Blodgett. The more detailed information about the calculations of Langmuir and Blodgett is contained in the work of Tribus [77]. Utilizing his own calculations and results of the calculations of Langmuir and Blodgett there were constructed the diagrams, on which in coordinates (p, Re_0) were carried out the isolines of the capture E (Fig. 5a) full of coefficient, local coefficient of capture at the critical point of cylinder E_0 (Fig. 5b) and acceptance angle α (Fig. 5c), which was equal to the half the

arc, included between extreme tangential trajectories.

According to the method, described in [14], were determined the trajectories of drops during the flow around of sphere and flat/plane plate.

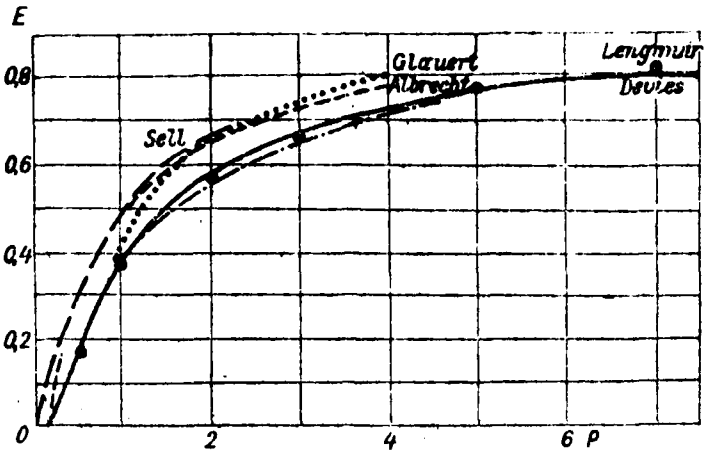

Fig. 4. Dependence of the complete coefficients of capture E on parameter p for round cylinders according to different authors. Points noted the values, obtained in the calculations of the author [14].

Page 25.

In spherical coordinates the function of current and velocity potential for a sphere are assigned by the equations

$$\psi = \frac{1}{2} u_0 r^2 \left[1 - \left(\frac{R}{r}\right)^3 \right] \sin \vartheta$$

$$\varphi = u_0 r \left[1 + \frac{1}{2} \left(\frac{R}{r}\right)^3 \right] \cos \vartheta,$$

whence easily is determined the velocity field around sphere, which

in dimensionless coordinates takes the form

$$\begin{cases} u_\xi = 1 + \frac{1}{2\rho^3}\left(1 - \frac{3\xi^2}{\rho^2}\right) \\ u_{\eta_1} = -\frac{3\xi\eta_1}{\rho^5}, \end{cases} \tag{1.26}$$

where $\rho = \sqrt{\xi^2 + \eta^2}$ - a dimensionless radius vector.

In the solution of system of equations (1.7) in velocity field, assigned by system of equations (1.26), were not considered the deviations from Stokes' law. It is possible to consider that results obtained in this case are sufficiently precise with $Re_0 < 10$, since the disregard of deviation from Stokes' law gives in this case the error in the determination of the coefficient of capture E not more than 5-10o/o.

Considerably more complicatedly is expressed velocity field for an infinite thin plate-strip/film.

In dimensionless coordinates the function of current [32] takes the form

$$\psi = \sqrt{\frac{1}{2}\left[\sqrt{(1 - \xi^2 + \eta^2)^2 + 4\xi^2\eta^2} - (1 - \xi^2 + \eta^2)\right]}.$$

Hence we obtain, that velocity field is assigned by the following equations

$$\begin{cases} u_\xi = \frac{\partial\psi}{\partial\eta_1} = \frac{\eta_1 + 2\xi^2\eta_1 - \eta_1\sqrt{\rho^4 + 4\xi^2\eta_1^2}}{\sqrt{2}\sqrt{\rho^4 + 4\xi^2\eta_1^2}\sqrt{\sqrt{\rho^4 + 4\xi^2\eta_1^2} - 1 + \xi^2 - \eta_1^2}} \\ u_{\eta_1} = -\frac{\partial\psi}{\partial\xi} = \frac{-\xi^3 + 2\eta_1^2\xi + \xi\sqrt{\rho^4 + 4\xi^2\eta_1^2}}{\sqrt{2}\sqrt{\rho^4 + 4\xi^2\eta_1^2}\sqrt{\sqrt{\rho^4 + 4\xi^2\eta_1^2} - 1 + \xi^2 - \eta_1^2}} \end{cases} \tag{1.27}$$

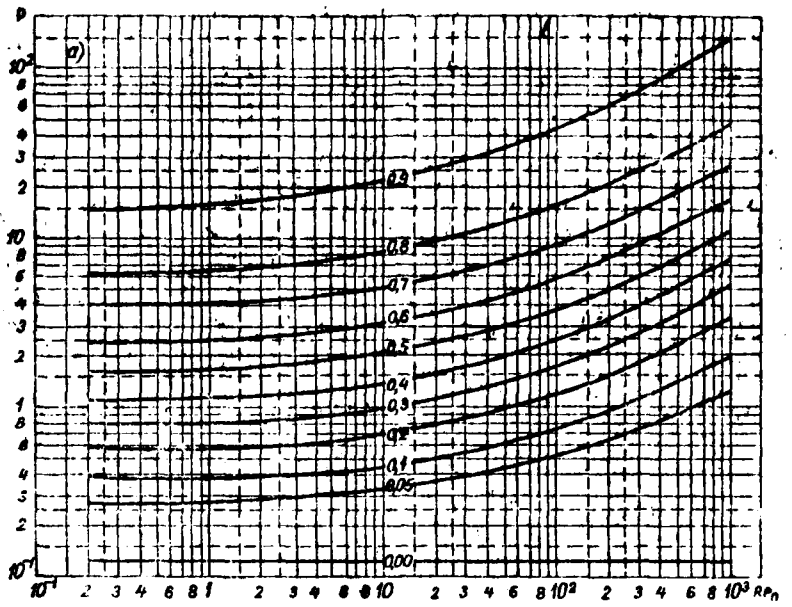

Fig. 5. a) the diagram of the dependence of total capture coefficient on parameters p and Re_0 for a round cylinder.

Page 26.

Here

$$\alpha = 1 - \xi^2 + \eta^2.$$

When velocity field is assigned by system of equations (1.27), the solution of equations (1.7) is so cumberscme which is impracticable without special computers. However, if we examine only the narrow central section of plate, then equations (1.27) considerably are simplified.

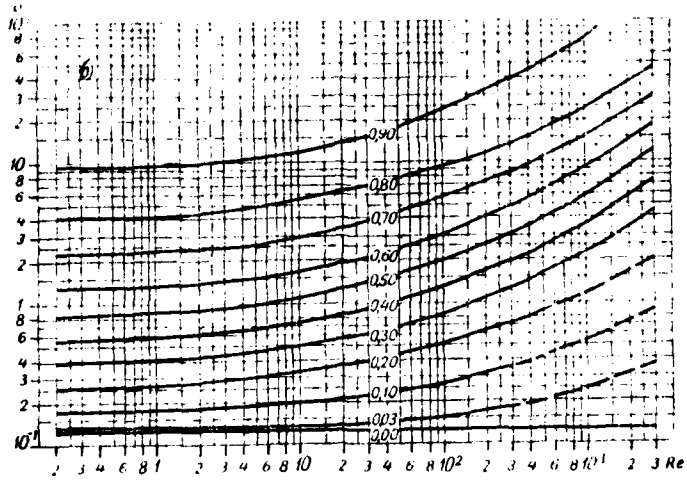

Fig. 5. b) the diagram of the dependence of the local coefficient of capture E_0 in critical point of round cylinder on parameters p and Re_0.

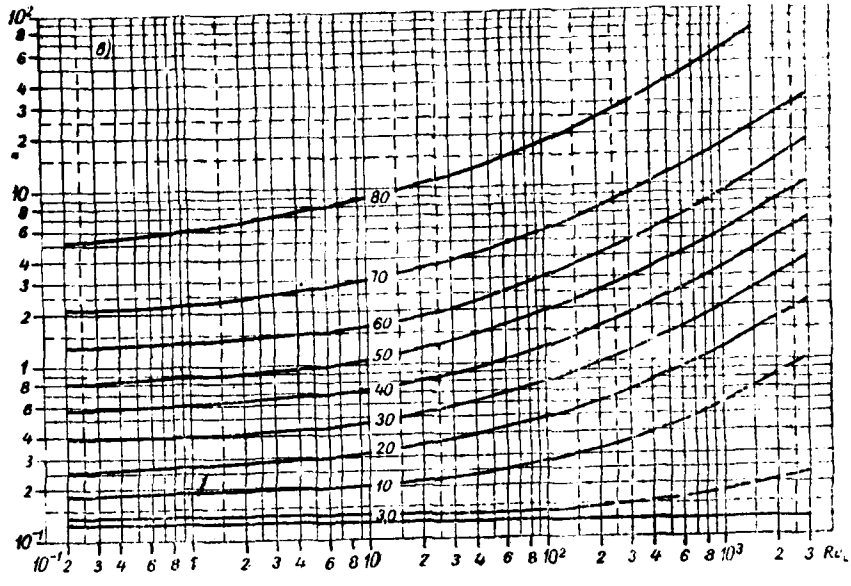

Fig. 5. c) the diagram of the dependence of the acceptance angle α for round cylinder on parameters ρ and Re_0.

Being limited to the trajectories, distant behind centerline at infinity not more than on $|\xi| = 0{,}01$, it is possible to consider that up to $|\eta| = 0{,}2$ occurs inequality $|\xi| \ll |\eta|$, then equations (1.27) are simplified and can be written in the form

$$\begin{cases} u_\eta = -\dfrac{\eta}{(1+\eta^2)^{1/2}} + O(\xi^2) \\ u_\xi = \dfrac{\xi}{(1+\eta^2)^{3/2}} + O(\xi^2), \end{cases} \tag{1.28}$$

where $O(\xi)$ - a low value of order ξ.

When $|\eta| < 0{,}2$ it is possible to simplify expressions (1.27), after placing $|\xi|, \eta| \ll 1$, then equations (1.27) they take the form

$$u_\xi = \xi\left(1 + \frac{1}{2}\xi^2 - \frac{3}{2}\eta^2\right) + O([\xi^2 + \eta^2]^{3/2}), \tag{1.29}$$

$$u_\eta = -\eta\left(1 + \frac{3}{2}\xi^2 - \frac{1}{2}\eta^2\right) + O([\xi^2 + \eta^2]^{3/2}).$$

With the aid of systems of equations (1.28) and (1.29), air speeds which assign field near centerline, it is sufficiently simple to calculate the trajectories of drops. Calculations were carried out without taking into account deviation from Stckes' law (Fig. 6), and

for one special case - the determination of corrections to the air intake of drops (Fig. 10) - taking into account this deflection.

B) the flow around wing profiles/airfoils.

The determination of the coefficients of capture for the bodies of the simplest forms and for round cylinders was especially the necessary stage in the resolution of the problem of icing. However, the obtained information about the character of the flow around different bodies of cloud drops with entire obviousness lead to the conclusion that during the study of the icing of the planes of the aircraft and its other parts with streamline profiles in section it is not possible to be limited to the calculations, made for round cylinders. On the other hand, the development of computational technology made it possible to approach directly the determination of the trajectories of drops, flowing around together with airflow about the more complicated, so-called wing profiles/airfoils. A similar problem was, of course, considerably more complicated and calculations are incomparably more labor-consuming than in the examination of the precipitation of drops to round cylinders.

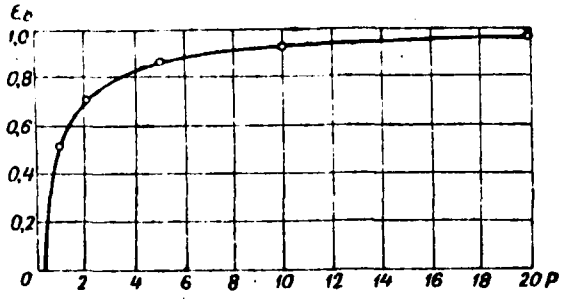

Fig. 6. Dependence of the local coefficient of capture E_0 at the critical point of the flat/plane plate, directed normal to flow on parameter p at $Re_0=0$.

Page 28.

Most completely a question of settling of drops to wing profiles/airfoils was investigated by Bergran in 1951 [44]. (Part of Bergran's findings were published by 1952 in his following article [45], dedicated to attempt find a simpler way of position finding of settling drops to wing profiles/airfoils, distributions of the collisions of drops according to the surface of wing and velocity of their collisions. The equations of motion of drop Bergran writes/records in a dimensionless form:

$$\begin{cases} \xi' = \dfrac{\psi}{\mathrm{Re}_0}\dfrac{C_d\mathrm{Re}}{24}(u_\xi - \xi') \\ \eta_1' = \dfrac{\psi}{\mathrm{Re}_0}\dfrac{C_d\mathrm{Re}}{24}(u_{\eta_1} - \eta_1'), \end{cases} \qquad (1.30)$$

where

$$\frac{\mathrm{Re}}{\mathrm{Re}_0} \quad \sqrt{(u_\xi - \xi')^2 + (u_{\eta_1} - \eta_1')^2}.$$

Calculations were given by it on the differential analyzers. In terms of assigned values φ, Re_0 and according to initial conditions the analyzer drew the trajectories of water drops.

In appendix 1 are given the tables of results of the calculations of Bergran.

On these tables it is possible to calculate the values of the coefficient of capture for the series/row of the values of parameters p and Re_0 (two-last columns in the tables appendix 1 have comprised we). Bergran examined four 15-percent Zhukovskiy profiles - symmetrical, at angles of attack 0.2 and 4° and the bent profile/airfoil with lift coefficient c_y =0.44 at zero angle of attack. The velocity field or current around profiles/airfoils was determined analytically, and for 15- percent symmetrical profile/airfoil NACA 65_2-015, velocity field was determined by the method of electrodynamic analogy.

L. M. Levin conducted in 1954 the calculations of the series/row of the trajectories of drops of approximately 90/0 of the symmetrical profile/airfoil NACA - 0009. In the same 1954 we carried out some trajectory calculations of the drops, depositing on a curved profile of the type NACA - 2215. This profile/airfoil does have a plane of aircraft LI-2.

The results of the calculations indicated do not yield to direct comparison, since they are related to the different parameters p and Re_0. Moreover, in this form these data give the solution only of the separate specific problems, which are of in general only limited interest. Therefore was logical to attempt to construct the grid of the values (or diagram) of the coefficient of capture E, making it possible to determine E with any p and Re_0.

It turned out that the data of Bergran and Levin make it possible to construct similar diagrams, if is known the behavior of function E(p) at very low and high values of p, at the different values of Re_0.

In the 2nd section of chapter I has already been mentioned about that which with decrease p to $p_{кр}$ E decreases to zero independent of value Re_0. The knowledge of values $p_{кр}$ is necessary for obtaining of complete representation about the coefficient of the capture of cloud drops by aircraft. Because of the works of Bergran and Levin a question about the numerical values of p for different streamline profiles of propeller-driven aircraft can be considered solved.

For Levin it was possible to obtain analytical expression $p_{кр}$ depending on thickness ratio $\bar{c}$, lift coefficient c_y and relative curvature f for different Zhukovskiy profiles. Decomposing/expanding his solution in series/row with an accuracy to the values of the 3rd order of smallness, Levin comes to convenient in practical use, truth to the somewhat bulky formula

$$p_{кр} = 0{,}296\bar{c}^2(1 - 2{,}31\bar{c} + 3{,}85\bar{c}^2 - 5{,}58\bar{c}^3) + 0{,}0127\,c_y^2[1 - 5{,}39\bar{c} + 14{,}5\bar{c}^2 - 25{,}7\bar{c}^3 - 0{,}0127\,c_y^2(1 - 19{,}25\bar{c})] + 2f^2[(1 - 2{,}31\bar{c} + 0{,}592\bar{c}^2 + 16{,}3\bar{c} - 24\bar{f}(1 - 4{,}37\bar{c}) - 0{,}622\,c_y^2(1 - 7{,}06\bar{c})] - 0{,}318f \cdot c_y[1 - 3{,}85\bar{c} + 6{,}51\bar{c}^2 - 4{,}33\bar{c}^3 - 0{,}127\,c_y^2(1 - 9{,}08\bar{c}) - 42\bar{f}^2(1 - 5{,}61\bar{c})]. \quad (1.31)$$

In Bergran's work [45] is given relationship/ratio $\psi_{cr} = 4\,\mathrm{Re}_0 \frac{\partial\sqrt{u_\xi^2 + u_\eta^2}}{\partial S} = 4\,\mathrm{Re}_0 G$, where S - a distance along the trajectory of drop in chord (let us recall that $p_{кр} = \frac{\mathrm{Re}_0}{\psi_{cr}}$), and are given the results of calculations G for the Zhukovskiy profiles and ellipses in dependence on relative thickness and a lift coefficient (application/appendix, fig. 34).

Bergran indicates that a similar graph/curve it is possible to use for any wing profiles/airfoils whose maximum thickness is arranged/located nearer to the spout of profile/airfoil. Errors due to the approximation of different profiles/airfoils Zhukovskiy's profile by the same relative thickness and the same lift are

unessential, since change $p_{кр}$ even to 10o/o exerts negligible effect on the size of coefficient and zone of capture.

Let us incidentally note that for high-speed/velocity profiles/airfoils whose thickening falls to the middle of chord, Bergran proposes to use the graph/curve, designed for an elliptical profile/airfoil (Fig. 34).

Comparison of $p_{кр}$ for 15- percent profile/airfoil, found from Levin's formula (1.31) with $\bar{c}=0$ and on the curves of Bergran (Tabl. 1), showed that they differ not more than to 2-3o/o.

On the basis of the calculations of Bergran and Levin and considerations about asymptotic property of change E with increase of p, and also data about $p_{кр}$ was possible to construct the diagrams of dependence of E on p and Re_0 for six profiles/airfoils.

Table 1. Values $f_{кр}$ for 15- percent Zhukovskiy profile.

c_y \ f	(1) По Левину			(2) По Бергран
	0	0,02	0,01	0
0,0	0,0049	0,0055	0,0071	0,0049
0,2	0,0052	0,0051	0,0060	0,0050
0,4	0,0061	0,0053	0,0055	0,0060
0,6	0,0076	0,0060	0,0056	0,0078

Key: (1). On Levin. (2). According to Bergran.

Page 30.

Before converting/transferring to the analysis of these diagrams, let us note that from the tables of Bergran and data of Levin it follows that the accuracy of the values E obtained by them with E<0.1 is such, that the errors in terms of absolute value can reach 0.02 and it is possibly more. Actually/really, for 15- percent symmetrical Zhukovskiy profile at $\alpha=4^\circ$ Bergran obtained in parameter $p=0.015$, and $Re_0=64$ and 256 values of E, respectively equal to 0.022 and 0.02 (see appendix, table 3), for a profile/airfoil with the angle of attack of $\alpha=2^\circ$ with $p=0.015$ and $Re_0=16$ is obtained value E=0.020, but for the same p and $Re_0=64$, value E=0.022 (table 2 of application/appendix) which is clearly erroneous. By that understated seems to us value E=0.045, obtained by Levin for profile/airfoil

NACA-0009 with p=0.027 and Re_0=110. The calculations of the coefficients of capture for very low values of p, which approach p_{cr}, are very complicated even during the use of computers.

Let us compare diagrams for determining the coefficient of capture E, constructed for the symmetrical profiles/airfoils of different thickness ratio - 9- percent NACA-0009 and 15- percent Zhukovskiy profile at zero angle of attack. In Fig. 7 are plotted the isolines of the equal to E for each profiles/airfoils.

From physical considerations it is clear that, other conditions being equal, the coefficient of capture E for NACA-0009 must be always more. However, we see that in Fig. 7 not all isolines of the equal to E for NACA - 0009 pass below appropriate isolines for a Zhukovskiy profile. This can be caused, on one hand, by an inaccuracy in calculation and construction of isolines and, on the other hand, apparently, fact that the coefficient of capture relatively little is changed with a change in the profile/airfoil of aircraft from 9-percent to 15-percent. Differences in the coefficients of the capture of the profiles/airfoils in question do not exceed 0.04, remaining, as a rule, less than 0.02.

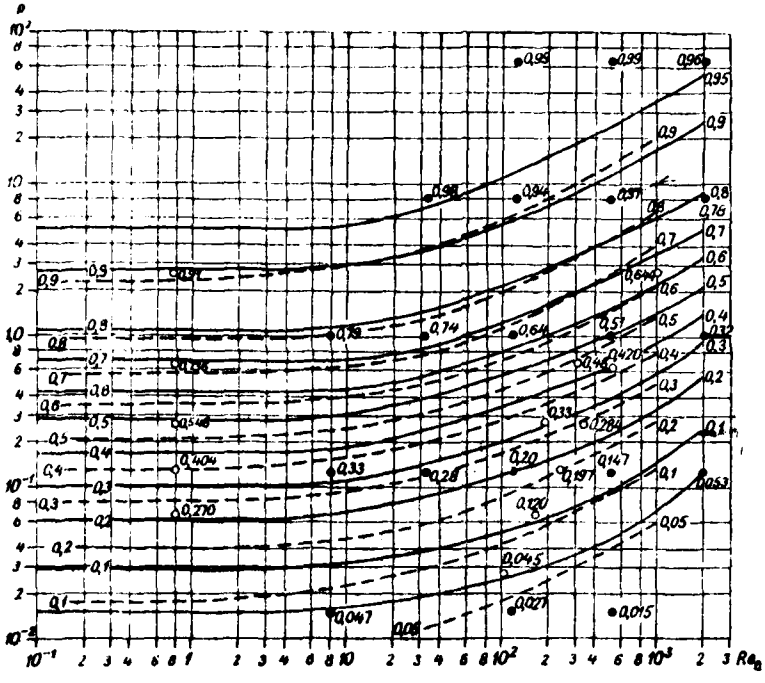

Fig. 7. Isolines of equal full or coefficient capture for 15o/o of symmetrical Zhukovskiy profile (solid lines) and for profile/airfoil NACA-0009 (broken lines) at zero angle of attack. 1 - Bergran's data, 2 - Levin's data.

Page 31.

From Fig. 7 it is clear that when E for 9-percent profile/airfoil proves to be less than E for 15-percent, then it is not possible to explain only by an inaccuracy in the construction of isolines. Sometimes easily can be noticed the inaccuracy in

calculations themselves (for example, as it was noted, value E=0.045 for NACA-0009 with p=0.027 and Re_0=110 it is clearly understated).

Being based on these considerations, it is possible to draw the general/common/total conclusion that for wing profiles/airfoils the coefficient of capture E was determined by Bergran and Levin with an accuracy to 0.02. About the fact that the error cannot be substantially more than this numeral, it testifies the fact that the isolines of the equal to E for profile/airfoil NACA-0009 virtually by pillar lie/rest below isolines E for 15-percent profile/airfoil, being deflected/diverted, as a rule, no more than to 0.02-0.04, that it could not occur with large random errors.

Consequently, changes of the coefficient of capture in dependence on thickness ratio lie/rest within the limits of values 0.00-0.04 with a change in the thickness ratio from 9 to 15o/o and cannot be reliable determined by the available calculations.

It is interesting to compare the coefficients of capture at different angles of attack α and camber of profile/airfoil. Let us note that during the calculation of the coefficients of capture for symmetrical Zhukovskiy profiles with the angle of attack, different from 0°, we took into consideration, that with an increase in the angle of attack α increases midsection the section (1.02 times at

$\alpha=2^\circ$ and 1.045 times at $\alpha=4^\circ$). The comparison of the constructed diagrams showed that the effect of the factors indicated small and does not exceed 15-20o/o with E>0.2, reaching 30o/o with E=0.1.

Summing up our conclusion/output about the complete coefficient of capture for wing profiles/airfoils, it is possible to say the following.

1. Relative errors for most reliable calculations for wing profiles/airfoils, carried out by Bergran and Levin, can reach 10o/o with E=0.2, decreasing with increase of E. In absolute value these errors, probably, do not exceed value of 0.02.

2. Effect of angle of attack in the range from 0 to 4° and thickness ratio in the range from 9 to 15o/o is comparatively small and becomes apparent in small oscillations/vibrations E about certain average/mean value on the order of +-0.02-0.03.

These two conclusion/output made possible to construct the single diagram, making it possible to determine the coefficient of the capture (when it is more than 0.2) for aviation profiles/airfoils in thickness ratio from 9 to 15o/o and angle of attack from 0 to 4°. It is possible to assume that this diagram will be suitable, also, for curved profiles, which fortifies itself by the comparison of data

for the bent Zhukovskiy profile with single diagram.

The construction of single diagram is carried out in Fig. 8a, in which are carried out the isolines from E=0.2 and it is above. Isoline E=0.1 is carried out by primes. In Fig. 8b this diagram is constructed in more demonstrative form - here along the axis of abscissas in logarithmic scale are deposited/postponed the values of parameter p, and along the axis of ordinates - value of the coefficient of capture E. Curves are constructed for the the different Re_0. In Fig. 8b it is clearly evident that E greatly slowly approaches its limiting values - to zero on the left side and virtually to unity to the right. This shape of the curve makes it possible with large confidence to interpolate value E between E=0 with p-p and E=0.2.

Page 32.

Since $p_{кр}$ most strongly depends only on thickness ratio and, furthermore, since change $p_{кр}$ even several times, as is evident from figure, do not exert substantial effect on shape of the curve E(p), then we for all 15o/o of profiles/airfoils extrapolated the curves E to value of E=0 in certain mid-position $p_{кр}$ (broken lines). For profile/airfoil NACA - 0009 dot-dash line is given extreme line with Re_0=0.

The knowledge of capture full of coefficient plays the significant role when it is necessary to determine the total quantity of ice, which grows on wing profile per unit time, for example during calculations of the necessary power for the thermal deicers.

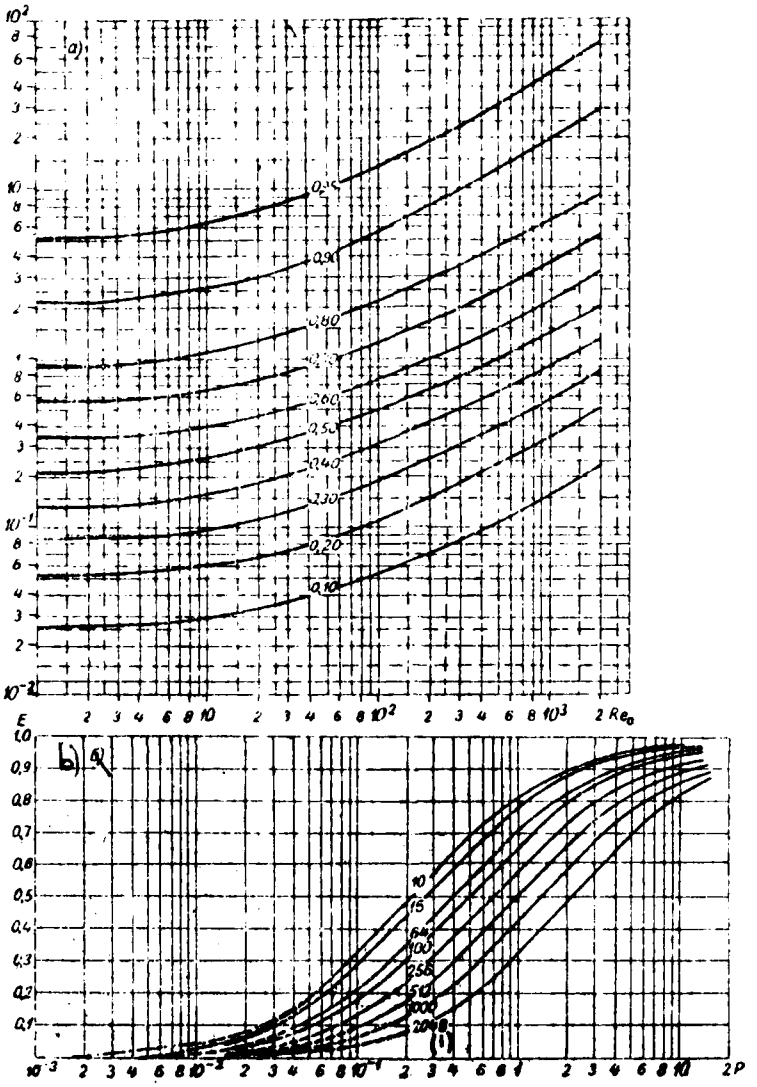

Fig. 8. a) The isolines of the capture E full of coefficient for wing profiles/airfoils with a thickness ratio of from 9 from 15o/o, b) the dependence of the capture E full of coefficient from parameters p and Re_0 (number by the curves) for wing profiles in thickness ratio from 9 to 15%.
Key: (1) V.

Page 33.

But in a whole series of the cases considerably larger value has knowledge of the icing intensity of the spout of the wing of aircraft, determined by the local coefficient of capture E_0. Unfortunately, we have available the considerably scantier information about the values of coefficient of E_0 in comparison with the data about the complete coefficient of capture.

In this connection it was represented by advisable to supplement existing knowledges with calculations for the asymmetric 15-percent profile/airfoil NACA-2215, lying at the root section of the plane of aircraft LI-2. The greatest difficulty is obtaining velocity fields around this nonanalytic profile/airfoil, i.e. the solution for this duct/contour Neumann's problem. For solving this problem we used known electrohydrodynamic analogy and as first approximation accepted the values of velocity fields, obtained on a simple electrical integrator of Elie's-12 type. Subsequently, after the series/row of smoothing and obtaining of the 2nd and 3rd approximation/approach by hand, with net point method, was constructed the potential field of

speeds, and thereupon the isolines of the equal horizontal and vertical velocities.

The trajectories of drops were obtained according to the method, described above (page 23 and further). For determining of E_0 were calculated the trajectories of drops of which one coincided at infinity with the extended chord of profile/airfoil, and two others (also at infinity) were located on both sides from it at a distance, equal to 0.005 from the chord length of profile/airfoil.

Accuracy obtained in this case in determination of E_0 is approximately/exemplarily equal to 10-15o/o.

All in our possession information about the local coefficient of capture in the spout of profile/airfoil E_0 is plotted/applied in Fig. 9.

As can be seen from figure, we have available a considerably smaller quantity of data about dependence of E on parameters p and Re_0 and not in state not for one profile/airfoil to construct sufficiently detailed diagrams. However, already on the basis of the available data it is possible to draw the conclusion that E_0 little depends on parameter Re_0. Therefore virtually for calculation E_0 in 15-percent profiles/airfoils it is possible to use dash curve (Fig.

9) without depending on value of Re_0. Error allowed in this case will hardly exceed 20o/o at very low values of E_0.

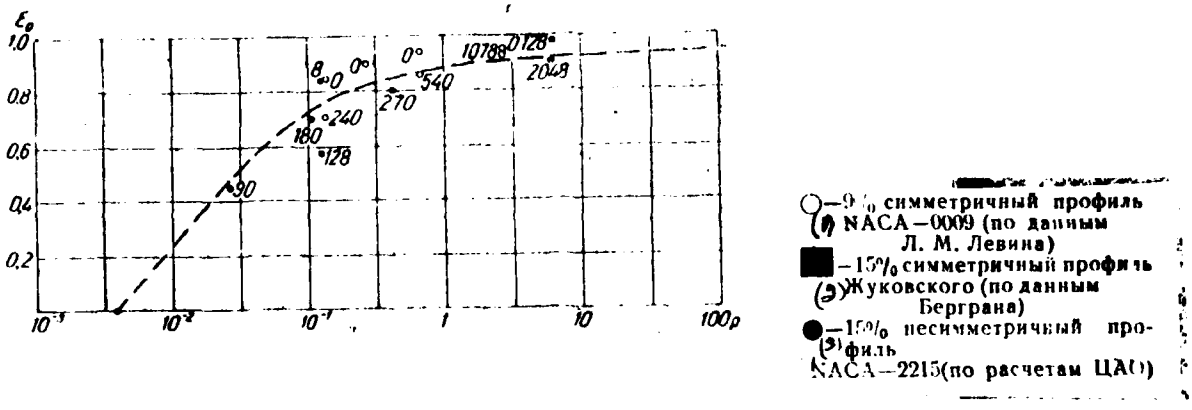

Fig. 9. The dependence of the local coefficient of capture E_0 in the spout of profile/airfoil on parameter p (numerals showed Reynolds numbers).

Key: (1). 9o/o the symmetrical profile/airfoil NACA-0009 (on Levin, these l. M.). (2). 15o/o symmetrical Zhukovskiy profile (according to Bergran's data). (3). 15o/o curved profile NACA-2215 (according to calculations by TsAO [Central Aerological Observatory]).

Chapter II.

AERODYNAMICS OF THE FLOW AROUND BODIES OF THE FLOW OF THE POLYDISPERSE AEROSOL.

1. Generalization of the concept of coefficient, capture.

Connection/communication of the coefficients of capture E and E_0 examined in the preceding/previous chapter with parameters p and Re_0 means that, other conditions being equal, they depend on a radius of drops r. Any cloud, however, consists of the drops of different sizes/dimensions, in other words, any real cloud is polydisperse.

To simultaneous account both aerodynamics of the flow around bodies of water drops and the polydispersion of cloud, it is possible to generalize the concept of the coefficient of capture and to introduce the so-called integral coefficient of the capture which we will designate in contrast to usual with wavy line above. Under the integral coefficient of capture $\tilde{E}$ we will understand the ratio of a quantity of water depositing on body to that which would settle in the absence of the effect of flow, i.e.

$$\tilde{E} = \frac{\int_0^{\infty} \frac{4}{3}\pi r^3 n(r) E(r) \rho_{\text{л}}\, dr}{\int_0^{\infty} \frac{4}{3}\pi r^3 n(r) \rho_{\text{в}}\, dr} = \frac{1}{w}\int_0^{\infty} \frac{4}{3}\pi r^3 n(r) E(r) \rho_{\text{в}} \cdot dr. \qquad (2.1)$$

However, by analogous form is determined the local integral coefficient of capture $\tilde{E}_{\text{л}}$. With the aid of function $\widetilde{E_1}$ the intensity of ice accumulation in any section of body will be written in the form

$$I = \frac{w}{\rho_{\text{л}}} u_{\infty} \tilde{E}_{\text{л}} \beta \text{ см/сек.} \qquad (2.2)$$

For determining the integral coefficients of capture whose knowledge is necessary during the construction of the quantitative theory of icing, should be known not only functions E(r) and $E_{\text{л}}$ (r), but also spectral distribution of cloud drops according to sizes/dimensions, i.e. function n(r).

2. The spectral distribution of cloud drops according to sizes/dimensions.

The diversity of factors and the complexity of the processes, which participate in the formation of clouds,, until now, did not make it possible to create the sufficiently completed theory, giving the possibility to determine the form of the function n(r). Therefore now our information rests only on experimental material. Before converting/transferring to survey/coverage and analysis of this

material, let us pause briefly at some fundamental questions, connected with the accumulation of material itself.

Page 35.

Cloud is the kind of aerosol and consists of a large number of drops, weighed in air. A number of drops into 1 cm^3 of air oscillates from ten to hundred. Thus, if we compare between themselves different, even adjacent parts of the cloud, then the density of spectral distribution in them is different. This difference is greater, the less the volumes. So, if we take the volume, equal to 1 mm^3, then it is possible that in it not at all will prove to be drops and then $n(r)=0$, but if this volume hits only one drop with a radius of r, then $n(r)$ will be expressed by delta function - $\delta(r)$. Arises the question, such as volume of air should be accepted for standard for determining the spectral distribution of drops in cloud. Some works in this region conducted in GGO P. V. D'yachenko as early as 1950 [5].

Mathematically a question can be formulated as follows.

Let us examine entire cloud as certain general population of drops, and a quantity of the measured drops N as certain selection from this totality. It is clear that in comparison with N the total

number of drops of the general population can be considered equal to infinity. It requests itself, if we consider that all drops are agitated in cloud randomly, how must be a number of drops in selection N in order with the assigned accuracy to describe entire general totality? Without stopping on the solution of stated problem, which would take away us beyond the framework of the present investigation, let us point out only immediate conclusions from its setting itself.

It is obvious that the greater N, the more precise one selection will transfer the general population. The accuracy of the determination of a radius or the drops of the greatest recurrence from the laws of mathematical statistics is proportional $\frac{1}{\sqrt{N}}$ [29]. Thus, for obtaining the correct representation about a radius of the drops of the greatest recurrence with the error more several percentages (during random mixing) it is necessary that N would be order of tens of thousands, i.e. volume was on the order of 100 cm^3.

For the catching of drops serve the plates, covered with oil or fume. The size/dimension of drops is determined with the aid of microphotography/micrographs. A quantity of measured drops on each frame in this case can reach several hundred, which corresponds to the volumes of the order of cubic centimeters. The determination of average sizes of drops from the method of multicylinders

corresponds to the volumes of the order of cubic meters and more. For obtaining the sufficiently representative data about the distribution of cloud drops according to sizes/dimensions by the method of microphotography/microphotograph it is necessary to take several tests/samples to plates and with each to produce on 2-3 photographs.

All most important works on the study of the microstructure of droplet clouds both in our country and abroad they were based on the principle of the taking of the samples of cloud drops with the fact or by another instrument as receiving part which served the microscope slide, covered with oil or fume. Spectrum determined thus of the sizes/dimensions of cloud drops differs from real because of the series/row of the systematic errors, characteristic to this method. Most essential deflection from the true spectrum causes the flow around air intakes of cloud drops, due to what is lost the large part of the small/fine drops. Researchers' majority either did not completely turn attention to this fact or it was limited to indication of it, without introducing the necessary corrections.

Page 36.

In connection with this it was represented by necessary in more detail to examine the errors, characteristic to the air intake of the system of TsAO and to calculate the necessary corrections. In work

[32] was given the detailed analysis of possible errors and were determined these corrections. Fig. 10 gives the graph/curve which makes it possible to find the value of correction factor $\alpha(r)$ depending on a radius of drops r. Thus, a true number of drops of the given radius n(r) was defined as the product of a number of grasped drops $n_{\text{изм}}$ on $\alpha(r)$.

Thus were finished stock, obtained during flights on an aircraft of the type LI-2 in in the period from 1949-1954 . Within this time by the group of the colleagues of the laboratory of the cloud investigations by TsAO under A. M. Borovikov's management/manual were studied hundreds of different clouds and were produced tens of thousands of microphotography/microphotographs of the separate tests/samples of cloud drops [3]. This material most in detail and fully describes cloud microstructure of the laminar forms both air-mass ones and frontal ones. Let us note that precisely the clouds of laminar forms are of greatest interest in the examination of the problem of icing, since they most frequently are encountered during flights.

The analysis of the materials of TsAO taking into account the corrections examined above showed that in all cases the experimental data are depicted sufficiently well as the formula of the form

$$n(r) = ar^2 e^{-br}. \qquad (2.3)$$

Formula (2.3) was initially proposed as early as 1951 [31]. It was compiled on the basis of A. M. Borovikov's data, obtained by it during the years 1948-1950. In the same year Best [46] proposed another formula

$$1 - F(x) = e^{-(x/a)^k}, \qquad (2.4)$$

where F(x) - the accumulated mass of water, i.e. portion of general/common/total liquid-water content, containing in drops by the diameter smaller than x, a and k - constant.

Finally, in 1954 L. M. Levin [12] found that the lognormal distribution so very describes well the experimental data about the distribution of drops according to sizes/dimensions.

Levin's formula takes the form

$$n(x) = \frac{1}{\sigma\sqrt{2\pi}\,x} e^{-\left[\ln \frac{x}{x_0}\right]^2 / 2\sigma^2}. \qquad (2.5)$$

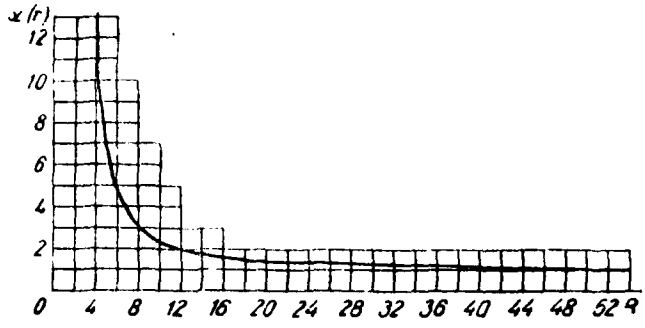

Fig. 10. Correction curve to the network air intake of drops.

Page 37.

After examining in detail all mentioned formulas, we arrived at the conclusion that they approximately/exemplarily equally correspond to experimental data. Large simplicity of formula (2.3) in comparison with (2.4) and (2.5) with approximately the same accuracy forced us to prefer it during practical calculations.

In formula (2.3) coefficients a and b can be expressed through liquid-water content w and average/mean (arithmetical) radius of drops r_{cp}.

Actually/really,

$$r_{cp} = \frac{\int_0^\infty rn(r)\,dr}{\int_0^\infty n(r)\,dr} = \frac{\int_0^\infty r^3 e^{-br}\,dr}{\int_0^\infty r^2 e^{-br}\,dr} = \frac{3}{b},$$

$$w = \int_0^\infty \frac{4}{3}\pi r^3 \rho_в \cdot n(r)\,dr = \frac{4}{3}\pi a \rho_в \int_0^\infty r^5 e^{-br}\,dr = \frac{4}{3}\pi a \rho_в \frac{5!}{b^6}$$

and, therefore,

$$n(r) = \frac{3^7}{4\pi \cdot 5!}\frac{w}{r_{cp}^6 \rho_в} r^2 e^{-3r/r_{cp}} = 1{,}45\frac{w}{r_{cp}^6 \rho_в} \cdot r^2 e^{-3r/r_{cp}}. \qquad (2.6)$$

The investigation of microstructure showed that the spectra of the distribution of drops in cloud were subjected to considerable oscillations/vibrations. Furthermore, it was explained that the spectra, constructed on the data about the sizes/dimensions of several hundred drops, which corresponds to volume on the order of 1 $см^3$, cannot correctly characterize cloud microstructure: for this are necessary in each case tens of thousands of drops.

It must be noted that due to some deficiencies/lacks in the technique of experiment - the loss of small/fine drops - formula (2.6) was actually obtained on the cut spectrum of drops, by a radius it is more 4μ. For radii $r<4\mu$ this formula can prove to be insufficient precise; however, the contribution of the appropriate fine drops to liquid-water content and is respectively into icing very small.

After feeding results to the many-year observations of TsAO, it proved to be possible to come to the conclusion/output that on the average cloud microstructure of laminar forms differs little one from another, i.e. that values r_{cp} in them are very close. The large oscillations in r_{cp} can be observed in isolatedes cloud of one and the same type depending on their phase state, presence or absence of residues/settlings, relative height/altitude in cloud and so forth, etc. These differences are greater than the difference between averaged values r_{cp} for clouds St, Sc, Ns and Ac. However, available statistical material did not make it possible thus far to more deeply trace the dependence of microstructure on separate factors. Table 2 given here characterizes mean radius r_{cp} in clouds of the type St, Sc, Ns and Ac, moreover clouds of the type St and Sc are illuminated somewhat in more detail - entire/all thickness of these clouds is broken into 3 layers: lower, average and upper. As one would expect, cloud drops in proportion to removal from lower cloud base are enlarged in accordance with previously known materials [3]. However, let us note that in the quite upper boundary where actually occurs the evaporation of cloud, r_{cp} can prove to be noticeably the less corrected values. The same is related also to lower boundary.

The extensive studies of cloud microstructure were carried out also in the USA under V. Lewis's guidance.

Some results of these works are given in table 3. Data are borrowed from the shape of khaulon [59].

In order to compare these data with results obtained by us, let us note that on the basis of formula (2.6) the median diameter of drops by volume $d_м = 2 \cdot 1{,}53\, r_{ср}$. In table 3 to the right $r_{ср}$ is designed on this relationship/ratio, i.e. $r_{ср} = \frac{d_м}{2 \cdot 1{,}53}$. Lewis's data completely satisfactorily will agree with our results. In V. Lewis's article [65] is given the detailed table of the repetition frequency of the different values of the mean effective diameters of drops depending on the type of cloudiness. We do not give here this table, since in the article it is not said, which is understood under mean effective diameter.

Since sometimes according to the data of TsAO $r_{ср}$ it oscillated in considerable limits - from 2.5 to 9 μ, subsequently all calculations were performed through formula (2.6) for the range of change $r_{ср}$ within the limits from 2 to 10 μ.

Table 2.

(1) Характеристика облаков	$r_{ср}$ (2) в μ
(3) Нижняя треть слоистых облаков	3,0
(4) Средняя треть слоистых облаков	4,2
(5) Верхняя треть слоистых облаков	5,3
(6) Слоистые облака в среднем (St)	5,0
(7) Нижняя треть слоисто-кучевых облаков	4,0
(8) Средняя треть слоисто-кучевых облаков	4,8
(9) Верхняя треть слоисто-кучевых облаков	5,5
(10) Слоисто-кучевые облака в среднем (Sc)	5,0
(11) Слоисто-дождевые облака (Ns)	5,0—7,0
(12) Высоко-кучевые облака (Ac)	4,5—5,0

Key: (1). Characteristic of clouds. (2). in. (3). Lower third of stratus. (4). Average third of stratus. (5). Upper third of stratus. (6). Stratus on the average. (7). Lower third of stratocumulus clouds. (8). Average third of stratocumulus clouds. (9). Upper third of stratocumulus clouds. (10). Stratocumulus clouds on the average. (11). nimbostratus clouds. (12). Altocumulus clouds.

Table 3.

(1) Форма облаков	$d_м$	(2) Диапазон диаметров капель	$r_{ср}$
(3) Кучевые	20,5 μ	3—56 μ	5,65 μ
(4) Слоистые	14,7 μ	3—50 μ	4,05 μ

Key: (1). Cloud form. (2). Range of diameters of drops. (3). Cumulus. (4). Laminar.

FOOTNOTE 1. $d_м$ - median diameter of drops by volume, i.e. in drops with a diameter of $d < d_м$ is contained as much water, as in drops from $d > d_м$ ENDFOOTNOTE.

Page 39.

3. Liquid-water content of supercooled clouds.

Water content of clouds - a quantity of condensed water, which is contained per unit of volume of air - is another important factor, which substantially affects icing intensity.

In the examination of the problem of icing basic interest are of the clouds of the laminar forms, to which was turned great attention during the investigation of microstructure. Most completely in our literature a question about water content of clouds of laminar forms was studied by V. Ye. Minervin in combined expeditions.

It is known that the liquid-water content, as microstructure, is subjected to considerable oscillations/vibrations. Instruments, that measure liquid-water content during several seconds, in which the drops recover from the volume of order of tens of cubic decimeters

AD-A083 374 FOREIGN TECHNOLOGY DIV WRIGHT-PATTERSON AFB OH F/G 1/3
PHYSICAL BASES OF AIRCRAFT ICING,(U)
AUG 79 I P MAZIN
UNCLASSIFIED FTD-ID(RS)T-1161-79 NL

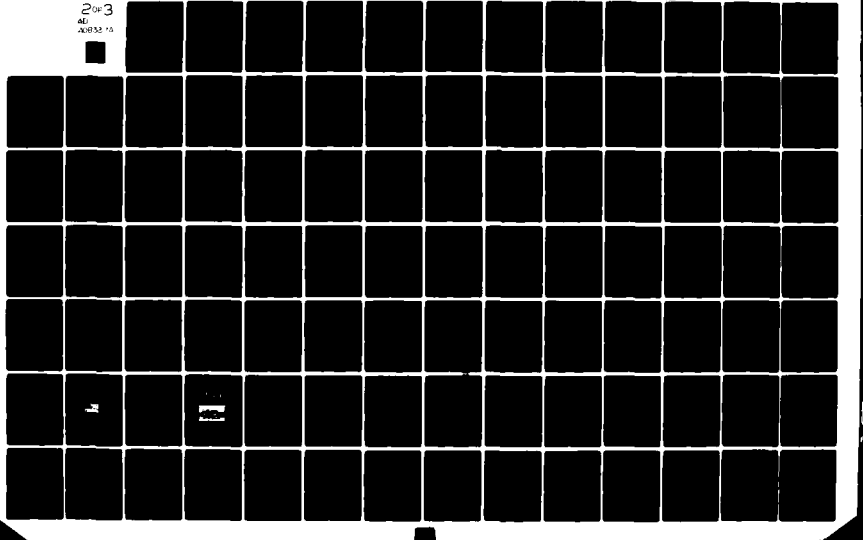

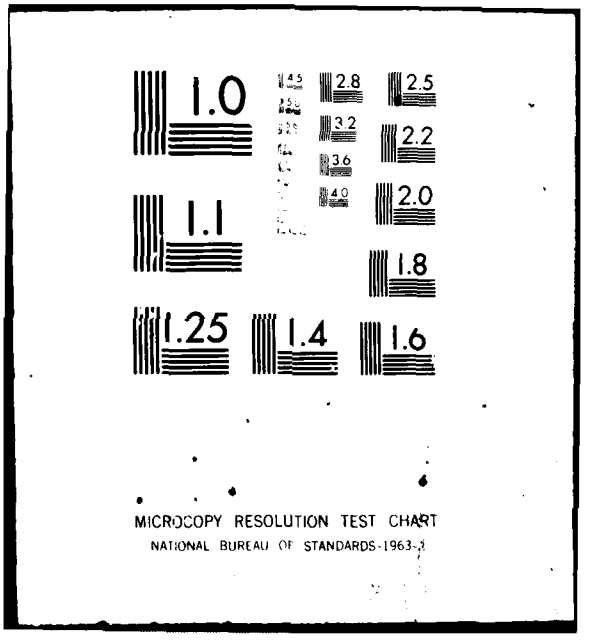
1.0
2.8
2.5
3.2
2.2
3.6
4.0
2.0
1.1
1.8
1.25
1.4
1.6
MICROCOPY RESOLUTION TEST CHART
NATIONAL BUREAU OF STANDARDS-1963-A

(instrument of Zaytsev [6] or Vonnegat [80]), indicate that it can change from one reading to the next to ten and even hundreds of percent. This means that in order to compose correct representation about average/mean water content of clouds, it is necessary to measure a quantity of the drop-forming water in volumes, hundreds times greater than this is required for a microstructure.

In the problem of fading there is the greatest interest in the knowledge of the values of the liquid-water content, averaged on the large sections, equivalent by volume 0.1-1 m^3 and by the extent of the order of kilometers. The method of ice-settling cylinders, widely utilized in American investigations and used by V. Ye. Minervin, gives precisely the same averaged values of liquid-water content. With examination of average/mean (but not extreme) values, naturally, it is possible to utilize the data, obtained by other instruments.

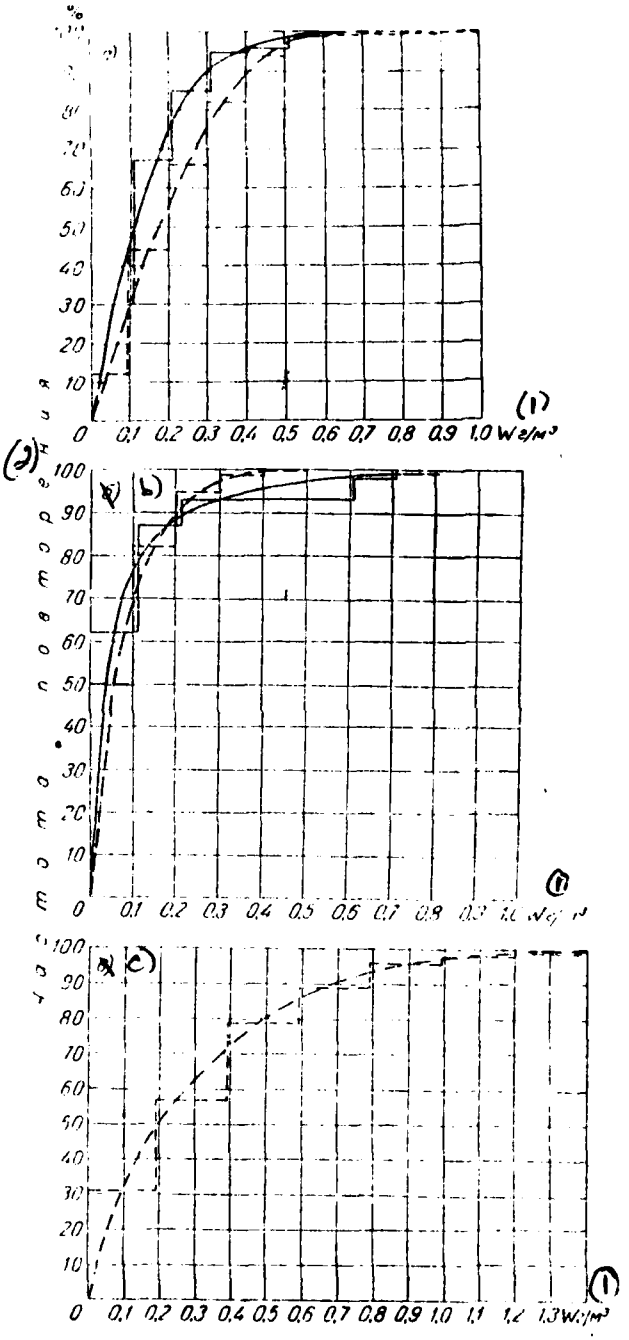
a)
80
70
60
50
40
30
20
10
0
0,1 0,2 0,3 0,4 0,5 0,6 0,7 0,8 0,9 1,0 W/m²
(1)
(2)
b)
100
90
80
70
60
50
40
30
20
10
0
0,1 0,2 0,3 0,4 0,5 0,6 0,7 0,8 0,9 1,0
(1)
c)
100
90
80
70
60
50
40
30
20
10
0
0,1 0,2 0,3 0,4 0,5 0,6 0,7 0,8 0,9 1,0 1,1 1,2 1,3 W/m²
(1)

Fig. 11.

Fig. 11. Curves of the accumulated repetition frequencies of liquid-water content for the clouds of the various forms: a) St, Sc - on Minervin of 100 cases (solid line), according to Lewis 372 cases (broken line), b) Ac, As - on Minervin of 16 cases (solid line), according to Lewis 264 cases (broken line), c) CU, Cb according to Lewis 324 cases.

Key: (1). g/m³. (2). Repetition frequency.

Page 40.

For our purposes it is more convenient entire to present data on liquid-water content in the form of the so-called graphs/curves of the accumulated repetition frequencies (Fig. 11), in which along the axis of abscissa are deposited/postponed the values of liquid-water content, and along the axis of ordinates - a number of cases in percentages, when liquid-water content did not exceed the assigned value. Both the data, borrowed from Lewis's article, and these of Minervin are obtained with the aid of ice-settling cylinders the time of exposure of which in the process of measurements oscillated from 1-2 to 10 min.

The results, given in Fig. 11, in each case are based according to V. Lewis approximately/exemplarily on 300 observations, on

Minervin in the case of St-Sc - in 100 observations, in As-Ac - in 16 observations. In spite of comparatively small statistics, on the basis of these graphs/curves it is evident that for the clouds of laminar forms a number of cases with liquid-water content w>0.5 g/m^3 does not exceed several percentages, and maximum values virtually do not exceed 1 g/m^3.

On data given L. T. Matveyev and V. S. Kczharin [1], the average/mean values of the liquid-water content of stratus even are less than obtained by V. Lewis and V. Ye. Minervin.

FOOTNOTE [1]. Proceedings of the Academy of Sciences of the USSR series geophysical, No 11, 1956. ENDFOOTNOTE.

In convective clouds liquid-water content on the whole noticeably greater - approximately/exemplarily into 20o/o of cases it exceeds 0.5 g/m^3, while into 2-3o/o - is above 1 g/m^3.

This conclusion/output, based on V. Lewis's data, qualitatively coincides with V. A. Zaytsev's results [6]. Large water content of clouds CU, according to V. A. Zaytsev, is caused by the fact that its measurements are related to more warm, summer clouds.

Summing up the numerous experimental investigations of water

content of clouds [6, 15, 65, 59] and their microstructure [3, 12, 34, 59, 65], it is possible to say the following relative to the droplet clouds of the laminar forms:

1. And liquid-water content and average sizes of drops can vary noticeably both for by one and the same of cloud form and in one and the same cloud.

2. In proportion to lift from lower cloud base both liquid-water content and sizes/dimensions of drops usually gradually grow/rise and only near quite upper cloud boundary sharply they decrease.

3. On the average of noticeable difference in cloud microstructure of laminar forms (St and Sc) it is impossible to reveal/detect.

4. With temperature decrease average/mean values of liquid-water content decrease.

4. Calculation of the integral coefficient of capture.

The introduced above integral coefficient of capture was determined by the expression

$$\tilde{E} = \frac{\rho_w}{w} \int_0^\infty \frac{4}{3} \pi r^3 n(r) E(r) dr. \qquad (2.7)$$

Thus, the integral coefficient of capture can be found, if is known the spectral distribution of cloud drops according to sizes/dimensions of n(r) and of the dependence of the coefficient of capture on the sizes/dimensions of drops E(r).

Substituting in equality (2.7) expression (2.6) for function n(r), let us have

$$\tilde{E} = \frac{3^6}{5! r_{cp}^6} \int_0^\infty r^5 e^{-3r/r_{cp}} \cdot E(r)\, dr. \qquad (2.8)$$

During the calculation of the intensity of ice accumulation in any section of body analogously is determined the local integral coefficient of capture $\tilde{E}_A$.

Page 41.

The coefficients of capture both complete E, and local E_A depend not only on the form of body, but also on its sizes/dimensions and speed of motion. Thus, the integral coefficients of capture for the body of the assigned form depend on three parameters: r_{cp} - characterizing the spectrum of the sizes/dimensions of cloud drops, C - certain significant dimension of body and u_∞ - flight speeds.

On the basis of the results of calculations E and E_A in 3 sections of chapter I and from that fact that the coefficient of capture can be considered virtually independent of the form of

profile/airfoil, if its thickness ratio is included between 9 and 15o/o (range of the profiles/airfoils which actually are encountered in cargo fleet), were calculated dependence of $\bar{E}$ on r_{cp}, chord lengths of profile/airfoil C and flight speed u_∞ In this case the range of velocity change ranged from 50 to 100 m/s, chord lengths of profile/airfoil from 1 to 400 cm and mean radii of cloud drops in limits from 2 to 10μ. The results of calculations are represented in the form of the corresponding diagrams in Fig. 12.

During the calculation of the integral local coefficient of capture in the spout 15o/o profile/airfoil E_0 the problem somewhat is simplified, since in the first approximation, it is possible not to consider dependence of E_0 on Reynolds number Re_0.

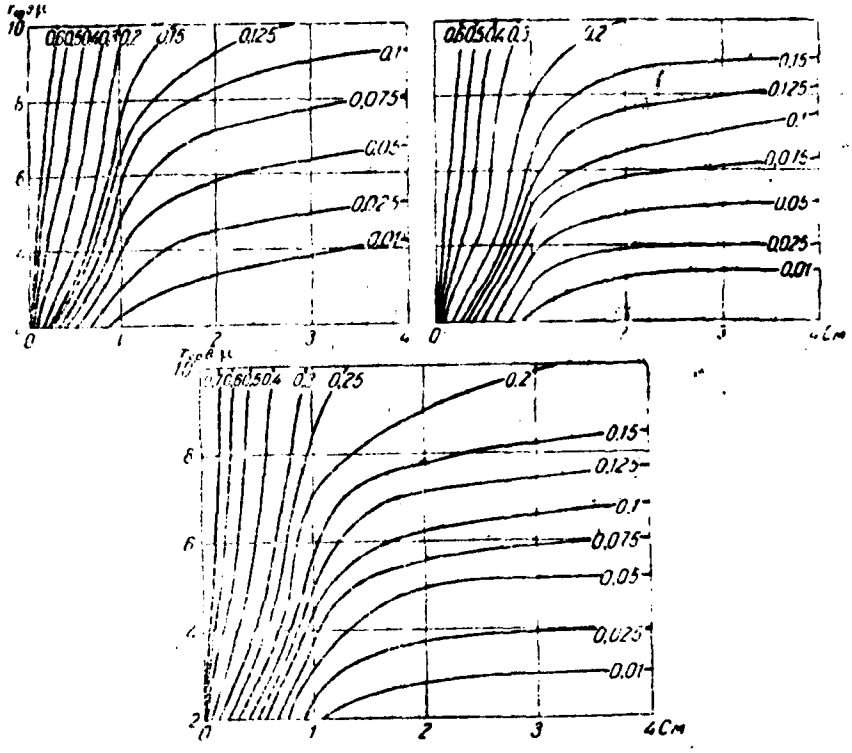

Fig. 12. Isolines of the complete integral coefficient of the capture of the aircraft profile/airfoil: a) u_∞ =50 m/s, b) u_∞ =75 m/s, c) u_∞ =100 m/s.

Page 42.

In this case of E_0 depends only on two parameters - r_{cp} and u_∞/C, however for convenience the final results of calculations are represented also in the form of diagrams (Fig. 13), in which is given dependence of $\widetilde{E_0}$ on r_{cp} and C at three values of speed u_∞.

It should be noted that dependence $\widetilde{E}_0$ only from two parameters r_{cp} and u_∞ / C makes it possible to more easily simulate the conditions of icing when us interests the intensity of ice accumulation on the spout of aircraft profile/airfoil.

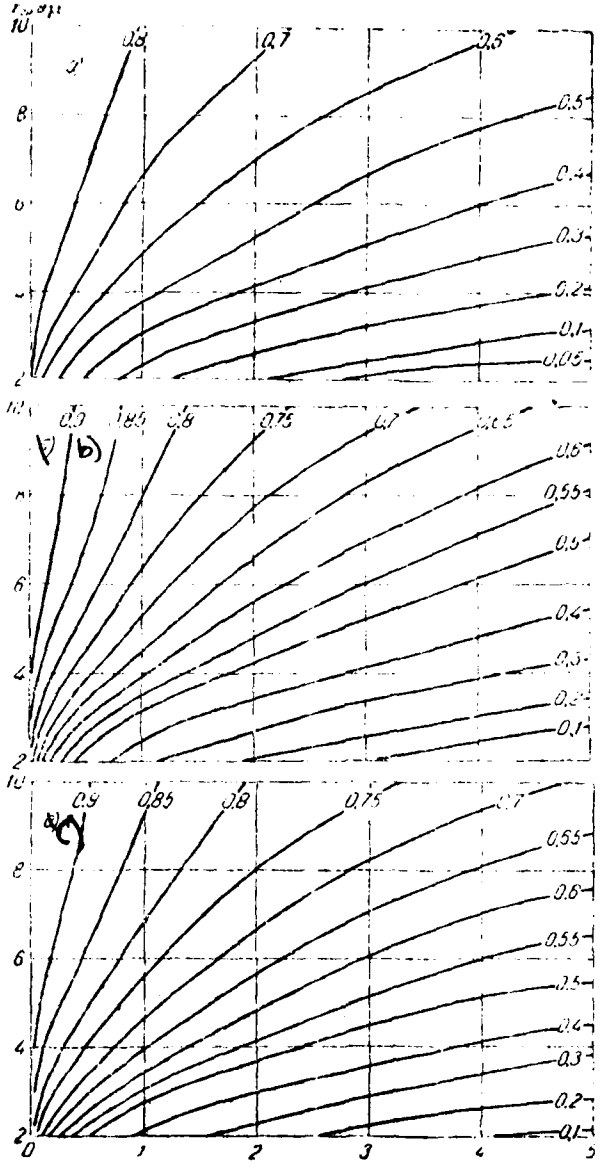

Fig. 13. Isolines of the local integral coefficient of capture in the nose/leading edge of the aircraft profile/airfoil: a) u_∞ =50 m/s, b) u_∞ =75 m/s, c) u_∞ =100 m/s. Along the axis of abscissas is deposited/postponed the chord length of profile/airfoil C m.

Page 43.

5. Connection/communication of intensities of icing of different aircraft components.

The dependence of the integral coefficient of capture on the sizes/dimensions of profile/airfoil and its form explains the well known fact of different icing of the different parts of aircraft. It suffices to say that the icing intensity flight aerologist's template/pattern can be almost three times of more than the icing intensity of the wings of aircraft. In this connection does arise the question - icing of what aircraft components one should accept as characteristic ones for the comparison with each other during flights under varied conditions? For example, in the Main Administration of the Hydrometeorological Service as standard is accepted the special template/pattern, established/installed in flight aerologist's window, in GVF usually is examined rate of icing of plane, etc. Furthermore, does arise another question, it is possible, knowing the icing intensity of one part, to judge about the icing intensity of another and that for this necessarily?

For a response/answer to these questions we return to expression (2.2), which is determining the icing intensity of body, and let us supply with index "E" of the values, which relate to certain by us to the standard

$$I_э = \frac{w}{\rho_{жэ}} u_{\infty} \beta_1 \tilde{E}.$$

Value β is the function of many variable/alternating, including speed of motion, water content of clouds, temperature and other factors. The value of the coefficient of capture $\tilde{E}$ depends on form and sizes/dimensions of the icing up body, spectrum of the sizes/dimensions of cloud drops and flight speed. On many factors depends $\tilde{E}$.

Therefore, it would seem, it cannot be obtained sufficiently simple method of determination from $\tilde{E}$ the icing intensity I of any another part. However, we investigate this question more attentive. It is easy to see that

$$I = I_э \frac{\rho_{жэ}}{\rho_ж} \frac{\beta}{\beta_1} \frac{\tilde{E}}{\tilde{E}_э}. \qquad (2.9)$$

The posed problem considerably will be simplified, if we place value $\frac{\rho_{жэ}\beta}{\rho_ж \beta_1}$ of the equal to unity. This assumption as this will be shown in Chapter III, in essence it is correct for cargo fleet ($u_\infty \leqslant 360$ km/h) with temperatures below - 5°. With too great liquid-water contents this assumption is not disrupted to -3° and

only at higher temperatures deflections from unity can become are sufficiently perceived.

With that made assumption of expression (2.9) substantially is simplified in it takes the form

$$I = I_0 \frac{\tilde{E}}{\tilde{E}_0}. \qquad (2.10)$$

Let us recall that

$$\tilde{E} = \frac{3}{50 r_{cp0}^6} \int_0^\infty r^5 e^{-3r/r_{cp}} \cdot E(r)\, dr.$$

Page 44.

If the values of the coefficients of capture E(r) were not changed in the process of icing, then for the selected standard and the part being investigated relation $\tilde{E}/\tilde{E}_0$ would be function only r_{cp} and, with the known structure of clouds, easily it would be determined from the relationship/ratio

$$I = I_0 \cdot F(r_{cp}).$$

So that the form of standard less possible would be changed in the process of icing, we selected the rotating cylinder. The diameter of cylinder had to be sufficient to large ones so that not strongly had to be large enough that on it would deposit the noticeable portion of cloud drops. As optimum, in the best way corresponding to the presented requirements, there was selected a cylinder with a

diameter of 5 cm. The instrument, as receiving part which serves the cylinder which rotates by 50 mm, was designed in NII [Scientific Research Institute] GMP by M. Ye. Azbel.

To strictly consider change $\tilde{E}$ in the increase of ice is not impossible. However, for such large bodies as the wings of aircraft, hardly should be expected the large changes $\tilde{E}$ in the process of icing, since the thickness of the layer of ice is too small in comparison with the sizes/dimensions of wing. Moreover, hardly should be expected the large changes $\tilde{E}$ in the build-up/growth of ice and for the series/row of other, too fine details of aircraft until grown ice changes significantly their form.

Taking into account the fact that the water, which deposits on the forward section of the cylinder, because of rotation is distributed all over surface of the latter, equation (2.10) should be written in the form

$$I = I_0 \frac{\pi \tilde{E}_A}{\tilde{E}_0}, \qquad (2.11)$$

where $\tilde{E}_A$ - local coefficient of capture in the position of aircraft which interests us, and $\tilde{E}_0$ - complete coefficient of capture for the cylinder with a diameter of 50 mm.

Relationship/ratio (2.11) is especially valuable when we want by standard to determine the intensity of ice accumulation on the spout of the wing of aircraft, since to measure directly the icing intensity of the plane or aircraft is extremely difficult. At the same time the icing of planes is the basic reason for deterioration in aerodynamic aircraft quality/rineness ratics.

After calculating dependence $\bar{E}$, on r_{cp} for flight speeds on 50, 75 and 100 m/s [1] and utilizing the results of calculations E_0, represented in Fig. 13, was found the dependence of conversion factor (SIO - profile/airfoil) from parameter r_{cp} and chord length of profile/airfoil C for the same three values of flight speed.

FOOTNOTE [1]. In calculations were accepted $\nu = 0{,}176$ cm^2/s, $\mu = 1.67 \cdot 10^{-4}$ g/cm and diameter of cylinder d=5 cm. ENDFOOTNOTE.

The obtained dependence is represented in Fig. 14.

Page 45.

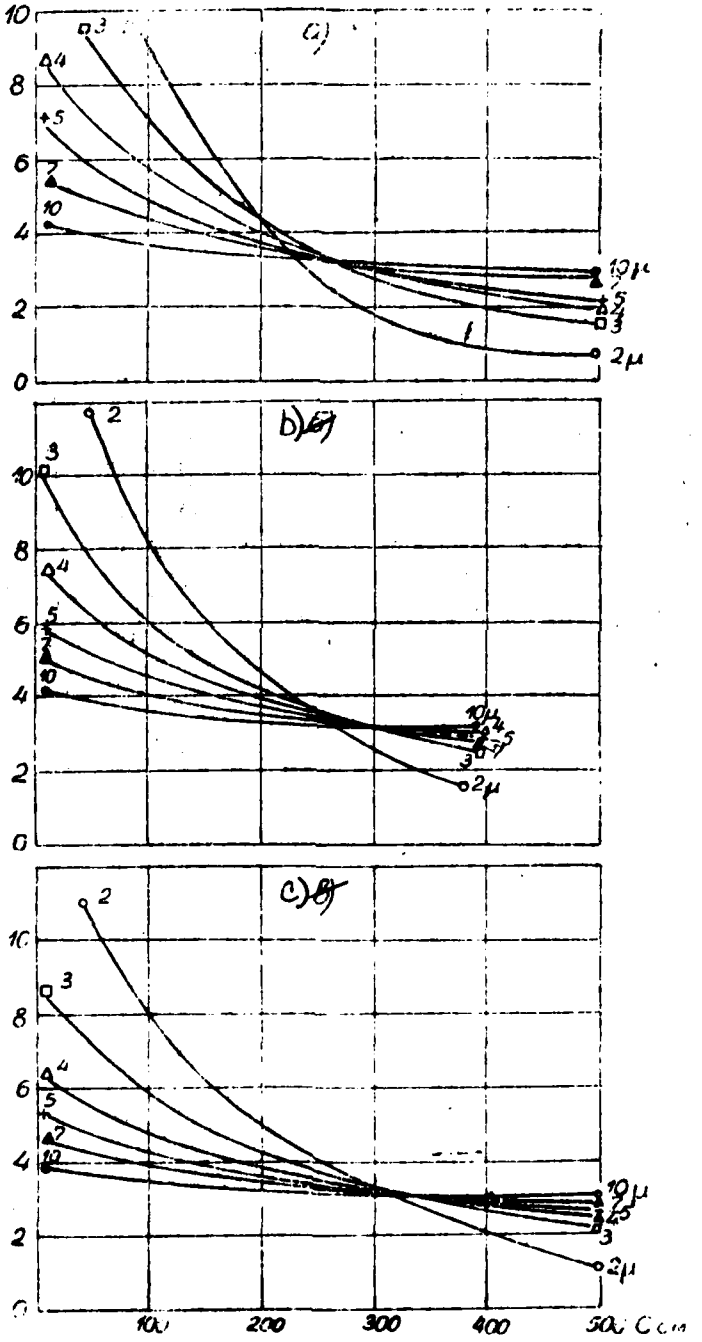

Fig 14.

Fig. 14. Connection/communication of conversion factor from icing intensity of standard (SIO) to icing intensity of plane in its frontal part with a chord length of profile/airfoil of C and spectrum of cloud drops r_{cp} (number by curves): a) u_x =50 m/s. b) u_x=75 m/s and c) u_x =100 m/s. Along the axis of ordinates are given the values of coefficient $\approx \frac{\tilde{E}_u}{\tilde{E}_3}$

Page 46.

The analysis of curves in Fig. 14 leads to very interesting conclusion about the fact that at the chord length of profile/airfoil from 2.8 to 3.2 m the conversion factor from /, to I profile/airfoil virtually remains constant, oscillating approximately/exemplarily to 10o/o about its average/mean value of 3.1 with a change in the flight speed from 50 to 100 m/s and mean radius of drops from 3 to 10.

The fact that the conversion factor in the examined case proved to be little depending on the type of clouds (r_p) and from speed fluctuations within limits of 200 to 350 km/h, gives the possibility of introducing permanent conversion factor for determining the icing intensity of the plane or contemporary transport aircraft of the type LI-2 and Il-12 in its center section (C=3 m). This conversion factor is equal to ~~3. In chapter IV it is shown that the practice confirmed the obtained conclusions.

Utilizing formula (2.11), it is possible to also design the general/common/total mass of ice depositing for plane. For this it is necessary $\tilde{E}_1$ to replace with the complete integral coefficient of capture $\tilde{E}$ and to multiply the obtained result for the area of the midship section of plane.

Then, whereas analogously utilizing curves in Fig. 12 for determining of $\tilde{E}$, it is easy to find values $\frac{\pi\tilde{E}}{\tilde{E}_0}$ and, knowing l_1 and the area of the midship section of plane, to determine the general/common/total mass of ice, deposited to plane.

Chapter III.

ROLE OF THE PROCESSES OF HEAT EXCHANGE IN AIRCRAFT ICING.

1. Coefficient of freezing (general/common/total relationships/ratios).

initially during the study of aircraft icing it was proposed that entire falling on aircraft water freezes at the moment of collision with its surface. However, to researchers it was always it is clear that with high temperatures (close to 0°) and at high flight velocities this assumption can be erroneous. Already Ludlam in 1951 [67], estimating the errors of ice-depositing instruments, which measure the liquid-water content and the sizes/dimensions of drops in supercooled clouds, paid serious attention to the possibility of the incomplete freezing of the depositing water.

Let us examine qualitatively the picture of the formation of ice on the surface of aircraft during the collision of the latter with the supercooled cloud or rain drops.

Analyzing the possible reasons, which lead to the freezing of supercooled water on the surface of aircraft, some authors came to the conclusion that it is caused by mechanical jolts, others were considered that the actual reason for the rapid freezing of drops are the ice crystalline particles, which fall to the surface of aircraft [25]. We are inclined to hold the second point of view with that stipulation, that is in no way compulsory the preliminary presence of crystalline particles on surface during the incidence/impingement to it of water drops. Actually/really, on the basis of the fact that the surface of aircraft is always contaminated, hardly one should expect that after the formation/education even very thin film of water its any possible prolonged existence in the supercooled form. Subsequently we will assume that if the conditions of heat exchange on the icing up surface of aircraft provide the diversion/tap of latent heat of freezing, i.e., if taking into account the heat of freezing the equilibrium temperature of surface remains below 0°, that entire water in this case fast enough is crystallized.

For this very reason we consider that a question about the very moment/torque of the beginning of freezing on the wing surface, from the point of view of the problem of icing, does not deserve considerable attention, since after the appearance of supercooled water crystallization begins virtually instantly.

Page 48.

It is interesting to rate/estimate, as will rapidly freeze the droplets of water, which fall to the already iced up surface. This question has large practical interest, since the lifetime of liquid droplets in contact with ice exerts a substantial influence on form and structure of deposited ice. It is necessary to know, does manage drop to freeze before to it falls the following drop or not.

Usually the rate of freezing of ice of the plane of aircraft does not exceed 0.1-0.2 mm/min, i.e., a layer with thickness of 10 μ grows for several seconds. Consequently, if the rate of the freezing of drop (rate of the advance of crystallization front) exceeds 10 μ/s, i.e., 0.001 cm/s, then drops knowingly manage to freeze to the arrival of the following.

Experiment shows that at sufficiently high temperatures of air the rate of the freezing of drop can prove to be less than indicated (which, possibly, and contributes to the formation of rough ice). A precise theoretical solution of the task of determining the rate of the freezing of the depositing water, is normal to the surface of settling, it represents not only not solved, but even clearly not formulated task.

Purely qualitative reasonings lead to the conclusion that the temperature field on the icing up surface takes the sufficiently complicated form. However, from the point of view of the problem of icing the fine structure of the pulsations of temperature on the icing up surface does not represent essential interest, and we therefore will examine certain mean temperature of surface t_s. However, let us note that with an increase in this mean temperature to zero errors they can increase. Until $t_s < 0$, we are assume that freezes entire deposited water, remembering in this case, that an increment in ice per unit time is smaller than a quantity of water depositing for the same time due to the evaporation of the certain fraction of ice. Designating through m, the mass of the water, which deposits per unit of this section per unit time, and through m_i - the mass of the water, which evaporates from the same section for the same time, can be written that the coefficient of freezing β, under which we will understand the ratio of ice frozen per unit time to the mass of those clashing with body for the same time of water drops, is equal to

$$\beta = 1 - \frac{m_i}{m}. \qquad (3.1)$$

With the specific quantity of water, which freezes per unit time per unit of area, the temperature of surface canachieve zero value. Let us designate through $m_{кр}$ a small quantity of water, which encounters the unit of area of aircraft for time unit with which the

temperature of the surface of icing reaches 0°. If a quantity of depositing water is more than $m_{кр}$, then will freeze only the part of it, whereas remaining part must remain in the liquid state. Further fate of nonfrozen water can be different - partially it evaporates from surface, partially is blown away and it is taken away by airflow, it is partially carried by flow to surface out of the zone of the settling where it can freeze, and finally partially water can prove to be within the growing layer of ice in the form of separate inclusions/connections. It is obvious that when $m_в > m_{кр}$ the freezing part of the supplementary (over $m_{кр}$) water is determined by the portion of the "cold", which is contained in this part of the water and, therefore, it is equal to

$$(m_в - m_{кр})(0 - t_0)\frac{c_в}{80},$$

where $c_в = 1$ - heat capacity of water.

It is easy to ascertain that in this case the coefficient of freezing takes the form

$$\beta = 1 - \frac{m_i}{m_в} - \left(1 + \frac{t_0}{80}\right)\left(1 - \frac{m_{кр}}{m_в}\right). \qquad (3.2)$$

Page 49.

Therefore, for the definition of the coefficient of freezing is necessary the knowledge of values as $m_в$, $m_{кр}$, m_i and t_0.

2. Some general information about heat exchange of bodies with gas flow.

Determination $m_{..}$ and $m_{|}$ is connected with the study of the heat balance of the icing up body. At the same time the investigation of heat balance for the surface of the moving/driving body and, in particular, the definition of temperature and the different points of its surface, in the case even if the latter is not moistened, is very complex problem both with the theoretical and with the experimental of the points of view. Most completely questions of heat exchange with the environment are resolved for the bodies of the simplest forms - the flat/plane plates, parallel to flow, and round cylinders. here there is no need for stopping during the examination of numerous works in this region, since in recent years appeared the series/row of the excellent mono-raffias, throwing light on questions of heat exchange during the motion of bodies in gases [1, 2, 4, 7].

We will not be so in detail to describe the achievements of theoretical and experimental studies in this region, but let us pause only at the basic physical representations, placed as the basis of the investigations of heat exchange and on latter/last known to us results.

Most fruitful hypothesis about the mechanism of heat exchange is

the hydrodynamic hypothesis which, actually, already became the theory of heat exchange in gases. The basic idea of this theory is of the affirmation of the identity of the mechanism of heat exchange the direct contact also phenomenon of hydrodynamic drag [4], which are considered as different reflections of a single primary process of substantial exchange. According to this theory displacement/movement and interaction, the elements/cells of medium is an initial cause of the diverse phenomena of exchange.

This theory is completely confirmed by experiment when dissipative terms are negligible, in this case the Prandtl number (Pr), which characterizes the degree of the identity of each process, is equal to one. In this case the temperature of body surface, which moves in the flow of gas, in the absence of heat withdrawal inside body (adiabatic surface) - the so-called adiabatic temperature of body (t_{ad}) - it is set equal to the temperature of stagnation Θ:

$$\Theta = t_0 + \frac{u^2_\infty}{2J\,c_p},$$

where t_0 [1] and u_∞ - respectively temperature and rate of the undisturbed flow.

FOOTNOTE [1]. t_0 they sometimes call thermodynamic, and Θ - is static by temperature. ENDFOOTNOTE.

At steady adiabatic temperature or surface the heat-flux density q is equal to zero. If because of any supplementary processes (for example, to inflow of heat from within) the temperature of surface $t_s \neq \Theta$, heat-flux density $q \neq 0$ and flow it is directed toward surface when $t_s < \Theta$ and from surface when $t_s > \Theta$.

Page 50.

In imperfect gases number Pr is not equal to one, so for air Pr=0.72 and even on adiabatic body surface temperature is not equal to Θ, the part of the energy dissipates because of internal friction. This effect is considered by recovery factor r which is determined by the relationship/ratio

$$r = \frac{t_{ad} - t_0}{\Theta - t_0}, \qquad (3.3)$$

where t_{ad} - real temperature on adiabatic body surface.

Numerical value of coefficient of r, determined on formula (3.3), varies from one point to the next. To study r as to the processes of heat exchange, are dedicated it is multiple investigations on which we also will not stop. Recently in aerodynamics increasing propagation obtains another determination of recovery factor r* [30], according to which $r' = \frac{t_{ad} - t_1}{\Theta - t_1}$, where t_1 - the temperature of the flow on the edge of the boundary layer. With this definition, the determination of r* is comparatively simply - as a rule r* differs little from $\sqrt{Pr}$ and is not changed along profile/airfoil. However,

entire/all difficulty in this case is transferred to the determination of temperature t_1, without knowledge by which it cannot be found r*. Distribution r along the duct/contour of round cylinder can be found in work [4].

Theory shows [4] that all formulas, obtained during the study of heat exchange at the low speeds or motion, remain valid and for high rates, if the temperature of medium is is replaced with the temperature of adiabatic wall $t_{ад}=t_0+\frac{ru_\infty^2}{2Jc_p}$. Thus, if because of some supplementary processes the temperature of body t_s is different from adiabatic, then there is heat flow to surface, equal to

$$q_1=-\alpha(t_s-t_{ад}), \qquad (3.4)$$

where α - a heat-transfer coefficient.

Actually, relationship/ratio (3.4) serves as determination α, i.e., under heat-transfer coefficient α should be understood the heat-flux density, which falls to one degree of the deflection of the real temperature of body surface from adiabatic. If $t_s>t_{ад}$, then heat is abstracted/removed from surface, if $t_s<t_{ад}$, then heat is fed to surface.

3. Different approaches to the study of the processes of the heat exchange of body with gas flow under conditions of icing.

To questions of the determination of the equilibrium temperature of the icing up surface dedicated his numerous works English researcher Hardy [56, 57, 58]. One of his latter/last works, carried out together with Brown, is dedicated to the determination of the kinetic temperature of the screw/propeller of aircraft under conditions of icing [58].

Page 51.

The authors write/record equation for determining the temperature of the moistened surface, which moves in cloud t_s'' (in the case of absolutely non-heat-conducting profile/airfoil) in the form $t_s'' = t_s' - 0{,}622 \frac{L_{исп}(e_s - e_1)}{c_p P_1}$, where t_s'' - equilibrium temperature of the moving/driving moistened surface,

t_s' - the equilibrium temperature of the moving/driving dry surface,

e - vapor pressure,

$L_{исп}$ - latent heat of vaporization of water.

S
ubscript 1 is related to conditions on to the edge of boundary layer.

For an absolutely heat-conducing profile/airfoil, i.e., for a profile/airfoil, which accepts one equilibrium temperature all over surface, the authors construct the appropriate equation by integration along the length the duct/contour of the equation of the form

$$k_h \rho_a v_0 c_p (t_S' - t_S'') = k_в \rho_a v_0 \cdot \frac{e_s - e_1}{P_1} \cdot 0{,}622 L_{исп},$$

where v_0 - the resultant velocity of the motion of screw/propeller,

k_h - a coefficient of convective thermal conductivity (dimensionless),

$k_в$ - a coefficient of the evaporation of water (dimensionless).

For the profile/airfoil of screw/propeller NACA 2409 authors brought calculations to quantitative results.

In 1971 Traybus [78], investigating the advantages of fluctuating vision in the thermal deicers, writes/records heat-flux density in the icing up surface with the aid of three functions Θ_1, Θ_2 and Θ_3 introduced to them with the dimensionality of temperature each, and new by the dimensionless variable b. In these designations general/common/total inflow of heat q must be equal to

$$q = f_c A (\Theta_1 - \Theta_2 - \Theta_3) \overset{(1)}{\text{при}}\ t_s < 32^\circ F,$$

where

$$\Theta_1 = t_s (1 + 0{,}47\, b) + 2{,}90\, L B^{-1} P_s = \Theta_1 (t_s, B, b)^\circ F,$$
$$\Theta_2 = \tau_\infty (1 + b) + 2{,}90\, L B^{-1} P_\infty + 127\, b = \Theta_2 (\tau_\infty, B, b)^\circ F,$$
$$\Theta_3 = \left(\frac{r}{c_p} + b\right)\left(\frac{u^2_\infty}{2gj}\right) = \Theta_3 (b, u_\infty)^\circ F,$$
$$b = \frac{R_w c_{pw}}{f_c}$$

and $$q = f_c \cdot A [\Theta_4 (t_s, B, b) - \Theta_4 (\tau_\infty, B, b) - \Theta_3 (b, u_\infty)] \overset{(1)}{\text{при}}\ t_s > 32^\circ F,$$

where $$\Theta_4 (t, B, b) = t (1 + b) + 29\, L B^{-1} P_s = \Theta_4 (t, B, b)^\circ F.$$

Key: (1). with.

In this case[1]

FOOTNOTE [1]. The dimensionality of all entering the formula values corresponds to the English system of units, in this case are preserved the designations of Tribus. ENDFOOTNOTE.

B - barometric pressure,

P_s - the elasticity of water vapors in surface,

P_∞ - the elasticity of water vapors in the free flow,

τ_∞ - the temperature of the free flow,

g - acceleration of gravity

f_c - the thermal conductivity (heat-transfer coefficient),

A - surface area,

L - latent heat of the sublimation of ice,

R_w - the settling velocity of water,

c_{pw} - the heat capacity of water.

Page 52.

The continuation of the work of Tribus was the article of Weiner, which appeared in the same 1951 [79].

Sufficiently in detail the conditions of thermal equilibrium were studied in 1953 by Messinger [68]. On the basis of the introduced by Tribus temperature functions Messinger brought all calculations to the appropriate traffic. It conducted calculations not only for the cases when t_s is more or less than 0°, but also for the case when $t_s = 0$ taking into account both the portion of freezing and portion of evaporation. as the independent variables in [68] are accepted flight speed u_∞, the temperature of undisturbed flow t_0 and parameter b, introduced by Tribus. Recovery factor r is accepted by constant and equal to 0.875; the author considers this as the average between his value with laminar - 0.85 and turbulent - 0.90 flow.

Messinger bypasses one of the essential difficulties, with which are encountered in concrete/specific/actual calculations, and namely - the task of the definition of the settling velocity of water (depending on liquid-water content and on the integral value of local the coefficient of capture) and local heat-transfer coefficient - after combining as Tribus, unknown parameters in one independent variable parameter b. Thus, the quantitative results, obtained by Messinger, can be used during calculations only when it is possible to determine the value of parameter b.

Let us note that in the calculations of Messinger the portion of evaporation for case $t_s > 0°$ is clearly reduced, since it considers evaporation as that occurring only from the surface of settling, while when $t_s > 0°$ water spreads beyond the limits of this zone. Consequently, and the values or rates determined by it, with which sets in the complete evaporation or the depcsiting water, they can be in this case substantially overstated. Further, the author and all other researchers, it considers that the drops completely give up entire their initial kinetic energy of body surface at the moment of collision. In fact that given up energy is considerably less, on the strength of the fact that the part of it forever lost during braking in air flow. However, virtually latter/last omission will not be reflected in results, since entire/all kinetic energy drops it plays extremely small role in the total heat balance of the icing up surface.

A somewhat cast approach to problem we meet in the collective work of cutter, Rasch and Baxter [52], that is actually the development of Ludlam's work [67], dedicated to the study of the effect of thermal processes on readings of different ice-depositing instruments. In this work the authors concentrate their attention in the calculation of the critical value of liquid-water content $w'_{кр}$.

this value, during which the temperature of the icing up surface reaches 0°.

4. Balance of the heat of the icing up surface.

Let us examine the in detail heat fluxes, directed to surface and from it during steady process of the icing when it is possible to consider it as constants t_s - the temperature of the icing up surface, t_0 - the temperature of air and u_∞ - the rate of motion. All given below relationships/ratios are related to the appropriate heat-flux densities.

1. Heat-flux density, caused by the deviation of temperature of surface t_s from equilibrium adiabatic t_{ad}, according to relationship/ratio (3.4) is equal to

$$q_1 = \alpha\left(\frac{r u_\infty^2}{2Jc_p} + t_0 - t_s\right). \qquad (3.5)$$

Page 53.

2. Density of heat flux caused by liberation of latent heat of freezing of depositing water, is equal to

$$q_2 = m_0 L_s, \qquad (3.6)$$

where m_1 - mass of water, which deposits per unit of surface per unit time.

L_3=80 cal/g - latent heat of freezing of ice with 0°. Relationship/ratio (3.6) is correct when $t_s < 0$ it is possible to consider that freezes entire deposited water.

3. Density of heat flux caused by transition of kinetic energy of drops into thermal with their shock from surface, is expressed by relationship/ratio

$$q_3 = \frac{m_0 u^2_\infty}{2J} \eta_1,$$

here η_1 - certain coefficient, which characterizes the fact that water depositing on surface gives up to this surface only part of its initial kinetic energy. We will assume/set $\eta_1 = 1$, thereby somewhat overstating term q_3, i.e., we will not consider that portion of energy which is taken away by forever air flow; in other words, it will assume that

$$q_3 = \frac{m_0 u^2_\infty}{2J} \qquad (3.7)$$

This assumption not cause noticeable quantitative changes, since estimation shows that even in the form (3.7) q_3 it is less than other terms hundreds times.

4. Heat flux, caused by cooling ice from 0° to temperature of

surface t_s, has density, equal to

$$q_4 = m_л \cdot c_л (0 - t_s) = - m_л c_л t_s, \qquad (3.8)$$

where $m_л$ - mass of ice, which freezes per unit time per unit of surface. When $t_s < 0°$, as it was noted in point/item 2, freezes entire deposited water and, therefore, $m_в = m_л$.

$c_л$ - heat capacities of ice, equal to 0.49 cal/g with 0°.

A number of factors contributes also to the heat removal from surface.

5. Heat-flux density, abstracted/removed for heating of supercooled water from temperature t_0 to 0°, is determined by expression

$$q_5 = m_в c_в (0 - t_0) = - m_в c_в t_0. \qquad (3.9)$$

6. Finally, evaporation (or sublimation) of ice from surface, caused by difference in saturation vapor pressure of water vapor above the icing surface and in undisturbed cloud leads to absorption (or liberation) of heat. The density of this heat flux it is possible to write in the form

$$q_6 = \pm m_i \cdot L_{...}$$

Page 54.

A strict definition of value m_i and consequently also q_6, is

sufficiently complex problem, than, apparently, and is explained by the fact that the majority of disagreements in the calculations of different authors occurs during the calculation of value q_6 [15, 21, 52, 68].

We will not stop on the reasons, which led some authors to clearly erroneous results - partially they are examined in V. Ye. Minervin's work [15].

Work [52] gives without bases/bases the expression for q_6, which in our designations takes the form

$$q_6 = \alpha\left[\frac{1550}{P_0}(e_0 - e_{t_0})\right],$$

where P_0 - pressure in the undisturbed flow,

e_0 and e_{t_0} - saturating vapor pressure at temperature with respect to 0° and t_0°.

According to Tribus and Messinger, this term (in our designations) will be written in the form

$$q_6 = \alpha \cdot 2{,}90\, L_{cy6}\frac{(e_0 - e_{t_0})}{P_0},$$

in this case the coefficient of 2.90 of Messinger is called empirical. It is easy to see that the numerical coefficient in

expression for q_6, accepted by Fritos [78], and following by them in terms of Weiner [79] and Messinger [68] differs from the coefficient, accepted by windbag, Rasch and Baxter [52]. Let us try to approach the determination of this coefficient from theoretical positions.

The conclusion/output of the expression given below, which is determining the heat loss to evaporation, we base on hypothesis, analogous hydrodynamic theory of heat exchange, i.e., let us assume that the evaporation is one of the manifestations of substantial exchange. Let us explain this in more detail.

The quantity of water m_i, evaporating for time unit is characterized by the intensity of the moisture exchange of boundary layer with surrounding air. Considering that the moisture exchange is realized by the same mechanism, that also heat exchange and exchange of air masses, it is possible to equate the intensity of the moisture exchange of a difference in the moisture content air masses exchanged per unit time. In this case it is assumed that in atmospheric boundary layer is saturated according to relation to ice at temperature of surface t_s, and in that not disturbed - it is saturated relative to water at temperature t_0. On the basis of the hydrodynamic theory of heat exchange, the mass of gas (air), which is adequate/approach unity of boundary layer per unit time (in g/cm² s), is equal to $\frac{\alpha}{c_p}$ or, if we express the exchange of air not in mass,

but in volumes, i.e., in $\frac{см^3}{см^2 \cdot с}$ then we will obtain $\frac{\alpha}{\rho_a c_p}$. Then the mass of that taken away from the same surface for the same time of moisture, i.e., in our designations m_i, is equal to

$$m_i = \frac{1}{\rho_a} \frac{\alpha}{c_p} \Delta\rho_n. \qquad (3.10)$$

Here

ρ_a - air density,

$\Delta\rho_n$ - a difference in the densities of saturated vapors of the water above ice at temperature of surface t_s and above water at temperature of air t_0.

Page 55.

Relation $\Delta\rho_n/\rho_a$ can be found in the courses of physics of the atmosphere (for example [33]): $\frac{\Delta\rho_n}{\rho_a} = 0{,}622 \frac{e_{t_{s.n}} - e_{t_{0.n}}}{P_0\left(1 - \frac{e_{t_{s.n}}}{P_0}\right)\left(1 - \frac{e_{t_{0.n}}}{P_0}\right)}$ or, with an accuracy to small ones of second order $\left(\frac{e_{t_{s.n}} + e_{t_{0.n}}}{P_0} \approx 0{,}01\right)$ it is possible to write $\frac{\Delta\rho_n}{\rho_a} = \frac{0{,}628}{P}(e_{t_{s.n}} - e_{t_{0.n}})$. Substituting this expression in equation (3.10) and multiplying obtained value m_i for heat of sublimation of ice at temperature t_s - $(L_{t_s.\text{суб}})$ let us have

$$q_6 = \alpha \frac{0{,}628 \cdot L_{t_s.\text{суб}}}{c_p}\left(\frac{e_{t_{s.n}} - e_{t_{0.n}}}{P_0}\right). \qquad (3.11)$$

If we approach determination of q_6 from the point of view of the

analogy between of thermal conductivity and diffusion [56], then is obtained the expression, analogous to equation (3.11), with supplementary factor $k_w k_h$, where k_w - a coefficient of the evaporation of water (dimensionless), k_h - a coefficient of heat transfer (dimensionless). From comparison with the empirically obtained coefficients of the psychometric equation of Hardy found that relation k_w/k_h is changed from 0.996 with - by 17.8° to 1.007 at +15.6°.

Minervin in 1956 [15], utilizing an analogy of thermal and diffuse processes, L. S. Eygenson [39] in detail developed in monograph obtained the relationship/ratio, similar to expression (3.11), with cofactor k/a, where к - a diffusion coefficient, a - a coefficient of thermal diffusivity. According to Hardy, $\frac{k_w}{k_h}=\left(\frac{k}{a}\right)^{0.3}$.

Without stopping on a question, who of two authors indicated is more than rights/laws in theoretical substantiation, let us note that Hardy's results, obtained by it during the comparison of the corresponding equations with the psychometric formula, testify that the cofactor, which appears in equation (3.11) unessentially differs from unity. The thereby is confirmed the soundness of the hypothesis accepted by us, with an increase in the rate when turbulent exchange begins to prevail above the molecular, this hypothesis must be justified still more.

Before converting/transferring to the construction of the equation of heat balance on this surface, let us focus attention on the following.

During the determination of inflow of heat q_2 we assumed that freezes entire deposited water, i.e., they counted $q_2 = m_n L_3$. However, it is possible that the evaporating part of water m_i does not manage to freeze. In this case should be written $Q_2 = (m_n - m_i) L_3$. But during the determination of heat withdrawal due to evaporation one should in expression (3.11) take heat of vaporization of water $L_{исп}$.

Thus, either $q_2 = (m_n - m_i) L_3$ and in this case $q_6 = m_i L_{исп}$, or $q_2 = m_n L_3$, but already in this case $q_6 = m_i L_{суб}$.

It is easy to see that also the equation of the balance of heat remains without change. Therefore when $t_s < 0$ let us assume/set

$$q_2 = m_n L_3, \text{ a } q_6 = m_i L_{суб}.$$

Page 56.

The error of Windbay, Nasch and Baxter [52] lies in the fact that they took $q_2 = m_n L_3$, and during calculation q_6 was utilized coefficient of 1550, equal, as it is easy to be convinced, to

relationship/ratio $\frac{0,622\,l_{исп}}{c_p}$.

We also do not have foundations for allowing instead of relation $\frac{0,628}{c_p} \approx 2,60$ coefficient or 2.90, used by Tribus, etc., and exceeding the ratio indicated approximately/exemplarily by 10%.

Thus, we wrote in an explicit form of expression for all the main heat fluxes which determine the balance of heat on the icing up surface. Here is not taken into consideration the radiation heat withdrawal, which plays negligible role.

Thus, the density of the resulting heat flux, which is adequate/approach the icing up surface, can be written in the form

$$q = q_1 + q_2 + q_3 + q_4 - q_5 - q_6 =$$
$$= \alpha\left(\frac{r u_\infty^2}{2Jc_p} + t_0 - t_s\right) + m_в L_s + m_в \frac{u_\infty^2}{2J} - m_в c_s t_s +$$
$$+ m_в c_в t_0 - \alpha \frac{0,628 L_{t_s\,\text{суб}}}{c_p}\left(\frac{e_{t_{s.в}}}{p_0} - \frac{e_{t_{0.в}}}{p_0}\right). \qquad (3.12)$$

In the absence of heat exchange with the internal surface of the icing up body net flux q is equal to 0 formula (3.12) takes the form

$$\alpha\left[\frac{r u_\infty^2}{2Jc_p} + t_0 - t_s - 0,628 \frac{L_{t_s\,\text{суб}}}{c_p}\left(\frac{e_{t_{s.в}}}{p_0} - \frac{e_{t_{0.в}}}{p_0}\right)\right] =$$
$$= m_в(L_s - c_s t_s + c_в t_0). \qquad (3.13)$$

5. Calculation of the coefficient of freezing.

Expressions (3.1) and (3.2), freezing β which characterize coefficient, can be converted, after replacing values m_i, $m_{кр}$ and $m_в$ with appropriate water content of clouds. Actually/really, if we designate through $w_{кр}$ such liquid-water content with which the settling per unit of body surface for time unit reaches critical value $m_{кр}$, i.e. $w_{кр} = \frac{m_{кр}}{u_\infty \cdot \tilde{E}_в}$ is analogous through w_i that portion of water content of clouds, which compensates evaporation, i.e., $w_i = \frac{m_i}{u_\infty \tilde{E}_в}$ and finally through w - actual liquid-water content, i.e., $w = \frac{m_в}{u_\infty \tilde{E}_в}$, then it is possible to write that

$$\beta = \begin{cases} 1 - \frac{w_i}{w} \text{ при } (1) \ w < w_{кр} \\ 1 - \frac{w_i}{w} - \left(1 + \frac{t_0}{80}\right)\left(1 - \frac{w_{кр}}{w}\right) \text{ при } (1) \ w > w_{кр}. \end{cases} \quad (3.14)$$

Key: (1). with.

Thus, for determination β it is necessary to know the actual liquid-water content w, the temperature of air t_0 and to find values $w_{кр}$ and w_i.

Page 57.

a) The calculation of critical liquid-water content.

For determination $w_{кр}$ let us turn to equation (3.13). Taking into account that in this case $t_s = 0$ and $m_s = w_{кр} \cdot u_\infty \tilde{E}_n$, let us have

$$\frac{w_{кр}}{\tilde{E}_n u_\infty} \frac{\left[-t_0 + \frac{0{,}628 L_{сув}(e_0 - e_{t_0})}{c_p P_0} - \frac{r u^2_\infty}{2 J c_p}\right]}{80 + t_0 + \frac{u^2_\infty}{2J}} = \frac{a}{\tilde{E}_n} [K_1(t_0, u_\infty, P_0) - r K_2(t_0, u_\infty)], \quad (3.15)$$

where

$$K_1(t_0, u_\infty, P_0) = \frac{-t_0 + \frac{0{,}628 L_{сув}}{c_p} \frac{(e_0 - e_{t_0})}{P_0}}{\left(80 + t_0 + \frac{U^2_\infty}{2J}\right) U_\infty},$$

$$K_2(t_0, u_\infty) = \frac{u^2_\infty}{2 J c_p \left(80 + t_0 + \frac{u^2_\infty}{2J}\right)}.$$

Thus, $w_{кр}$ depends on a whole series of the parameters and, first of all, from the temperature of air t_0 and flight speed u_∞ and, as show calculations, to a lesser degree from pressure P_0 and recovery factor r. Furthermore, $w_{кр}$ depends on such complicatedly defined

values, as heat-transfer coefficient α and the integral local coefficient of capture $\tilde{E}_{\Delta}$.

It should be noted that the dependence on r begins to become apparent by noticeable form only at comparatively high speeds (more than 100 m/s). Furthermore, when is studied icing in the vicinity of critical point, it is possible with large accuracy to count r=1, since at this point occurs total stagnation, as for instance, at the critical point of the round cylinder r=1 for Mach's any numbers from 0.4 to 0.9 [4].

The values of functions $K_1(t_0, u_\infty, P_0)$ and $K_2(t_0, u_\infty)$ were designed virtually for entire range of values t_0, u_∞ and P_0 possible during the flights of low-speed aviation.

The results of calculations are represented in Fig. 15. From the figure one can see that with $u_\infty < 10^2$ m/s the relative role K_2 in comparison with K_1 is small and it always decreases with decrease t_0.

For determination $\omega_{кр}$ it is necessary to know also $\frac{1}{\tilde{E}_{\Delta}}$. About the integral coefficient of capture we in detail spoke above, in chapter III, and brought the diagrams, making it possible to determine $\tilde{E}_{\Delta}$ for cylinders and series/row of profiles/airfoils. However, the determination of heat-transfer coefficient α represents the complex

problem which it is necessary to examine in somewhat more detail. The theory of the heat exchange of different bodies, which move in gas flow, unfortunately, is not yet developed so so that it would be possible with sufficient confidence to use the theoretical relationships/ratios, which are determining heat-transfer coefficient.

Page 58.

During the experimental investigation of the processes of heat exchange usually appears itself the dependence between the criterion of Nusselt $Nu=\alpha C/\lambda$, which characterizes the heat exchange of bodies with medium and Reynolds number $Re_0 = \frac{a_\infty C}{\nu}$. As a rule, this connection/communication can be represented in the form

$$Nu = a \cdot Re_0^n, \qquad (3.16)$$

where a and n - some constants, which depend not only on the form of body, but also on the range of Reynolds numbers. So M. A. Mikheev [17] gives the following values of a and n depending on Re_0 for round-cylindrical bodies during the calculation of the average according to the duct/contour of heat-transfer coefficient (Table 4).

For us the knowledge of heat-transfer coefficient for a cylinder is of independent interest, since the rotating cylinder (SIO) served as standard for determining the icing intensity in experimental flights.

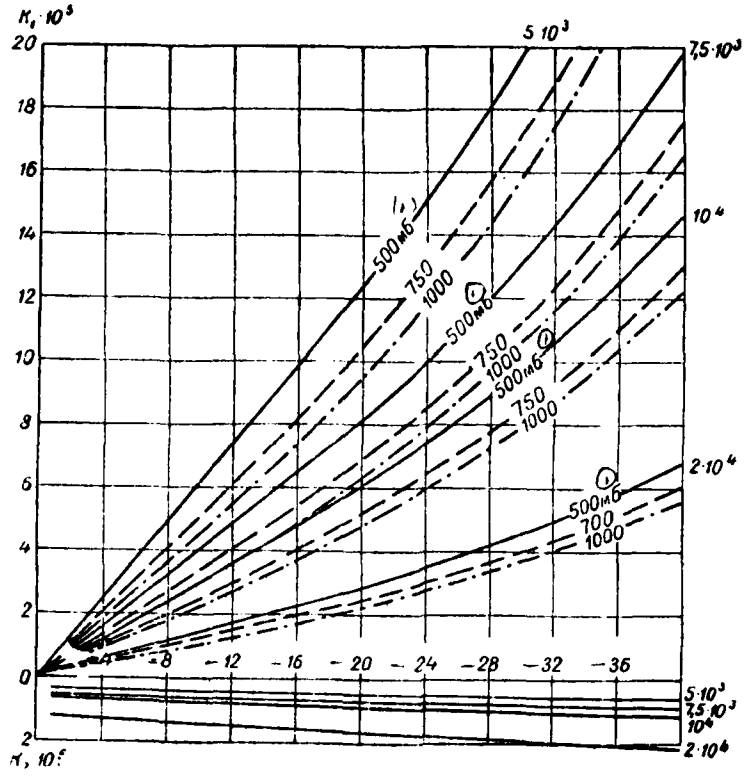

Fig. 15. Are upward along the axis of ordinates deposited/postponed the positive values of function $K_1 \cdot 10^5$, down - the positive values of function $K_2 \cdot 10^5$. Numbers by the curves indicate the values of the flight speed "b_0" in the middle of curves - pressure P_0.

Key: (1). mb.

Page 59.

In view of this were designed on Mikheev's given table the values α

for the cylinder with a diameter or 50 mm depending on flight speed $\nu = 0{,}167$ on cm²/s and $\lambda = 5.5 \cdot 10^{-5}$ cal/cm s °C.

FOOTNOTE 1. Value $\lambda = 5.5 \cdot 10^{-5}$ cal/cm s. deg. corresponds to temperature of -10°C. Generally the dependence λ on temperature very is not strong, namely at 0°C $\lambda = 5.05 \cdot 10^{-5}$ cal/cm s deg., but at -20°C $\lambda = 5.38 \cdot 10^{-2}$ cal/cm s deg. ENDFOOTNOTE.

The results of calculations are represented in Fig. 16.

Is considerably less studied the heat emission of the bodies of more complex form. Coefficients a and n in criterial relationships/ratios depend substantially on that, are found we in the region of laminar or in the region turbulent boundary layer. The first occurs to $Re_0 \approx 10^5$, the second - with $Re_0 > 10^6$. In the range Re_0 from $2 \cdot 10^5$ to $2 \cdot 10^6$ is located the transition layer for which it is not possible to indicate a precise criterial relationship/ratio, since in this case number Nu depends not only on Re_0, but also on the degree of the roughness of the surface and other factors.

All known to us experimental works regarding the heat-transfer coefficients α of wing profiles/airfoils, carried out both in our country and abroad, they indicate that the range of the oscillations/vibrations or heat-transfer coefficient for different profiles/airfoils and conditions is included within the limits $1 \cdot 10^{-3}$–$1 \cdot 10^{-2}$ cal/cm² s °C.

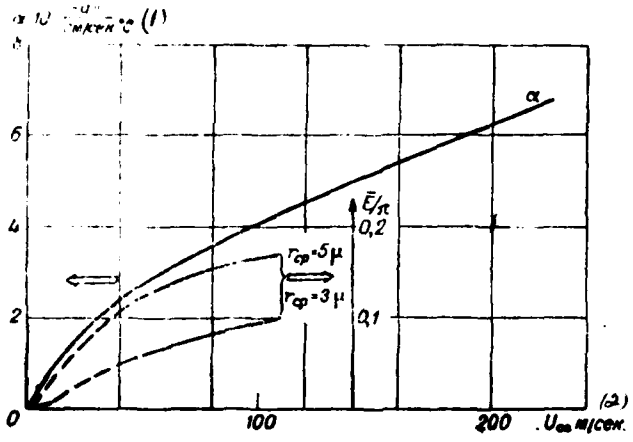

Fig. 16. Connection/communication of average heat-transfer coefficient α for a round cylinder with the speed of blowout (axis of ordinate to the left), dependence E/w for 50 mm of cylinder on $r_{ср}$ and $u_{со}$

Key: (1). cal/cm/s °C. (2). m/s.

Table 4.

Re_0	a	n
5–80	0,81	0,40
80–$5\cdot10^3$	0,625	0,46
$5\cdot10^3$ и выше (1)	0,197	0,60

Key: (1). and it is above.

Page 60.

So, in several examples of Tribus [78] α varied from $2 \cdot 10^{-3}$ to $3 \cdot 10^{-3}$ cal/cm^2 s°C. For Hardy [56] the curves of the dependence α on position on the wing profile of aircraft C=46, constructed on the basis of the works of Squire [74], indicate the change α from $1 \cdot 10^{-3}$ to $4 \cdot 5 \cdot 10^{-3}$ cal/cm^2 s°C. To the same result lead the calculations α according to known distribution the pressures along profile/airfoil, based on semi-empirical formulas.

Thus, for wing profiles/airfoils we can comparatively reliably indicate the boundaries of possible values α. However, obtaining precise values α for concrete/specific/actual profiles/airfoils and flight conditions exceeds the limits of the present investigation. In each specific case α can be determined either experimentally or with one or the other degree of approximation on the basis of the available relationships/ratios, which connect α with profile pressure distribution.

It must be noted that researchers' series/row determines heat-transfer coefficient somewhat differently from this accept in the present work, namely, they determine α from the relationship/ratio

$$q_1 = \alpha \left(\frac{r u_1^2}{2Jc_p} + t_1 - t_s \right), \qquad (3.17)$$

where t_1 and u_1 - respectively temperature and speed on the boundary of boundary layer. Let us recall that we determined α from the relationship/ratio

$$q_1 = \alpha\left(\frac{r u_\infty^2}{2Jc_p} + t_0 - t_s\right), \qquad (3.5)$$

where t_0 and u_∞ - temperature and speed of the undisturbed flow.

It is easy to see that both these expressions would be identical, if r=1, since in this case $t_0 + \frac{u_\infty^2}{2Jc_p} = t_1 + \frac{u_1^2}{2Jc_p}$. However, in the real case, with r<1, these expressions do not coincide. Actually the inadequacy of relationships/ratios (3.17) and (3.5) is included faster not in different determinations α, but in the different determinations of recovery factor [1].

FOOTNOTE [1]. It is more detailed with these two determinations of recovery factor it is possible to become acquainted in Hilton's monograph [30]. ENDFOOTNOTE.

Returning to expression (3.15) we see that there is entire necessary and sufficient for determination w_{xp} for an instrument SIO. For convenience in the calculations the same Fig. 16, in which is given the dependence α and u_{∞}, depicts dependence of $\tilde{E}/r$ on u_∞ and r_{c_p}.

FOOTNOTE 2. Factor 1/w reflects the fact that on the average the increase of ice flows/occurs/lasts evenly all over circumference of rotating cylinder. ENDFOOTNOTE.

Values w_{kp} in some special cases, designed with the aid of diagrams Fig. 15 and 16, give in Table 5. In this case the value of recovery factor r for SIO accept equal to 0.85 (directly for end connections of the profile/airfoil should be accepted r=1, 0).

More detailed calculations indicate that already at temperature $t_0 < -5°$ w_{kp} it exceeds the usually encountered values of water content of clouds (Fig. 11). Moreover, even with t_0=-3° (as is evident from Table 5) and flight speed $v \leq 75$ m/s (270 km/h), water content of clouds, as a rule, is less w_{kp}.

Page 61.

However, in individual, exclusively rare cases water content of clouds can prove to be more than w_{kp} even with t_0=-10°. Therefore in specific examples with large liquid-water contents always it is necessary to keep in mind the possibility of the involuntary freezing of the depositing water.

For wing profiles/airfoils relation $\frac{a}{E}$ (it can be) is approximately/exemplarily 3-5 times less than value $\frac{3\pi}{f}$ for an instrument SIO. Thus $\omega_{кр}$ for the spout of profile/airfoil several times is less than $\omega_{кр}$ for the cylinder which rotates by 50 mm, and sufficiently frequently it can reach the values of liquid-water content virtually encountered in clouds. Thus, one should sweep in form that for the center section of the plane in the individual, completely probable cases p it can prove to be lower than for an instrument SIO.

B) The temperature of the icing up surface and evaporation from it.

In the absence of heat exchange with internal surface the temperature of surface t_s is connected with flight conditions on the equation of heat balance (3.13). However, the complicated dependence of separate terms of this equation on temperature t_s does not make it possible to in general solve it relatively t_s.

Comparatively simply it is possible to determine the temperature of surface t_s in the particular case when a quantity of depositing water $m_в = m_в$ i.e. in accuracy compensates the evaporation of ice from it.

Table 5.

t_0	$w_{0,5}$ (1) (м/сек)	p_0 (2) (мб)	$r_{ср}$ (г)	$w_{кр}$ (3) (г/м³)
−3	$5 \cdot 10^3$	1000	3	0,477
			5	0,231
		500	3	0,721
			5	0,351
	$1 \cdot 10^4$	1000	3	0,053
			5	0,079
		500	3	0,168
			5	0,096
−10	$5 \cdot 10^3$	1000	3	1,881
			5	0,911
		500	3	2,614
			5	1,206
	$1 \cdot 10^4$	1000	3	0,684
			5	0,592
		500	3	1,025
			5	0,788

Key: (1). (m/s). (2). (mb). (3). (g/m³).

Page 62.

Then, on the basis of that [1] that $m_i = 0{,}628 \frac{\alpha}{c_p} \frac{e_{t_{0,5}} - e_{t_{0,0}}}{P_0}$ and, substituting in equality (3.13) for m_i this expression m_i, we will obtain

$$\frac{r_{кр}^2 \omega_{0,5}}{2 A c_p} = t_0 - t_0 + \frac{0{,}628}{c_p} \frac{\alpha (e_{t_{0,5}} - e_{t_{0,0}})}{P_0} \left(L_{t_0, кон} + t_0 - t_0 - \frac{\alpha}{2} \right). \quad (3.18)$$

FOOTNOTE [1]. Cm the section of 4 present chapters. ENDFOOTNOTE.

When deriving the equation (3.18) we proceeded from that fact that as a result the water, depositing on body surface and which was being located thus far at temperature t_0, evaporates and is converted into water vapor at temperature t. Since the heat, necessary for this conversion, must not depend, in view of the reversibility of process, from that, in what way we to this come, then it it is possible to equate with the heat, spent on heating water from t_0 to t, and its subsequent evaporation at temperature t. For this very reason into relationship/ratio (3.18) enters either heat of cooling ice 0° down to t, or the heat of the freezing of water.

The solution of equation (3.18) is represented in the form of the nomogram (Fig. 17), the method of the use of which following: from the lower horizontal scale of speed (for example $u = 60$ m/s) should be to be raised on vertical straight line to the curve of assigned r (r=0.9), then, moving over horizontal, to reach the intersection with assigned line t_0 (for example -10°) finally being discharged from point of intersection on vertical line down, to scale t, read the response/answer, in this case, -8.6°. The made path is shown in figure by arrow/pointer.

It is obvious that with aircraft icing a quantity of depositing water is more than evaporating. Consequently temperature t, determined according to relationship/ratio (3.18), Budde lower than

actual, since in equality (3.18) is not considered the inflow of heat, caused by the freezing of the supplementary part of the deposited water. If we disregard/neglect kinetic energy of the depositing water drops, then it is not difficult to ascertain that for the more precision determination of value t_s it is possible to use the same nomogram (fig. 17), if we instead of u_∞ proceed from certain "given" speed

$$u_n = u_\infty \cdot \sqrt{1 + \frac{2Jc_p\tilde{E}(L_{t_{s.s}} + t_0 - t_s)(w - w_i)}{\alpha r u_\infty}}. \qquad (3.19)$$

FOOTNOTE 1. Dependence u_n and on t_s is comparatively small and during calculations of radicand with a sufficient degree of accuracy it is possible to take as t_s the equal to the value, found from equality (3.18). ENDFOOTNOTE.

Correction found thus can reach completely noticeable value. For example, with $\tilde{E}=0.5$, $w=0.2\cdot10^{-6}$ g/cm^3, $\alpha=5\cdot10^{-3}$, r=1 and $u_\infty=10^4$ cm/s this correction is equivalent to an increase in the speed more than twice.

At the known value of the temperature of icing up surface t_s does not comprise large work to calculate the mass of ice m_i, evaporating from a unit of surface per unit of time, and the value of water content of clouds w_i, necessary for the compensation of this

evaporation.

Page 63.

Actually/really,

$$m_i = \alpha \cdot K_3(t_s, t_0 P_0) \tag{3.20}$$

and, therefore,

$$w_i = \frac{\alpha}{E_A u_\infty} \cdot K_3(t_s, t_0, P_0), \tag{3.21}$$

where

$$K_3(t_s, t_0, P_0) = \frac{0.628}{c_p} \frac{e_{t_s, n} - e_{t_0, n}}{P_0}. \tag{3.22}$$

Fig. 18 gives simple nomogram for determining the function K_3 in dependence on values t_0, t_s and P_0.

For illustration in table 6 are given values t_s and w_i, for SIO in some special cases (water content of clouds is accepted equal to 0.2 g/m³).

Thus, after determining w_∞ and w_i and knowing liquid-water content w and temperature t_0 clouds, it is possible according to equation (3.14) to find the coefficient of freezing β. For an example the same Table 6 in latter/last column gives values β. From table it is evident that even at temperature of air -3° value β is very close to unity, if the speed of aircraft does not exceed 200 km hour.

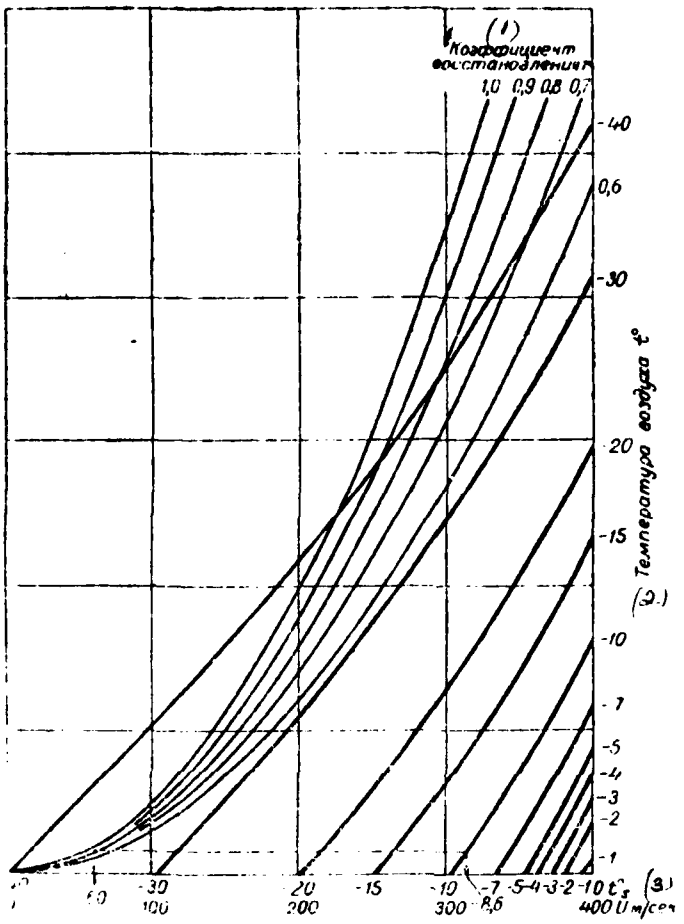

Fig. 17. Nomogram for determining the temperature of icing up surface . The method of use is described in text.

Key: (1). Recovery factor. (2). Temperature of air. (3). m/s.

Page 64.

At conclusion of present chapter let us note that the detailed analysis of the process of heat exchange conducted on the surface of aircraft under conditions of icing makes it possible to answer one more virtually very important question. Namely, to what temperature it is necessary to ensure heating the surface of aircraft during flights in dry air in order during flights in clouds to guarantee the prevention of icing.

In order to guarantee the absence of icing, inflow of heat to the unit of surface for time unit q (i.e., density of the heat flux applied to internal surface) must ensure its heating to 0° and completely compensate the heat removal so that in this case would not occur the freezing of the deposited water. Consequently it is possible to write that

$$q = \alpha(0 - t_{\text{вх}}) + \alpha L_{\text{исп}} \frac{0{,}628}{c_p} \frac{(e_0 - e_{t_0})}{P_0} + m_в c_в (0 - t_0) - m_в \frac{u^2_\infty}{2J}. \quad (3.23)$$

From other side this same inflow of heat q provides in dry air heating surface to certain unknown temperature $t_г$. Thus, occurs the equality

$$q = \alpha(t_г - t_{\text{вх}}). \quad (3.24)$$

Equalizing right sides (3.23) and (3.24), we will obtain

$$t_г = L_{\text{исп}} \cdot \frac{0{,}628}{c_p} \frac{(e_0 - e_{t_0})}{P_0} + \frac{w u_\infty \cdot \tilde{E}}{\alpha}\left(|t_0| - \frac{u^2_\infty}{2J}\right) \quad (3.25)$$

or, disregarding term $\frac{u^2_\infty}{2J}$ (with $u_\infty < 100$ m/s this is completely admissible), finally it is possible to write

$$t_г = 600 \cdot K_в(0, t_0, P_0) + \frac{w u_\infty \tilde{E}}{\alpha} |t_0|. \quad (3.26)$$

Table 6.

$t_{a'}$	u_{∞} (1) (см сек)	P_0 (2) (мб)	$r_{ср}$ (мк)	t_s (°С)	w_i (3) (10^{-3} м)	β
-3	$5 \cdot 10^3$	1000	3	-1,3	0,013	0,935
			5	0,3	0,013	0,935
		500	3	1,3	0,029	0,855
			5	-0,3	0,029	0,885
	$1 \cdot 10^4$	1000	3	0	0,0143	0,221
			5	0	0,0082	0,141
		500	3	0	0,0253	0,720
			5	0	0,0145	0,427
-10	$5 \cdot 10^3$	1000	3	-7,8	0,0045	0,977
			5	-6,55	0,0061	0,969
		500	3	-7,8	0,009	0,955
			5	-6,55	0,0113	0,943
	$1 \cdot 10^4$	1000	3	-4,50	0,0135	0,932
			5	-3,1	0,0111	0,945
		500	3	-4,5	0,0253	0,873
			5	-3,1	0,0213	0,893

Key: (1). (cm/s). (2). (mb). (3). (g/m^3).

Page 65.

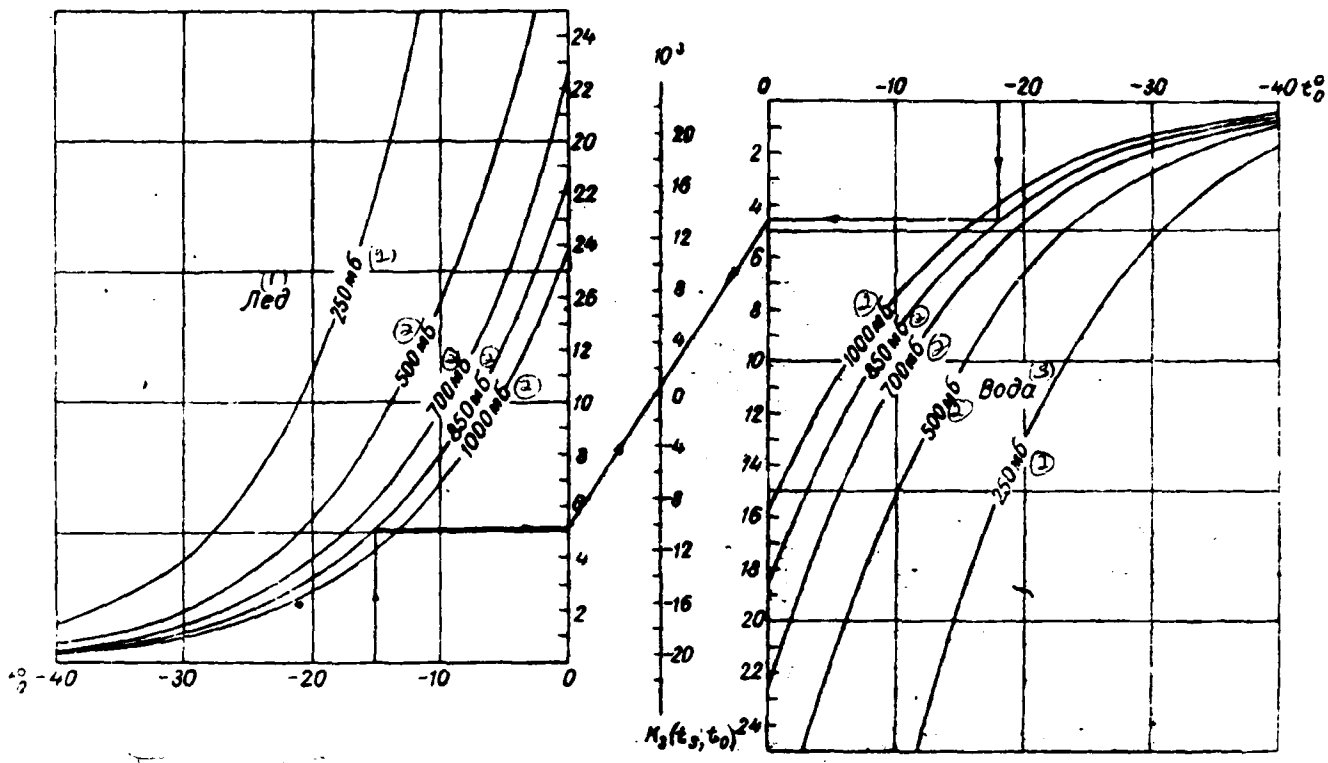

Fig. 18. Nomogram for determining function $K_3(t_0, t_g, P_0)$. Arrow/pointer showed an example of determination K_3 with $t_0=-18°$, $t_g=-18°$ and $P_0=850$ mb.

Key: (1). Ice. (2). mb. (3). water.

Page 66.

From relationship/ratio (3.26) it is evident that t_1 first of all, depends substantially on t_0, i.e., from that temperature with which we want to completely eliminate the possibility of ice formation. So already with $t_0=-20°$ even with the quite minimum liquid-water content, which ensures only the wettability of surface, overheating t_1-t_0 must exceed 30°, and upon consideration of a maximally possible value of liquid-water content and coefficient of capture this overheating must reach to 40-50°.

Such power of deicers it is hardly possible to ensure without the essential weighting of aircraft and considerable deterioration in the flight characteristics. For this very reason it seems to us by advisable during the construction of the thermal deicers for the protection of the planes of aircraft to everywhere pass to the method of the fluctuating preheating, proposed by Tribus [78].

Chapter IV.

EXPERIMENTAL STUDIES OF THE ICING OF PROPELLER-DRIVEN AIRCRAFT.

1. Purpose and procedure of experimental flight.

The construction of the theory of icing, led to quantitative results, not only does not eliminate the need for conducting the experimental studies of aircraft icing, but moreover, are posed new problems, considerably expanding series of question, included earlier during the experimental study of icing.

Up to 1950 our basic experimental material on aircraft icing in USSR was the material, accumulated on the network/grid of the points/items of aircraft sounding of the Main Administration of the Hydrometeorological Service. Up to 1948 on these points/items they conducted only qualitative observations of the icing of different aircraft components, seen from flight aerologist's place. Since 1948 in flight aerologist's window at a distance of 30 cm from edge was established/installed the special template-indicator of icing. It is the considerably reduced model of the wing of heavy aircraft. On the

front of the template/pattern are plotted/applied the alternating black-white bands with a width of 15 mm. The thickness of grown ice is determined from measuring pin - the indicator with a length of 5 cm with divisions by 5 mm. In the presence of icing the flight aerologist notes height/altitude and time of the beginning of icing, thickness of grown ice for separate time intervals, form and form of icing and height/altitude and time of the end/lead of the icing.

Despite the fact that this observation still it is not possible to name/call quantitative, since the estimation of the icing intensity and extent (extensiveness) of the zones of icing, obtained on the basis of observations of template/pattern, is sufficiently rough, in the first stages of the research of physics of icing these observations had vital importance. They made it possible to gather vast low-quality material about different forms and forms of icing, to obtain the specific statistical data, etc. Many results of these observations were used in I. G. Pchelko's works [23].

However, during the detailed research of physics of icing, in principle it is not possible to be satisfied by similar low-quality observations, since they do not give the possibility to connect icing with such basic parameters of clouds as liquid-water content and distribution of cloud drops according to sizes/dimensions. Furthermore, the determination of icing intensity to templet should

be recognized very rough and inaccurate.

Page 68.

Therefore it was necessary to manufacture the new procedure of the experimental study of icing, making it possible to carry out quantitative measurements with sufficient accuracy and giving possibility to connect special features/peculiarities in the character of icing with the physical parameters, characterizing the state of the atmosphere, and for flight conditions. It was necessary so as far as possible to remove the element/cell of subjectivity in the estimation of icing.

To the development of new procedure contributed the fact that in the laboratory of the cloud investigations by TsAO [Central Aerological Observatory] was accumulated large experiment in the study of different sides of physics of clouds. These works, initiated in A. M. Borovikov even on balloon during the years 1946-1947 [3], led to the creation of the aircraft flying laboratory equipment with which continuously was improved. On this flying laboratory, beginning with 1950, by the group of colleagues under A. M. Borovikov's management/manual were conducted yearly special flight expeditions for the study of cloud microphysics, icing, on the analysis of the three-dimensional/space structure of the frontal cloud systems and

other phenomena. Basic part of these flights passed to the supercooled clouds of laminar forms in the presence in them of icing.

In 7 years were carried out more than 300 such flights, with the common coating, exceeding 1000 hours, of them about 300 hours fell to flights under conditions of icing.

The in detail flying laboratory was described in the series/row of works; therefore below we will give only the enumeration of the basic instruments, established/installed on aircraft, and their arrangement/position (Fig. 19).

1. Aerographs.

2. Air intake of drops (Fig. 20).

3. Micro-camera mount.

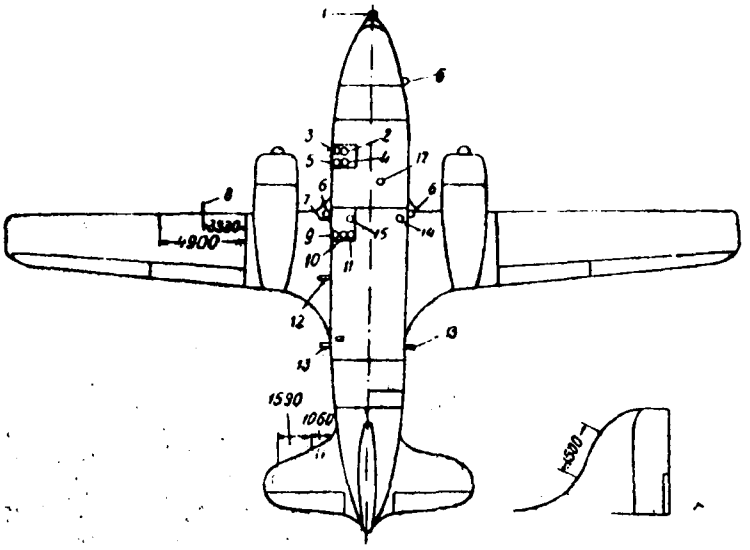

Fig. 19. The schematic of the arrangement/position of instruments in the aircraft of IL-14: 1 - aerograph, 2 - automatic recorder of the speed, 3 - pressure recorder, 4 - electric clocks, 5 - electric plate, 6 - thermometer, 7 - indicator of icing, 8 - measuring dowel, 9 - altitude indicator, 10 - variometer, 11 - speed indicator, 12 - instrument for the measurement of water content; 13 - automatic recorder of icing (SIO), 14 - micro-camera mount, 15 - automatic recorder of temperatures (ST-23).

Page 69.

4. Different instruments for measuring water content of clouds, constructing/designing V. Ye. Minervin, based, for supercooled

clouds, on principle of ice-settling cylinders, and construction/design of V. A. Zaytsev - on the principle of filter paper.

5. Instrument stand to which are fastened/strengthened altitude indicators, speed and overloads, compass, watches. To this same stand is fastened/strengthened the toggle switch from the electric bell on signal of which was conducted the simultaneous measurement of different parameters.

Besides those enumerated, on board aircraft, depending on the task of this concrete/specific/actual flight, were located some other instruments.

During the study of aircraft icing, the basic goal of investigations in our first expeditions it was:

1. The explanation of the dependence of the character of icing on the varied conditions, under which occurs ice accumulation.

2. Explanation of dependence of character of icing on form and sizes/dimensions of icing up body.

3. Obtained of precise quantitative data about icing intensity

of bodies of cylindrical form, for which at that time were fulfilled theoretical calculations with purpose of checking results of theory.

For the accomplishment of the outlined objective was made the set of the templates/patterns of various forms (Fig. 20) which with the aid of special rod were carried far beyond the edge of aircraft (further 0.5 m). Into set entered: the disks with a diameter of 40 mm; the sphere with a diameter of 40 mm; cigar-shaped body of revolution with maximum cross section, also equal to 40 mm; the elliptical cylinders, directed at different angles toward flow, rectangular plates and, the finally round cylinders of different diameters both rotating, and not rotating.

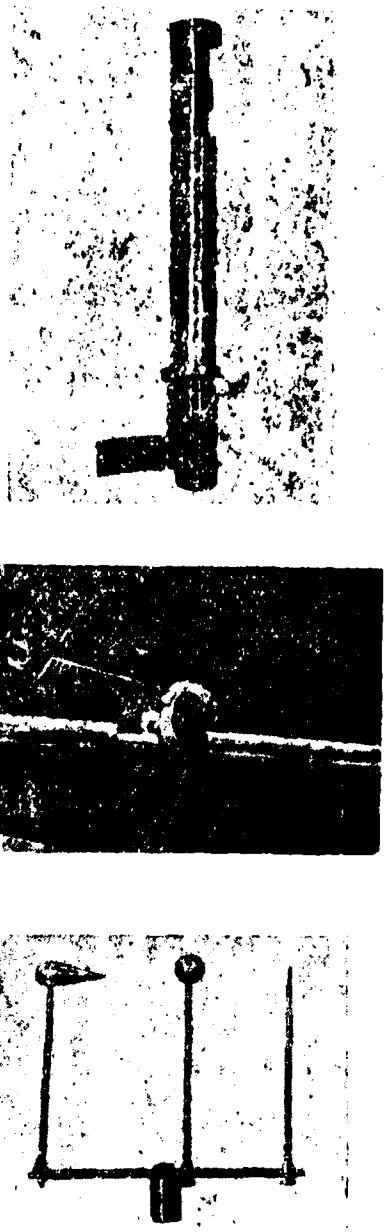

Fig. 20. Air intake of the tests/samples of cloud drops (above), some templates/patterns, which were being applied for studying the

dependence of the means of ice deposit on the form of profile/airfoil.

Page 70.

In the presence in flight the icing, besides observations with the aid of special templates/patterns continucusly conducted also qualitative observations of different parts of aircraft, which were undergoing icing, and after flight aerologist's standard template/pattern. All observations were accompanied by detailed records, sketchings and photographs. In the period of icing were conducted usual temperature sounding, measurement of liquid-water content and cloud microstructure, recording the flight conditions - speed, height/altitude, course and so forth and finally was maintained detailed flight log.

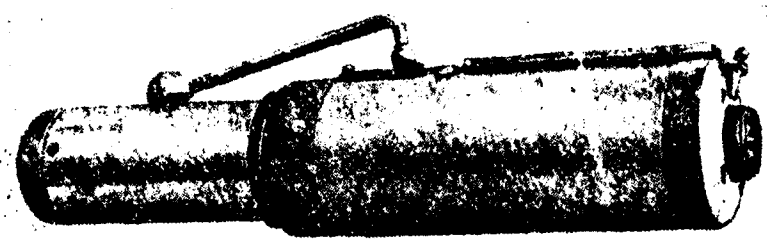

Fig. 21a. Aircraft meter of icing - appearance of instrument to work.

Fig. 21b. Aircraft meter of icing - type of instrument after work.
(On cylinder it is visible grown ice with strongly uneven surface).

The target of later in-flight studies (1955-1956) was conducting the experimental check, presented in chapter III theory of the recalculation of icing intensity from standard to plane and study of the three-dimensional/space extent of the zones of icing in different synoptical positions. On a latter/last question we stop will not, since it exceeds the scope of this work.

For the accomplishment of the first objective the instrument part of flying laboratory was completed new, developed and prepared by that time in NII GMP by M. Ye. Azbel, by instrument SIO (aircraft meter of icing - Fig. 21), receiver part of which was 50 mm the rotating cylinder.

Since basic part of the instruments, utilized during the study of icing (air intake of cloud drops, instruments, which measure the liquid-water content, SIO and series/row of others), is placed outside aircraft, it was necessary to explain, what effect has on reading of these instruments the disturbance/perturbation, introduced into medium by aircraft during its motion. For this purpose was used the Pitot tube, with the aid of which it was possible to determine with sufficient accuracy or the boundary of the zone of disturbance/perturbation into the field of velocities and the

cylindrical resistance thermometer, which made it possible tc rate/estimate the boundaries of the zone of disturbance/perturbation in temperature field.

The first expeditions (1950-1954) were conducted on the flying laboratory, equipped on an aircraft of the type LI-2, the latter (1955-1956) - on the aircraft of IL-14.

Entire complex of observations in the first expeditions was fulfilled in essence by the colleagues of TsAC: by A. M. Borovikov, Z. V. Tonkova, A. A. Reshchikova, V. Ye. Minervin, N. M. Bokarev and by author; in separate flights participated other colleagues. Latter/last expeditions on IL-14 were conducted together with the State of NII GVF, from which in them accepted participation O. K. Trunov, G. M. Balashov and V. R. Yushkevich. In these expeditions, besides the complex of observations noted above, was conducted the study of the effect of different form of icing on operational-flight aircraft quality/fineness ratios.

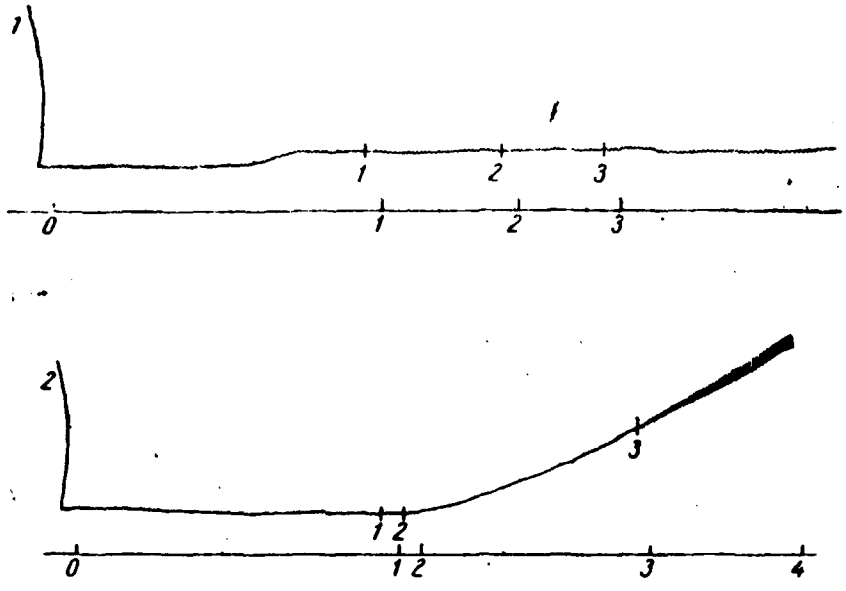

Fig. 21c. Aircraft meter of icing - examples of tape recording of the instrument: 1 - in flight from 11/XII 1955, 2 - in flight from 16/XII 1955.

Page 72.

Route and mode/conditions of each of the flights were determined depending on overall sinoptic situation in flying area and were more precisely formulated directly during conducting of flight itself. As an example let us examine one of the flights.

Flight, carried out on 12 April 1956, passed on route Vilnyus - Riga - Vilnyus - Minsk - Vilnyus, in rear of cyclone, in uniform air mass. During this day middle latitudes of the European territory of the USSR were engage by the vast area of reduced pressures, one of centers of which at noon was located above the northwestern part of Baltic states (Fig. 22). From center in Novgorod, Vyshniy Volochok and Moscow is passed a front of occlusion. In rear of cyclone, on the territory of Latvia and Lithuania, is passed the series/row of secondary cold fronts. A similar sinoptic situation provided development in these areas of restless stratocumulus, but with the places and very powerful/thick cumulonimbus cloudiness.

During the probing, produced during takeoff in Vilnyus 10 hours (Fig. 23), aircraft opened layers Sc at the height/altitude of 500-1550 m. Above it was clear. In clouds was observed the icing.

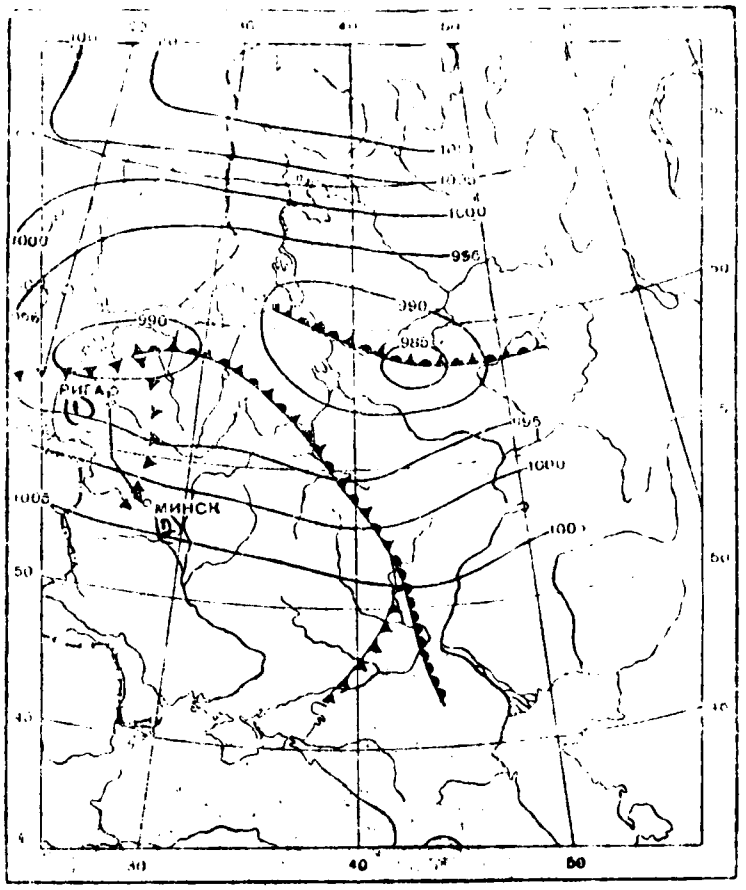

Fig. 22. Example of synoptical situation in flight 12/IV 1956 on route Vilnyus - Riga - Vilnyus - Minsk - Vilnyus.

Key: (1). Riga. (2). Minsk.

After probing the aircraft went in Rigni's direction, being located always near lower cloud base, sometimes even to short period leaving of them (in the places where the clouds raised themselves). Cloudiness was restless - sharply was changed the height/altitude of the lower and upper cloud boundaries and their power. Icing was observed always, in this case its intensity (on SIO) was changed from 0.04 to 0.13 mm/min. Water content of clouds, measured by the instrument of Zaytsev, oscillated from 0.07 to 0.29 g/m^3. In the second half flight on section Vilnyus - Riga the intensity of icing is considerably feeble (to 0.02-0.01 mm/min). Liquid-water content fell to 0.04-0.02 g/m^3. The simultaneous decrease of the liquid-water content of the drop part of clouds and icing intensity coincided with precipitation from the clouds or snow. During entire flight was perceived the turbulence from weak to that moderated. However, the straight/direct correlation of changes in the intensity of turbulence and icing it was not observed.

Upon the return from Rigni to Vilnyus, the aircraft flew in essence nearer to the upper edge of clouds. Here just as it is earlier, in the section of path nearest to Riga the icing intensity remained approximately/exemplarily permanent and weak: 0.07-0.09 mm/min. The extent of the zone of weak intensity was ≈130 km in upper boundary (in lower it reached 200 km). Subsequently the intensity of icing began sharply to be changed, growing/rising to 0.12-0.13 mm/min

and falling to 0.02-0.03 mm/min. As earlier, direct connection/communication of the intensity of turbulence with icing intensity to reveal/detect not succeeded.

In section Vilnyus - Minsk the power of clouds decreased to 300-400 m. In other respects their character remained as before.

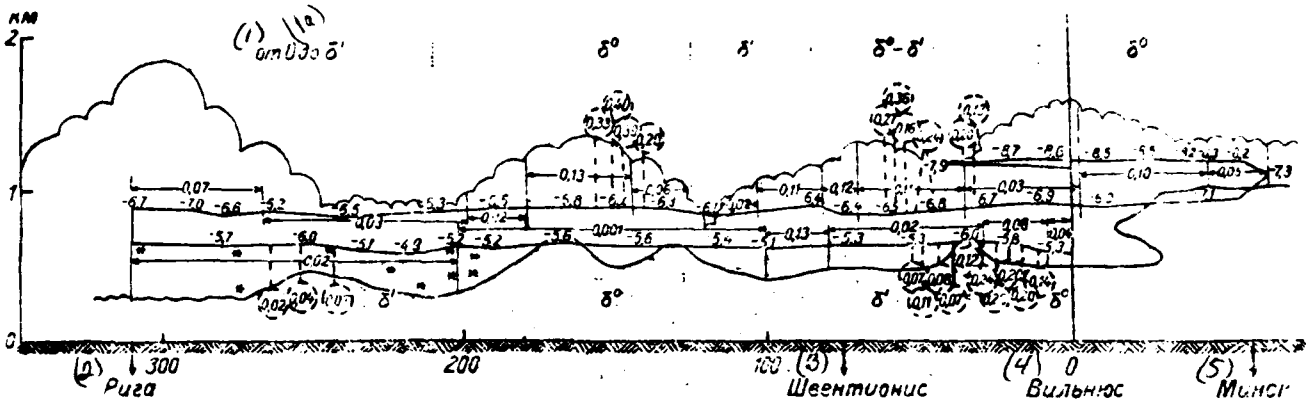

Fig. 23. Vertical section or clouds in flight 12/IV 1956 on route Vilnyus - Riga - Vilnyus - Minsk - Vilnyus. ---- the flight trajectory. By numerals they are shown: the temperature, water content of clouds in g/m³ (in small circles) and icing intensity SIO in mm/min. σ - bumping or aircraft (σ° - is weak, σ' - moderated), ✳— snow.

Key: (1). from. (1A). to. (2). Riga. (3). Shventionis. (4). Vilnyus. (5). Minsk.

Page 74.

Thus, in present flight was inspected the zone of the icing of clouds Sc in uniform air mass. It is possible to consider that it covers entire mass of clouds both in the horizontal and in vertical

the directions (temperature in cloud was changed from -5 to -9°). This same result was obtained also in other flights.

Before passing directly to the analysis of the assembled experimental material, let us pause briefly at one more moment/torque.

As is known, to icing are subjected the most diverse parts of aircraft, from rivets to planes, control vanes, etc. Structure and form of ice deposits substantially are modified from completely transparent glassy ice to white milky, from smooth and even to strongly uneven, U-shaped. The icing of one form does not exert a substantial influence on flight aircraft quality/fineness ratios and does not represent danger, another - on the contrary, it strongly makes its lift-drag ratios worse: raises drag, decreases the lift, etc.

The extreme diversity of forms and structure of ice deposits becomes apparent, as this was discovered, not only depending on the flight conditions and characteristics of cloud, but also on form and sizes/dimensions of the icing up body.

This complicated dependence of form and structure of deposited ice on numerous factors and existed disconnection of researchers

contributed so that up to now still there is no conventional single classification of the forms of icing.

Direct participation in prolonged flight expeditions for the investigation of icing during 6 years allowed us to compose the classification (table 8) proposed in 3 sections of present chapter of the types of icing, in which were reflected the form, the structure and the type of the surface of growing ice. The analysis of available material showed that this classification sufficiently in detail transfers the encountered forms of icing, and the possibility of light coding it makes its virtually very convenient.

2. Effect of the disturbance/perturbation, introduced by aircraft to the measured parameters of cloud.

As has already been mentioned, in the period of observation of aircraft icing were conducted continuous instrument/tool observations of different parameters of cloud and flight conditions, namely, after temperature, flight speed, liquid-water content and cloud microstructure, etc. It is logical that the receivers of these instruments were carried outside and they were arranged/located in immediate proximity of aircraft and therefore they were located in other in that or disturbed degree to the zone of flow. Therefore, first of all, does arise question, is possible readings of these

instruments to relate to the undisturbed medium or these readings characterize certain disturbed zone and require the introductions of the corresponding corrections.

The possibility of this type of the errors due to the perturbation of flow was for the first time by us expressed into 1953 more in connection with the study of the errors for the aircraft air intake of drops [32]. The conclusion that containing in this work the probable error, introduced due to the aircraft which perturbs actions in the measured range of dimensions does not exceed 5o/o for the drops of any sizes/dimensions, was based on very rough qualitative reasonings.

Page 75.

Therefore it is expedient in more detail to examine the perturbing effect which introduces into current of traffic of aircraft.

A) the field of velocities and temperatures around aircraft.

Fig. 19 gives schematically the fuselage contour of the aircraft of Il-14 and are shown of the place of the arrangement/position of one or the other receivers of meteorological elements.

For measuring of velocity fields was made the tube with a length of 120 cm with the aid of which it was possible to measure certain value, proportional to the dynamic head. Speed indicator was connected to tube and, thus, it was possible to count off the values of the airspeed in some relative unity. In rate measurement at the assigned distance from edge the tube together with special nozzle was turned around its axis to the maximum reading of speed indicator how was reached the parallelism of nozzle to airflow.

For measuring the temperature field served universal temperature-sensing device P-1, fastened/strengthened to the end/lead of the tube with a length of 80 cm. As the monitor of temperature served receiver ST-23.

The measurements of rate and temperature were conducted through every 5 cm along the normal from the edge of aircraft. In this case the rate was measured with an accuracy to 5o/o, temperature - with an accuracy to 0.3°. The results of measurements showed that the zone of the disturbance/perturbation (zone, on outer edge of which the parameters of medium virtually are not changed during removal/distance from edge) it grows/rises from 8 cm at point 1 (Fig. 24) to 20 cm at point 3. Rate within the zone of disturbance/perturbation grew/rose along the normal from fuselage to the outer edge of zone, which attests to the fact that the zone of

disturbance/perturbation is boundary layer. The high transverse sizes/dimensions of layer testify about its turbulent character.

The temperature of the stagnant flow (static temperature) virtually was not changed with removal/distance from the edge of aircraft. The latter means that the dissipative terms do not play the significant role and the zone of the disturbance/perturbation of its own thermodynamic temperature of flow coincides with the zone of the field distortion of velocities.

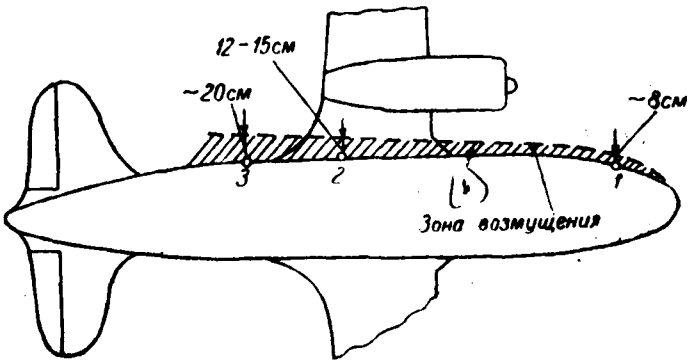

Fig. 24. Diagram of the zone of the disturbance/perturbation of air flow near the fuselage of aircraft. 1 - lateral window of the chief pilot; 2 - third window of passenger compartment, 3 - latter/last window of passenger compartment.

Key: (1). Zone of disturbance/perturbation.

Page 76.

One should especially note, that even so the boundary layer at point 2 has thickness of 12-15 cm, on boundary its rate approximately/exemplarily to 100/0 is more than at infinity. This is explained by the fact that point 2 is located directly above the wing of aircraft at a distance where still manifests itself the disturbance/perturbation, introduced by wing into flow. Apparently on the same reason the rate, attained on the boundary of zone at point

3, by several percentages lower than rate at infinity.

Thus, the conducted investigations of the fields of velocity and temperature lead to the following conclusions:

1. The zones of the disturbance/perturbation both the field of velocities and their own temperature field of the moving/driving flow coincide. In this case virtually the zone of disturbance/perturbation coincides with boundary layer and increases along fuselage towards its tail section approximately/exemplarily as $\sqrt{l}$ (l - distance from the face grinding of fuselage), reaching the latter/last window of passenger compartment has $\approx$20 cm.

2. Instruments, which use for measuring one or the other parameters of undisturbed flow, so that them would not affect field distortion of velocities, must be placed in forward fuselage section at a distance not less than 15 cm from edge, in rear - not less than 30 cm. In this case one should remember, that the rate in the third window of passenger compartment to 10o/o is more than the rate of aircraft that must be considered by the introduction of the corresponding corrections.

B) distortions, introduced by the aircraft into the spectral distribution of drops according to sizes/dimensions and their

quantity per unit of volume of air.

In order to define, as is changed the spectral distribution of drops according to sizes/dimensions, and their quantity per unit of volume in immediate proximity of the fuselage of aircraft due to the disturbance/perturbation, introduced by the latter during motion, let us examine the flow pattern of fuselage of cloud drops.

Fig. 25 schematically shows the flow around fuselage of air the flow around fuselage of air and drops of two different radii. It is easy to see that directly along side fuselage can exist the certain "dead" zone, where do not fall the drops of given size/dimension. It is obvious that the sizes/dimensions of this zone are different this zone they are different for different drops. In order to rate/estimate these sizes/dimensions, let us examine the stopping distance of the drop of the assigned radius, which began to move along the normal to the surface of fuselage with the assigned initial velocity. Let us consider in the first approximation, that the general/common/total motion of drop is composed of its motion along the flow line of air and along the normal to this line.

In detail the calculations of the stopping distance of drop taking into account deflection from Stokes' law are given in 2 sections of V chapter. Here let us note that, if we as reference

length accept the stopping distance of Stokes drop λ_0, then real stopping distance can be expressed by the formula of the form

$$\lambda_1 = \lambda_0 \frac{3}{0,17^{2/3}\mathrm{Re}_0}\left(\operatorname{arctg}\frac{1}{\sqrt{0,17\,\mathrm{Re}_0^{2/3}}} - \frac{\pi}{2} + \sqrt{0,17\,\mathrm{Re}_0^{2/3}}\right).$$

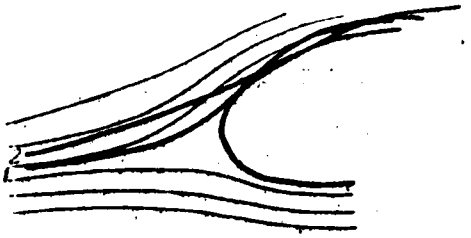

Fig. 25. Schematic of the flow around the fuselage of aircraft of air flow (thin lines) and of cloud drops of different sizes/dimensions (1 and 2).

Page 77.

Dependence of λ/λ_0 on Re_0 is represented in Fig. 26.

Estimating stopping distance in centimeters $\ell = (\lambda/\lambda_0)(2ur^2/9\mu)$, we see that for the drops of radius 10 μ ℓ does not exceed 5 cm, even if normal component of the rate of drop with respect to flow attains 100 m/s. Thus, hardly one should expect that the dead zone can exceed 5 cm. Obvious further that the zone of the disturbance/perturbation, introduced into the flow of "true liquid" by the motion of aircraft, cannot be substantially more than the zone of the disturbance/perturbation of air flow.

Above it was mentioned, that the air-stream velocity was

different from rate at infinity (in limits of accuracy of measurement) only in a comparatively narrow boundary layer, which was being expanded from 8 cm in 1st pilot's window to 20 cm in the latter/last window of passenger compartment.

To us it seems that the reasonings outlined above sufficiently convincingly indicates the fact that all utilized in flying laboratory instruments whose receivers were placed at the distances, exceeding 30-40 cm (air intake or the tests/samples of cloud drops, meters of liquid-water content, SIO, etc.), with a high degree of accuracy are measured the parameters, which relate to the undisturbed air flow.

3. Classification of the forms of icing.

As has already been mentioned above, for explaining the dependence of the character of icing on form and sizes/dimensions of the icing up body was investigated the icing of the bodies of various forms. The assembled material consists of many tens of sketchings and photographs of ice accumulation on spheres, disks, rectangular plates, cigar-shaped bodies, models of wings, elliptical cylinders, etc., which make it possible to trace the evolution of these forms, and also several hundred quantitative observations of the icing of cylinders in diameter 2, 10, 20, 34, 50 and 70 mm both rotating and

motionless ones.

The basic results of the analysis of the assembled experimental material are reduced to the following.

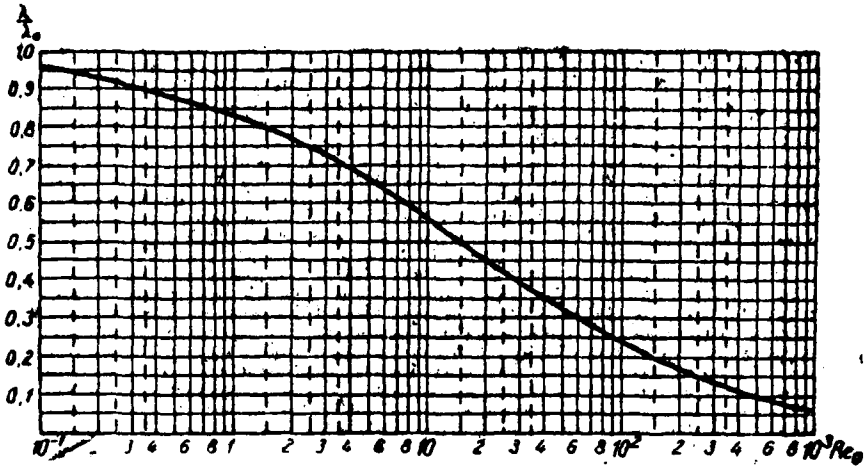

Fig. 26. Inertia landing run (stopping distance) of drop (axis y-OV), which has initial Reynolds number Re_0 (axis x-OV), expressed in the units of the inertial path of Stokes drop.

Page 78.

1. Grown ice on external parts of propeller-driven aircraft by pillar is determined by character of settling on them supercooled cloud drops and by process of freezing of deposited drops. Sublimation factors do not play the noticeable role (which completely coincides with the results of calculations in chapter III). Of this it is easy to be convinced, placing one body in the aerodynamic shadow of another, and in this case the shaded body it will not be covered by ice.

2. Diversity of different forms of icing affects changes in form, structure of surface and on structure of grown ice. Any form of icing it is convenient to consider as deflection from "ideal", accepting as the "such ideal" icing when the layer of grown ice is small and repeats the form of the body (for a cylinder - this is crescent-shaped form). The surface of ice smooth, color is milk-white. Ideal icing occurs with sufficiently low temperatures and low liquid-water contents.

Table 7 gives several cases of ideal icing.

Ideal icing is possible only when the deposited drops freeze virtually instantly, without spreading, the zone of settling drops in this case virtually coincides with the zone of the icing of body.

In the process of the icing when the thickness of grown ice becomes comparable with the sizes/dimensions of body, the form of ice gradually differs from ideal. This occurs the more rapid the greater water content of clouds.

Ideal icing easily can be explained, also, on the basis of the theoretical positions, developed in the preceding/previous chapters.

Actually/really the form of ideal icing is transferred well by the character of a change of the local coefficient of capture when the coefficient of freezing can be considered equal to unity, i.e., at sufficiently low temperatures. The milk-white color of ideal icing is explained by heterogeneity in the structure of ice, caused by the presence of an enormous quantity of the smallest air bubbles, which were being formed between the rapidly frozen drops of water.

Deflections from ideal icing can be observed on all three factors together or separately. About one means of deflection we already spoke above, namely, that with prolonged icing the thickness of the layer of ice becomes compared with the sizes/dimensions of body. In this case both the color and the surface of ice remain virtually without change. Often in this case from the edges of basic ice outgrowth ice has needle-shaped structure. This needle-shaped structure in edges can be explained, if we examine the flow pattern of body of cloud drops and to consider that in the edges of the ice deposit of air-stream velocity are comparatively great, and the local coefficients of capture on the strength of the fact that the flow is almost parallel to body, they are small. Action of both these factors contributes to the efflorescence of ice from edges.

Table 7.

(1) Дата	(2) Температура (градусы)	(3) Водность (г/м³)	(4) Вид облаков	(5) Запись по коду
17/III 1951 г.	—7	0,07	Ns	III
20/III 1951 г.	—13	0,07	Ac	III
25/III 1951 г.	—9	0,2	Ns	III

Key: (1). Date. (2). Temperature (degrees). (3). Liquid-water content (g/m^3). (4). Cloud species. (5). Recording on code.

Page 79.

Most frequently, when the grown ice is compared according to the thickness with the sizes/dimensions of body, the smallest heterogeneities on surface which earlier appeared by completely smooth, they grow to the fact that the surface becomes rough. Furthermore, so that the thickness of ice would achieve noticeable sizes/dimensions (on too small bodies) necessary that the liquid-water content would be sufficiently great. Latter/last fact contributes so that ice becomes less porous, in it it is less than air bubbles and its color is changed from milk-white to cloudy-white.

If flight occurs at sufficiently high temperature ($t>-5-7^{\circ}$), drops do not manage to freeze instantly and under the action of

AD-A083 374 FOREIGN TECHNOLOGY DIV WRIGHT-PATTERSON AFB OH F/G 1/3
PHYSICAL BASES OF AIRCRAFT ICING,(U)
AUG 79 I P MAZIN
UNCLASSIFIED FTD-ID(RS)T-1161-79 NL

3 OF 3
AD
A083374

END
DATE FILMED
DTIC

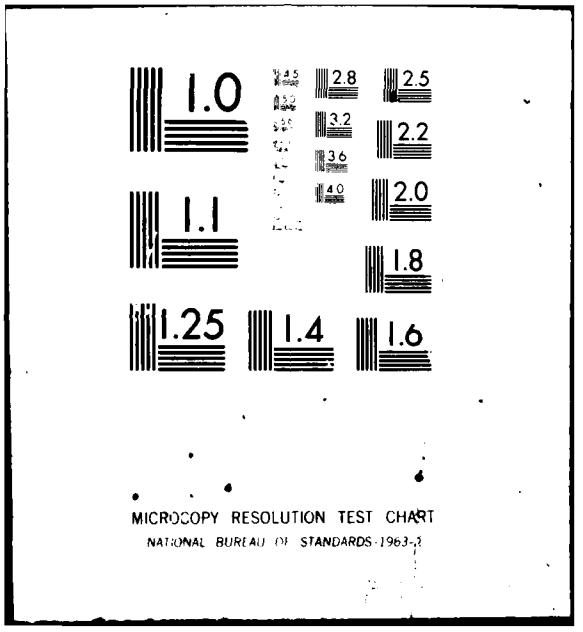
1.0
1.1
1.25
1.4
1.6
1.8
2.0
2.2
2.5
2.8
3.2
3.6
4.0
MICROCOPY RESOLUTION TEST CHART
NATIONAL BUREAU OF STANDARDS-1963-A

powerful/thick airflow somewhat are related to the edges of body. Under these conditions the increase of ice from edges occurs more rapidly and the frontal part of it becomes at first flat/plane (if earlier it was curved), and then U-shaped or as it occasionally referred to as, double-humped.

To the conversion of flat/plane form into U-shaped contributes not only the examined effect of the spreading of liquid, but also a change in the flow pattern. Actually/really, it is not difficult to see that the coefficient of capture in the edges of flat/plane body must be more - to edges cumulative effect of the deflecting force of flow on drop along the length the path of the latter decreases. This qualitative conclusion/output was have checked we experimentally. Actually/really, the edge of flat/plane disks and flat/plane rectangular plates despite all conditions they iced up more rapidly, forming characteristic ice rim.

The fact that the drops freeze not instantly, contributes so that ice of less porous ones, in it is less than air pockets and it, therefore, more is transparent.

Finally, with high temperatures and large liquid-water contents frequently is observed transparent ice whose surface is strongly uneven, and form can be very whimsical. This character of icing is

explained additionally to the factors enumerated above by the possibility of the noticeable fluctuations in liquid-water content, which lead to the dissymmetry of settling water and at first insignificant separate protuberances/prominences, which facilitate appearance, which grow subsequently into large/coarse mounds, as is evident, for example, in Fig. 21. As a rule, ice in this case either transparent or weakly turbid. The latter should be explained the presence in ice no longer air, but water inclusions, on the strength of the fact that at high temperatures, as shown in chapter III, freezes all depositing water. Ice formation at high, close to zero temperatures when manages to freeze all deposited water, sometimes is characteristic by the presence of the ice flows, which exit for the zone of settling drops. Latter/last phenomenon is observed at temperatures, as a rule, higher than -2, -3°.

Numerous observations of the icing of bodies made it possible to manufacture the simple system (code) of the recording of the encountered forms of icing, represented in Table 8. With the aid of the code it is possible with sufficient completeness to easily and rapidly write any form of grown ice encountered in practice. The code consists of three numerals the first of which reflects the form of grown ice, the second - the degree of transparency (color) and the third - the degree of the surface roughness.

As examples of the use of the code table 9 gives several cases of the icing of cylinders the diameter of 3 mm and their decoding, and also three photographs (Fig. 27) of the icing of different form, above which are shown the numerals of the code.

In conclusion let us again note that simultaneously the form of the icing of different bodies (for example, template/pattern and of plane) can be various (and is transmitted, therefore, by the different numerals of the code).

Page 80.

Therefore during the determination of effect on flight aircraft quality/fineness ratios of one or the other form of icing one should indicate, on what aircraft component this form is determined. Apparently the disregard of this factor was one of the reasons, on which the different authors in different ways estimated the role of that or another form of the icing (see, for example [10]).

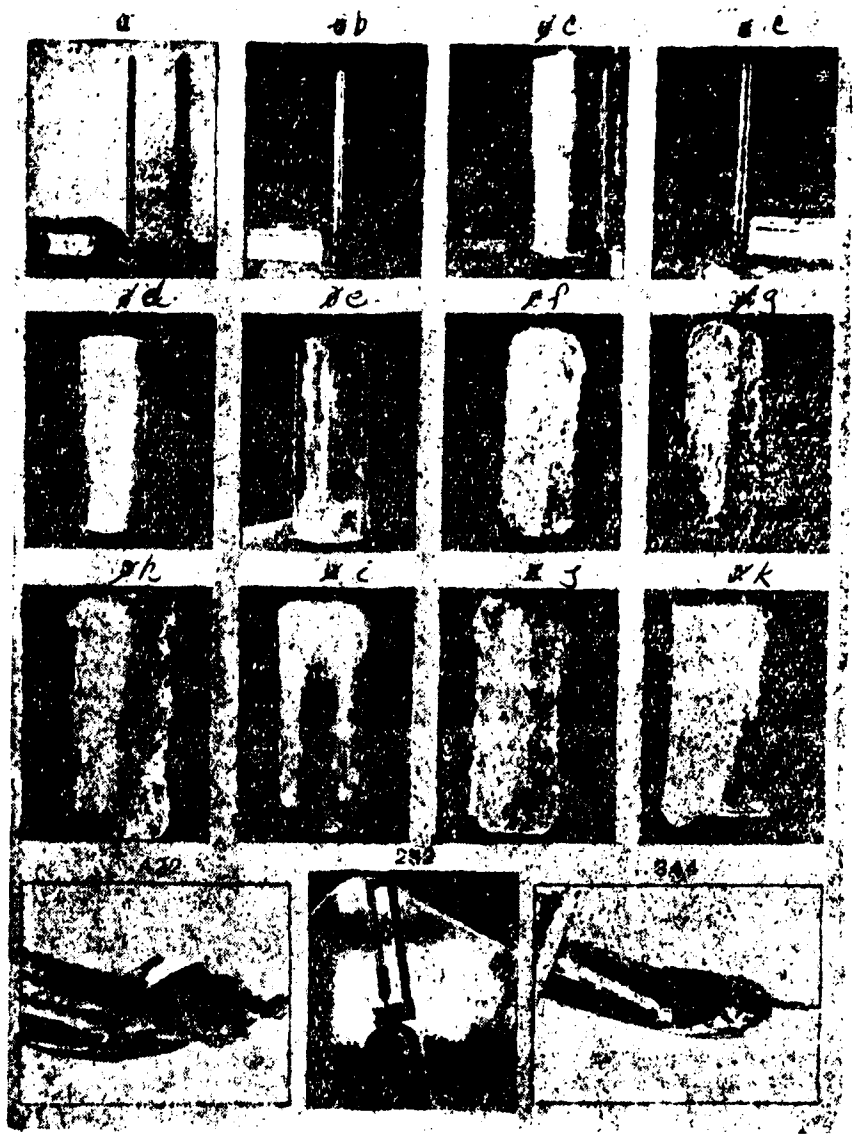

Fig. 27. Examples of the coating of the icing of different form.

4. The experimental check of theoretical calculations.

Bringing/finishing theory to numerical results makes it possible to conduct not only its qualitative, but also quantitative comparison with experimental results. In chapter II is shown that the intensity of the increase of ice on body can be written in the form

$$I = \frac{3}{\rho_л} u_\infty w \tilde{E}_л. \qquad (4.1)$$

First of all, logically, one ought not to have drawn a comparison of theory with experiment on the rotating cylinders, because their form and coefficient of capture in the process of icing are changed comparatively little. The instrument, used for this purpose, was three connected with the axis of the cylinder of the different diameters: 0.30, 1.99 and 6.93 cm. Cylinders were given in rotation with the aid of the electric motor, placed within larger of them. Distance from the edge of aircraft to the nearest cylinder exceeded 50 cm. Instrument was placed at the rear window of passenger compartment.

Table 8.

Цифра кода (1)	(2) Форма ледяного нароста	(3) Степень прозрачности (цвет)	(4) Степень шероховатости поверхности
1	(5) "Идеальная" (серпообразная - для цилиндрических тел, лукообразная - для тел вращения)	(6) Молочно-белый	(7) Гладкая
2	(8) Нарост сравним с размерами тела	(9) Мутно-белый	(10) Шероховатая
3	(11) С краев ледяные наросты принимают игольчатое строение	(12) Мутный	(13) Шероховато-бугристая
4	(14) Корытообразная или другая причудливая форма	(15) Слабо замутненный	(16) Бугристая
5	(17) Видны ледяные потеки	(18) Прозрачный	(19) Сильно бугристая

Key: (1). Numeral of the code. (2). Form of ice growth. (3). Degree of transparency (color). (4). Degree of surface roughness. (5). "ideal" (crescent-shaped - for cylindrical bodies, moon-shaped - for bodies of revolution). (6). Milk-white. (7). Smooth. (8). Outgrowth is compared with sizes/dimensions of body. (9). Cloudy-white. (10). Rough. (11). With edges ice outgrowths accept needle-shaped structure. (12). Turbid. (13). rough-uneven. (14). U-shaped or other whimsical form. (15). Weakly turbid. (16). Uneven. (17). Are visible ice drips. (18). Transparent. (19). Strongly uneven.

Table 9.

№ п/п (1)	(2) Дата	(3) Температура (°C)	(4) Водность (г/м³)	(5) Форма облачности	(6) Запись по коду	(7) Индекс рис. 27
1	4/XII 1952 г.	—10,7	0,04	Sc	121	а
2	4/XII 1952 г.	—15	0,21	Sc	211	б
3	18/XII 1952 г.	—5,7	0,18	Sc (Ns)	311	в
4	16/XII 1952 г.	—4,9	0,11	Ns (Sc)	321	г
5	18/XII 1952 г	—3,9	0,06	Ns	242	д
6	21/XII 1952 г.	—4,5	0,32	St	333	е
7	21/XII 1952 г.	—5	0,30	Ns	232	ж
8	22/XII 1952 г.	—1,1	0,21	St	423	з
9	23/XII 1952 г.	—8,4	0,31	St	343	и
10	23/XII 1952 г.	—9,1	0,47	Sc	322	к
11	23/XII 1952 г.	—8,4	0,31	St	221	л

Key: (1). No in sequence. (2). Date. (3). Temperature (°C). (4). Liquid-water content (g/m³). (5). Form of cloudiness. (6). Recording on code. (7). Index of Fig. 27.

Page 82.

During work with these cylinders (November-December 1954) the flights occurred predominantly in stratus and nimbostratus clouds. Data of the measurements of the thickness of ice frozen on cylinders are given in Table 10.

For the analysis of the data given in table 10, let us turn to equation (4.1). In this equation most variable value is w. Value β/ρ_* at temperatures lower than -5° can be accepted as constant for all cylinders. Then, assuming/setting flight speed on constant and

designating through I_1, I_2, I_3 icing intensities, and through $\tilde{E}_1$, $\tilde{E}_2$, $\tilde{E}_3$ - integral coefficients of the capture of the corresponding cylinders, can be written

$$I_1 : I_2 : I_3 = \tilde{E}_1 : \tilde{E}_2 : \tilde{E}_3. \qquad (4.2)$$

Since actually flight speed u_∞ does not remain constant and, furthermore, it does not remain constant in the process of the icing of cylinders and the spectrum of the distribution of the sizes/dimensions of drops r_{cp}, relationship/ratio (4.2) is approximate.

The practical limits of deviation of rate from the average/mean value of 190 km/h did not exceed 10-20 km. Hardly one should expect that r_{cp} for the same time interval oscillated more than to 0.5-1 μ about average/mean value of 4.5 μ. Taking into account possible vibrations u_∞ and r_{cp} it was established that in the increase of ice ratio $\tilde{E}_2/\tilde{E}_1$ could vary approximately/exemplarily from 0.55 to 0.72 at the most probable value, equal to 0.63 (one should consider that in this case somewhat they are changed and the diameters of cylinders, that it can introduce supplementary error $\approx$5o/o), and $\tilde{E}_3/\tilde{E}_2$ - approximately/exemplarily from 0.36 to 0.52 at the most probable value, equal to $\approx$0.43.

Table 10.

№ п/п (1)	Дата (2)	Время (3)	Толщина намерзшего льда (мм) на цилиндрах диаметром: (4)			Форма облака (5)
			3 мм	20 мм	10 мм	
1	21/XI 1954 г.	14.04—14.11	9,5	5,1	3,2	Sc
2	27/XI 1954 г.	11.25—11.29	3,6	2,5	0,3	Sc
3	27/XI 1954 г.	12.23—12.31	3,9	2,9	1,1	Sc
4	30/XI 1954 г.	15.39—15.50	3,5	2,1	0,1	Sc
5	30/XI 1954 г.	16.05—16.16	8,0	4,7	1,3	Sc
6	30/XI 1954 г.	16.32—16.42	7,0	4,3	1,5	Sc
7	1/XII 1954 г.	9.39— 9.43	3,7	2,6	0,7	Ns
8	7/XII 1954 г.	16.04—16.14	2,7	1,5	0,4	Frnb
9	8/XII 1954 г.	8.34— 8.54	4,3	2,1	0,3	St
10	8/XII 1954 г.	9.07— 9.15	8,5	5,6	1,7	Sc
11	8/XII 1954 г.	9.29— 9.34	7,0	4,0	1,0	Sc
12	8/XII 1954 г.	9.54— 9.58	6,3	3,1	0,1	Sc
13	9/XII 1954 г.	12.36—12.47	1,5	0,5	0,1	St (Sc)
14	9/XII 1954 г.	13.41—13.51	5,0	2,6	0,7	St (Sc)
15	9/XII 1954 г.	13.53—14.00	6,0	3,3	0,9	St (Sc)
16	9/XII 1954 г.	14.10—14.15	4,0	2,6	1,7	St (Sc)
17	9/XII 1954 г.	14.20—14.25	4,3	2,6	0,8	St (Sc)
18	9/XII 1954 г.	14.41—14.46	7,1	4,3	1,3	Sc
19	10/XII 1954 г.	9.25— 9.31	1,8	1,1	0,4	St (Sc)
20	10/XII 1954 г.	10.04—10.13	3,9	2,2	0,5	St
21	10/XII 1954 г.	10.17—10.24	2,7	1,5	0,2	St
22	10/XII 1954 г.	12.46—12.54	3,6	2,0	0,5	St
23	10/XII 1954 г.	12.59—13.09	3,7	1,7	0,3	St

Key: (1). No in sequence. (2). Date. (3). Time. (4). Thickness of frozen ice (mm) on cylinders with diameter. (5) Cloud form.

Page 83.

The comparison of experimental data with theoretical calculations shows that the amplitude of the oscillations of the relation to the icing intensity 20 mm of cylinder I_2 to the icing intensity 3 mm of cylinder I_1 is more than this is expected according to theory. Namely I_2/I_1 oscillated in limits from 0.33 to 0.74 at

average/mean value of 0.57. However, ratio I_3/I_2 oscillated in limits of 0.14 to 0.65 (if we jump points in thickness of grown ice it is less than 0.1 mm) about average/mean value of 0.32. In either case the experimental values of relations proved to be than somewhat lower predicted by theory in the first case approximately/exemplarily to 10o/o and the secondly approximately/exemplarily to 25o/o. Apparently, great value in these systematic errors has the fact that the measurements of the thickness of grown ice, as a rule, began from thin cylinder, by the diameter of 3 mm, and concluded with 70-mm. Since measurement was conducted within the aircraft where the temperature was more than 0°, then is possible the layer of ice on 20 mm and still more the layer of ice on 70 mm cylinders managed somewhat to thaw to the moment/torque of measurement. Furthermore, the diameter of large cylinder was measured not by micrometer, but by vernier caliper, which, naturally, decreased the accuracy of reading.

In spite of some shortages in the procedure of experiment, obtained results should be considered it sufficiently well agreeing with theory.

In expeditions 1955 and 1956 we obtained the possibility somewhat otherwise to approach testing of theoretical relationship/ratio (4.2). For this purpose was used the already mentioned previously instrument SIO, which with an accuracy to 0.1 mm

continuously recorded the thickness of ice.

Utilizing theoretical calculations, it is possible, measuring the intensity of ice accumulation on SIO - 1 in form (4.1), to determine the value of liquid-water content $w_{сно}$. Value $w_{сно}$ found thus characterizes average/mean liquid-water content in certain section. In calculations $\rho_л$ given below it was assumed/set by the equal to 0.3 g/cm².

On the other hand, at our disposal was located the instrument of Zaytsev [6], making it possible to directly measure the values of liquid-water content $w_з$. However, the liquid-water content, determined by the instrument of Zaytsev, characterizes sections ten times less than the liquid-water content, calculated according to data of SIO. Therefore to that time interval Δt, for which was determined the average/mean intensity of the increase of ice on SIO, sometimes was 5 more than the measurements of liquid-water content by the instrument of Zaytsev or which was located more average/more mean in the section in question value $w_з$.

The results of comparison $w_{но}$ and $w_з$ are given in table 11, where in the 1st row are given values $w_з$, in the 2nd - $w_{си}$, in the 3rd - number of measurements $n_з$, from which was determined value $w_з$, in the 4th - number of drops according to which was located $r_{ср}$, given

in the 5th row, in the oth - deflection of some values of liquid-water content from others $\Delta w = w_{СИО} - w_3$ and in the 7th - ratio $\Delta w/w_3$ in percentages.

It should be pointed out that values $r_{ср}$, given in the 7th row, are not sufficiently representative, since they are based on a comparatively lean microstructural material. Meanwhile for obtaining more or less reliable information about r_p, as was mentioned in chapter II, it is necessary that the measured spectra would contain thousand and even tens of thousands of drops. The errors in determination $w_{СИ}$, due to incorrect determination $r_{ср}$ can reach tens of percent.

Pages 84-85.

However, in spite of this, table 11 it shows that the deflections Δw on the whole do not exceed the values, obtained by V. Ye. Minervin during the comparison of different instruments, which measure the liquid-water content. The presence of such deflections reflects, first of all, the special feature/peculiarity of the vibrations of liquid-water content in clouds and the fact that the liquid-water content, measured by the instrument of Zaytsev, characterizes the too small volumes of cloud, ten times it is less than the volumes, characteristic for $w_{СИО}$. The results of comparison w_3 and $w_{СИО}$ testify

about a good agreement of theory with experiment. It must be noted that for the problem of icing a more characteristic value is w_{liq}, i.e. the liquid-water content, which characterizes the noticeably larger sections of clouds, than w_3.

A number of cases, represented in table 11, can be doubled, if we draw the results of measurements in the absence of microstructural observations. Taking as for these latter r_p equal to 5μ, it was obtained by table 12.

Table 11.

(1) Дата	(2) 8 апреля 1956 г.	(2) 9 апреля 1956 г.						(2) 10 апреля 1956 г.						
(4) Время	13.32 13.33.5	11.23—11.35	11.27—11.26	12.16—12.21	12.30—12.34.5	12.31.5—12.40	12.40—12.43	13.16—13.25	13.25—13.28	13.28—13.31	13.34—13.40	13.40—13.45	13.49—13.53	15.15—15.18
№ п/п (5)	1	2	3	4	5	6	7	8	9	10	11	12	13	14
$w_з$	0,06	0,02	0,07	0,03	0,08	0,28	0,33	0,36	0,47	0,13	0,01	0,31	0,20	0,05
$w_{сио}$	0,13	0,005	0,04	0,02	0,11	0,28	0,37	0,23	0,38	0,11	0,01	0,16	0,17	0,01
$n_з$	1	2	1	3	3	4	3	9	5	6	1	1	3	3
n	—	416	1204	—	367	1119	1315	2502	623	101	114	1010	602	162
$r_{ср}$	6,7	2,9	4,1	3,3	6,5	4,2	6,3	4,8	6,5	7,0	8,2	6,5	2,8	3,4
Δw $w_з - w_{сио}$	−0,07	0,015	0,03	0,01	−0,03	0,0	−0,04	0,13	0,09	0,02	0,00	0,18	0,03	0,04
$\frac{\Delta w}{w_з} \cdot 0$	−116	75	43	33	−37	0	−12	36	19	15	0	53	15	80

(2) 12 апреля 1956 г.							(3) Среднее квадратичное отклонение
10.30—10.36	10.36—10.46	11.00—11.30	11.34—11.38	12.42—12.49	13.04—13.11	13.11—13.40	
15	16	17	18	19	20	21	22
0,19	0,08	0,06	0,16	0,37	0,24	0,29	—
0,25	0,08	0,06	0,16	0,36	0,32	0,18	—
6	6	7	1	3	6	4	—
313	554	293	140	744	1686	1398	—
2,7	2,4	3,0	3,7	2,8	2,9	3,8	—
−0,06	0,00	0,00	0,00	+0,01	−0,08	0,11	$6{,}5234 \cdot 10^{-2}$
−32	0	0	0	3	−33	38	43

Key: (1) Date; (2) 8 April 1956; (3) Root-mean-square deviation; (4) Time; (5) No. in sequence.

Table 12.

(1) Дата	(2) 8 апреля 1956 г.							
(4) Время	13.30—13.31	13.31—13.32	13.43—13.48	13.48—13.50	13.50—14.27	15.17—15.26	15.26—15.32	15.32—15.37
№ п/п (5)	1	2	3	4	5	6	7	8
$w_э$	0,29	0,19	0,14	0,06	0,035	0,10	0,17	0,06
$w_{сно}$	0,11	0,005	0,12	0,06	0,002	0,12	0,01	0,05
$n_э$	1	1	2	2	2	7	3	3
$\Delta w = w_э - w_{сно}$	0,18	0,185	0,02	0,00	0,33	−0,02	0,16	0,04
$\frac{\Delta w}{w_э}$ %	62	97	14	0	94	20	94	17

(6) 9 апреля 1956 г.									(7) 10 апреля 1956 г.			(8) 12 апреля 1956 г.		(9) Среднее квадратичное отклонение
11.18—11.23	11.25—11.27	11.28—11.31	11.31—11.31	12.44—12.48	12.48—12.52	12.52—12.58	12.58—13.05	13.05—13.12	13.12—13.14	13.15—13.16	15.18—15.26	15.26—15.30	12.19—12.52	13.11—13.17	
9	10	11	12	13	14	15	16	17	18	19	20	21	22	23	24
0,18	0,15	0,13	0,08	0,15	0,27	0,115	0,08	0,12	0,15	0,51	0,22	0,04	0,020	0,13	--
0,10	0,18	0,09	0,09	0,10	0,23	0,07	0,07	0,08	0,30	0,64	0,09	0,05	0,09	0,01	-
1	2	2	3	1	5	4	4	6	1	1	1	4	3	1	-
0,08	−0,03	0,01	−0,01	−0,01	0,04	0,015	0,01	0,01	0,15	−0,13	0,13	−0,01	0,11	0,09	$8,072 \cdot 10^{-2}$
44	−20	30	−11	−2	15	39	12	33	100	25	59	25	55	69	1

Key: (1) Date; (2) 8 April 1956; (3) Root-mean-square deviation; (4) Time, (5) No. in sequence.

Pages 86-87.

Here root-mean-square deviation w_3 from $w_{\text{сно}}$ increased approximately/exemplarily one and a half times; however, also in this case of disagreement w_3 and $w_{\text{сн}}$ bear qualitatively and quantitatively the same character, as the vibration of the instantaneous[1] values of liquid-water content of the relatively averaged value, indicated by V. Ye. Minervin.

FOOTNOTE [1]. By "instantaneous" we understand the values of liquid-water content, obtained by the instrument of Zaytsev and the drop-forming water which characterize the content in volume on the order of 10-20 l. However, values $w_{\text{сно}}$ characterize volumes thousands times large. ENDFOOTNOTE.

Finally, in these expeditions 1955-1956 were checked other theoretical calculations, presented in chapter II and the characterizing interconnection icing intensities of standard - (SIO), template-indicator and the plane or the aircraft of Il-14. The thickness of grown ice on plane was determined from the graduated

dowel, fastened/strengthened in the middle of the wing where the chord of section was equal to 310 cm. Readings were conducted with the aid of binoculars, with an accuracy to 2-3 mm. So that this low accuracy of reading would not lead to significant errors, was constructed the time/temporary graph/curve of the increase of ice on plane and SIO, after which the intensity of the increase of ice was determined from the slope tangent of straight lines, levelling off broken lines in the time intervals of order of tens of minutes. The results of a similar processing are given in Table 13. The first three columns are related to materials 1955, the others - to 1956. If we reject/throw the case of 16 December 1955, which we will examine separately, then it is evident that virtually relation I_n/I_0 is changed in the very small limits: from 2.6 to 3.3, differing from average/mean value of 3.0 not more than for 13o/o. The obtained results confirmed the theoretical calculations, made in chapter II (Fig. 14). As can be seen from Fig. 14 according to theory this relation must be changed from 2.75 to 3.25 with rate change from 50 m/s (180 km/h) to 100 m/s (360 km/h) and mean radii of drops r_p from 3.5 to 10 μ. In this case the most probable values (with $u_\infty = 70$ m/s and $r_{cp} = 4 \div 5\mu$) relation I_n/I_0 are equal to 3.1.

The insignificant understating of relation $\frac{I_n}{I_0}$ in comparison with theory is completely regular, since on the average the coefficient of freezing in end connections of the profile/airfoil is

less than in SIO (see Chapter IIA).

Table 13 shows that relation $\frac{I_n}{I_0}$, according to theory, does not depend on liquid-water content and icing intensity - latter, as can be seen from table, they were changed sometimes more than 5 times.

In flight on 16 December on 1955 anomalous deflection $\frac{I_n}{I_0}$ from average/mean value can be explained by the specific character of the increase of ice. In this flight the icing was most intense of those all occurred into 1955-1956. Icing intensity I_0 reached to 0.65 mm/min. And despite the fact that the temperature on stand thermometer was -5, -6°, the coefficient of freezing on plane β_n was, apparently, less than unity. Furthermore, on receiving cylinder grew transparent and very uneven ice (Fig. 21), thanks to which "linear" icing intensity in mm/min artificially was overstated, due to incomplete filling volume. The fact is that the protuberances/prominences of ice increase more rapidly because they take away/gather the water, intended for filling of adjacent indentations. This artificial overestimate of "linear" icing intensity it would be possible to formally consider, introducing the effective density of ice ρ_n. However, this formal account does not give practical results, since ρ_n, nevertheless remains the value of unknown. The appearance of grown ice of the type, given in Fig. 21, gives grounds to assume that ρ_n is less than unity by tens of

percent, that already one can completely explain examined above anomalous value $I_n / I_s = 2{,}4$.

Summing up that presented, it is possible to say that virtually with an accuracy to 15c/c conversion factor from the icing intensity, recorded by SIO to the icing intensity of plane in its central section (with chord of *3 m), retain constant value equal to 3.0.

This fact, found theoretically and confirmed it is experimental, it made it possible to draw conclusion [19, 20] about the advisability of instrumentation of SIO to scheduled flights for the collection of the objective statistical data and timely information of pilot about the thickness of grown ice on the plane of aircraft.

Table 13.

(1) Дата	(2) 8 декабря 1955 г.	10 декабря 1955 г.	16 декабря 1955 г.	(3) 8 апреля 956 г.	9 апреля 1956 г.	
(6) Время				13.20—13.45	11.20—11.40	12.35—13.20
(7) № п/п	1	2	3	4	5	6
$I_в$	—	—	—	0,09	0,075	0,15
$I_п / I_в$	3,3	3,1	2,4	3,3	3,2	2,75
$I_в / I_ш$	—	—	—	0,44	0,45	0,36
$I_ш / I_в$	—	—	—	7,5	7,0	8,0

(3) 10 апреля 1956 г.			(3) 12 апреля 1956 г.			(4) Среднее значение	(5) Максимальное отклонение (в %)
13.10—14.00	14.16—15.20	15.05—15.35	11.20—11.50	12.05—13.05	13.30—14.00		
7	8	9	10	11	12	13	14
0,14	0,14	0,04	0,052	0,06	0,225	—	—
3,2	3,0	2,6	2,8	2,7	2,8	3,0	13
0,59	—	0,33	0,33	0,32	0,55	0,42	40
5,5	—	7,9	8,5	8,3	5,1	7,2	26

Key: (1). Date. (2). December. (3). April. (4). Average/mean value. (5). Maximum deflection (in o/o). (6). Time. (7). No in sequence.

The fact that sometimes representations obtained thus about the thickness of grown ice on plane will prove to be erroneously high, is not obstruction to the made recommendation, since under such conditions ice on plane has specific channel-shaped form and it is more dangerous than the smooth outgrowth of ice. Therefore the artificial overestimate or real rate of icing seemingly compensates the increasing danger due to the specificity of form.

Since many previous works were based on observations of icing with the aid of flight aerologist's template-indicator, it was represented by advisable to examine connection/communication of degree and intensity of the increase of ice on template/pattern with the appropriate characteristics on plane and SIO. The results of this comparison can be illustrated by the 3rd and 4th rows tables 13, from which it appears, that the ratio of intensities of ice formation on plane to the appropriate intensity on template/pattern I_n/I_m oscillates in the wider limits (after being deflected ≈20-25o/o) about certain average/mean value, equal to ≈0.4. Accurately also in large limits it oscillates and $I_m/I_{CИO}$ varying approximately/exemplarily from 3.2 to 8.5. These numerals correspond according to vibration theory in r_{cp} in clouds approximately/exemplarily from 3 to 6.5 μ, which will be in complete

agreement with our microstructural investigations.

The given above data and corresponding reasonings are related to aircraft IL-14. On it was unfortunately today for us possible to conduct similar investigations on an aircraft of the type LI-2; however, the agreement of theory with the experiments, made on the aircraft of IL-14 gives grounds to assume that and for LI-2 it is possible to use the results of the theoretical calculations, made in chapter II.

Page 89.

Chapter V.

ICING OF HIGH-SPEED AIRCRAFT.

1. Features of icing at high velocities of flight.

Violent aeronautical development in recent decade led to the fact that jet-propulsion technology began to acquire ever increasing weight both in the serviceman and in civil air fleet. Logical therefore to examine, what special features/peculiarities introduces into the problem of icing high-speed/velocity aviation. For this let us return to the fundamental principles, which characterizes the intensity of the icing

$$I = \frac{w}{\rho_л} u_\infty \beta \cdot E_0 \qquad (2.2)$$

For rates $u_\infty < 100$ m/s already at temperatures of lower than -5° basic difficulty in the use/application of equation (2.2) presents the determination of the integral coefficient of capture $\tilde{E}_1$, coefficient β differs little from unity. With an increase in the

velocity coefficient E, increases, approaching in the spout of profile/airfoil the specific limiting value which easily is located with the known form of profile/airfoil. At the same time decreases the coefficient of freezing β, becoming actually important value in equation (2.2), to be determined.

Therefore in present chapter to more advisably begin investigation not with examination $\tilde{E}$, as this was earlier, but from examination β.

In chapter III was studied the heat balance on the surface of the moving/driving body and according to relationship/ratio (3.18) was constructed the nomogram of Fig. 17, which makes it possible to calculate the temperature of the icing up surface in dependence on the flight speed and temperature of the undisturbed flow. In this same chapter it is incidentally shown about the validity of the used intermediate relationships/ratios and for high speeds. Let us note that the validity of a similar affirmation follows also of the monograph "Contemporary state of high-speed aerodynamics" edited by Khauert [2], Vol. 1, chapter X.

Let us return to Fig. 17. Let us recall that in the calculations on the basis of which is made nomogram given on this figure, it was assumed that water content of clouds w was equal to that value w_0.

which exactly compensates evaporation.

Page 90.

It is clear that if $w < w_i$, then icing will not be. But if $w > w_i$, then, in order from this same nomogram to find t_s, it is necessary to replace real flight speed u_∞ by that given u_n, equal to

$$u_n = u_\infty \sqrt{1 + \frac{2 c_p \tilde{E}(L_s, t_s + t_0 - t_s)(w - w_i)}{r u_\infty}}$$

The examined nomogram (Fig. 17) gives the possibility for each value of recovery factor r to construct the curve of the dependence of the temperature of airflow t_0 on speed u_∞, at which t_s turns into zero. Such curves are represented in Fig. 28 for different recovery factors r. The limits of change r are accepted equal to 1.0-0.7, since according to the known data of value r at any point of aircraft profile/airfoil they are included precisely within these limits. If necessary to easily construct analogous curves and for smaller values of r.

It is obvious that if with assigned r and u_∞ the temperature of air is higher than found from Fig. 28, the icing is impossible. Moreover, icing it can not be, also, at lower temperatures, if water content of clouds $w < w_i$. From Fig. 28 it is clear that at supersonic

speeds, for example 340 m/s, and to the temperature of air of -30°, an icing must not have the place at one point of profile/airfoil. At the same points where r>0.9, icing cannot be even with t_0=-40°.

One of features of the icing of high-speed aircraft consists in the fact that at high velocities of flight theoretically is completely feasible another mechanism of icing, different from that examined earlier, that becomes apparent even during flights in ice clouds. As is known, recovery factor r does not remain constant along the enclosure of wing, but it decreases in proportion to removal/distance from end connections from r=1 to r≈0.7. This distribution r leads to analogous distribution and the temperature of the wing surface, i.e., temperature is reduced in proportion to removal/distance from end connections of the profile/airfoil. Under specific conditions the temperature of end connections of the wing can prove to be higher than 0°, but it is further, being reduced, it can become negative, i.e., the zero isotherm will pass somewhere along profile/airfoil. Thus, even when flight occurs in ice clouds, is possible aircraft icing, since the crystalline particles of ice, which deposit on frontal aircraft component where temperature $t_s > 0°$, they can have time to melt, and then to be referred by the flow in the region of minus temperatures where the water is crystallized anew.

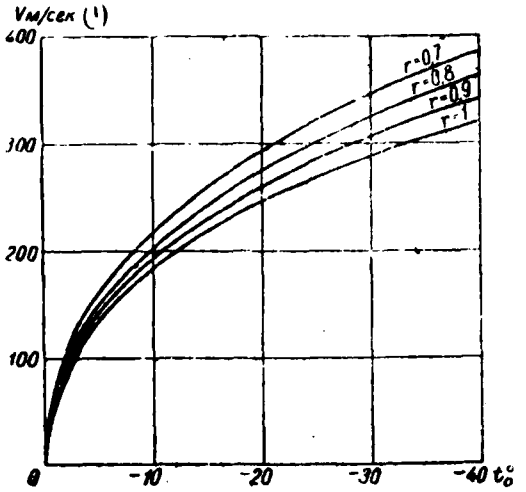

Fig. 28. Dependence of the flight speed u_∞, temperature of the moistened surface necessary for elevation to 0°, on the temperature of air t_0 with different recovery factors r.

Key: (1). s.

Page 91.

The temperature distribution indicated along wing can in principle lead to the increase of ice of the whimsical form when ice is formed at certain distance from frontal surface. This form of ice is especially dangerous, since it extremely makes aerodynamic aircraft quality/fineness ratios worse. Similar icing was noted in the literature [9, 23]. In I. G. Ponelko's report [23] are described

several such cases, which occurred at speeds 800-850 km/h and 600-700 km/h.

With known distributions of recovery factor r along wing profile it is possible to determine those conditions, under which it occurs icing of the type examined above and at what distance from the spout of profile/airfoil passes the zero isotherm.

The calculation procedure is such.

On assigned flight speed u_∞ and known r in spout (usually =1) is found that temperature of air t_1 (from Fig. 28), with which the temperature of wing in spout is equal to 0°. If the real temperature of air $t_0<t_1$, the examined mechanism of icing it is impossible. If $t_0>t_1$, then find similar r_1 (from the same Fig. 28), with which the temperature of surface is equal to zero. If the distribution r according to profile/airfoil is such, that in certain place $r=r_1$, then the examined mechanism of icing can occur. Line $r=r_1$ is the line of the zero isotherm and separates the frontal region of wing with the positive temperature on which the icing does not originate from the region of wing with minus temperature, where can occur the increase of ice. From theoretical calculations it is known that for some wing profiles/airfoils r sharply it falls from 1 at the critical point to 0.75 at a distance of $\approx$0.1 airfoil chord. Further r is

changed insignificantly, completing small vibrations about the curve, which is reduced approximately/exemplarily to 0.72 at the end of the profile/airfoil. In this case, the appearance of the zero isotherm and the mechanism of icing[1] noted above can take place, as is evident from Fig. 28, at flights in a velocity of 200 m/s (720 km/h) and temperature of air from -9 to -12°, at flights in a velocity of 250 m/s and temperature of air from -15 to -21°, at flights in a velocity of 300 m/s and temperature from -23 to -33°, at the speed of 340 m/s (M>1) from -31 to -45° finally at the speed of 370 m/s at temperature of lower than -39°.

FOOTNOTE [1]. Conditions presented below are necessary, but they are insufficient for similar icing, since it is completely probable that with not too large liquid-water contents, the evaporation from the overheated surface of aircraft will exceed wetting due to collision with cloud drops. ENDFOOTNOTE.

From the examination of the mechanism of icing, which leads to so dangerous a form of ice accumulation on the planes of high-speed aircraft, it is possible to draw an important quantitative conclusion. From Fig. 28 and values of speed and temperature corrected above, with which is possible the icing of the form in question, it follows that an increase in the velocity of flight on 30-40 m/s must ensure the destruction of conditions favorable for

similar icing and the cessation of further increase of ice. This "speed maneuver" in the series/row of cases completely attain for contemporary aircraft can prove to be the effective means of deicing of aircraft at the high subsonic speeds of flight. The absence at our disposal of experimental data does not make it possible, unfortunately, to check the expressed considerations.

In connection with the possibility of the supplementary mechanism of the icing of high-speed aircraft, a question about the coefficient of freezing acquires qualitatively another character.

Page 92.

The fact is that at such high speeds the portion of the heat, which is isolated with the freezing of drops, plays already small role in comparison with kinetic heating, and the derived speed u_n differs little from flight speed u_∞. In this case the temperature of surface t_s corresponds to that found from Fig. 17 and if $t_s < 0$, then the coefficient of freezing β is determined by formula (3.14), indicated in chapter III, i.e., $\beta = 1 - \frac{w_l}{w}$. Consequently, for determination β it is necessary, first of all, to determine w_l, that corresponds to obtained temperature t_s.

As it was shown in chapter III, w_l it is expressed by equation

(3.21)

$$w_i = \frac{\alpha}{\bar{E}_A u_{\infty}} \cdot K_s(t_s, t_0, P_0).$$

For determination $K_s(t_s, t_0, P_0)$ in chapter III was constructed a comparatively simple nomogram (Fig. 18). A question of the determination of heat-transfer coefficient α was also examined in chapter III. We will be restricted here only to repetition, that all known to us data attest to the fact that α virtually oscillates in the limits of 10^{-2}-10^{-3} cal/cm^2 s°C.

The absence of precise information about coefficient α does not give the possibility to find precise values w_i under varied conditions. However, it is possible that at sufficiently high flight velocities overheating the surface of aircraft can prove to be so/such considerable which quantity of cloud moisture depositing on this surface will be is knowingly insufficiently for the compensation evaporation from it. Is in other words possible such situation when $w < w_i$ and in this case, naturally, icing will not be even during flights in the such strongly supercooled clouds when the temperature of the surface of aircraft remains negative.

If in this case it is possible to rate/estimate value w_i to from below and show, that this value $w_{i\,min}$ more than the encountered values of water content of clouds w, this will mean that the icing is

impossible.

In order to rate/estimate from below the real values of liquid-water content w_1, necessary for the compensation for surface evaporation of aircraft, it follows, as is evident from (3.21), to rate/estimate from below value α and K_3 and on top - value $\tilde{E}_*$.

Thus, the knowledge of value $\tilde{E}_*$ is very important for evaluating the real possibilities of icing in flight with high speeds.

Before converting/transferring to estimate of the magnitude $\tilde{E}_*$, let us pause separately at the calculation of the coefficients of capture E at the supersonic flight speeds whose knowledge is necessary during the study of the integral coefficients of capture $\tilde{E}_*$.

2. Calculation of the coefficients of capture at supersonic flight speeds.

The profiles/airfoils of wings of high-speed aircraft differ significantly from the profiles/airfoils, used in subsonic aircraft. The greatest thickness of these profiles/airfoils is given to the middle: rhombiform or biconvex profiles. In present section we will examine the trajectories of drops about rhomboid profiles/airfoils.

In connection with the fact that is examined the supersonic flow, double wedge airfoil can be replaced with wedge (Fig. 29), since the character of the flow around end connections in this case does not affect the form of the rear half profile/airfoil.

The task of determining the trajectories of drops, which deposit on the wedge, which moves with the supersonic speed, mathematically considerably simpler than the analogous task at subsonic speeds can be led to the complete analytical solution.

Let us dismantle/select this task in more detail.

Infinite wedge with an angle at apex/vertex 2δ moves in with zero angle of attack with a certain speed of v_0, such, that $M_0>1$. We investigate such motion when in the apex/vertex of wedge is formed the attached shock wave, directed at angle ε toward the axis of the symmetry of wedge. To shock wave (upstream) the air is not disturbed, and drops move rectilinearly with constant velocity v_0. Behind shock wave (downstream) the parameters of flow (temperature, pressure, density and speed of its motion) are changed, due to which they are

curved and trajectory of drops.

Before converting/transferring directly to the trajectory calculations of drops, it is necessary to mean the shock-wave angle and the character of a change in parameters and speed of flow upon transfer through this oblique shock. The theory of this question is well known [2, 30]. For example, on the nomogram available in [30] (page 432, Fig. 336), possible knowing M_0 and δ [1], to find ε and M_1.

FOOTNOTE [1]. Here and throughout index 0 corresponds to the undisturbed flow (upstream), but index 1 - to disturbed flow (downstream from the jump of deviation). ENDFOOTNOTE.

However, knowing ε, on product $M_0 \cdot \sin \varepsilon$ from Fig. 30 (constructed according to the table, given in [2] on page 121), it is possible to find ratios ρ_1/ρ_0, P_1/P_0 and T_1/T_0.

After supplementing the indicated graphs/curves by known relationships/ratios $M_n = \frac{v_0}{\sqrt{\gamma RT_0}}$ and $M_1 = \frac{v_1}{\sqrt{\gamma RT_1}}$, where for air $\gamma = c_p/c_v = 1,4$ $R = 2,8704 \cdot 10^6$ cm^2/s^{3}deg - gas constant, we have complete possibility sufficiently simply from the known values of P_0, ρ_0, T_0 and v_0 to find P_1, ρ_1, T_1 and v_1.

Thus, task lies in the fact that to find the trajectory of the

motion of the drop of the assigned radius r, which flows around together with airflow about the wedge with apex angle 2δ. The direction of the motion of wedge coincides with its bisector (zero angle of attack).

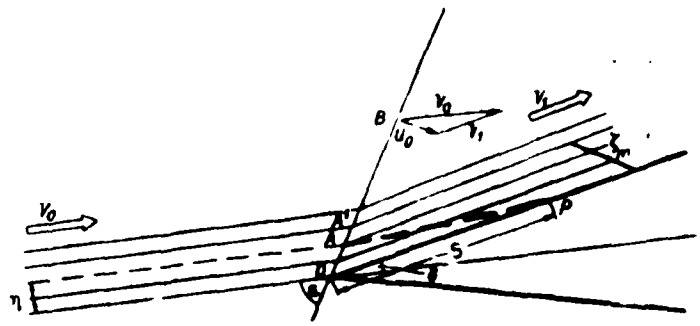

Fig. 29. The schematic of the flow around wedge of the supersonic flow of the aerosol (solid lines showed the trajectories of air particles, dash - trajectories of drop).

Page 94.

Motion occurs with attached shock wave. The parameters of air are upstream known - temperature $T_0=t_{\beta_0}+273$, pressure P_0, density ρ_0. Speed of flow to shock wave v_0. On the basis of these data, as it was shown above, are located values ε and parameters of air P_1, ρ_1, T_1 and the speed of its motion v_1 downstream.

For the first time this task was sufficiently clearly formulated also by Traybus and Giber [24], which brought its solution to numerical results for a series/row of the cases. Most completely it was solved by Serafin [75], for which it was possible to obtain the

trajectories of drops in parametric form. The basic ideas of Serafin are used in the solution of stated problem given below.

The assumptions, placed as the basis of the solution, remain the same as and in Serafin, namely:

1. The water droplets are always spherical and do not change size/dimension.

2. Gravitational force can be disregarded/neglected.

3. Air resistance to motion of drop they are resistance of viscous fluid.

4. Imbalance of forces, which act on drop from the moment of its incidence/impingement into shock wave and to output from it, can be disregarded/neglected during trajectory calculation.

The first three assumptions coincide with analogous assumptions during the solution of the tasks of flow with low speeds (Chapter 1).

Disregarding the imbalance of forces (point/item 4) does not cause doubt, since the thickness of shock wave is equal to several mean paths of molecules of air and is of the order of 25 0^{-5} mm [30], so that drop was under the effect of these forces of less than 10^{-8} s.

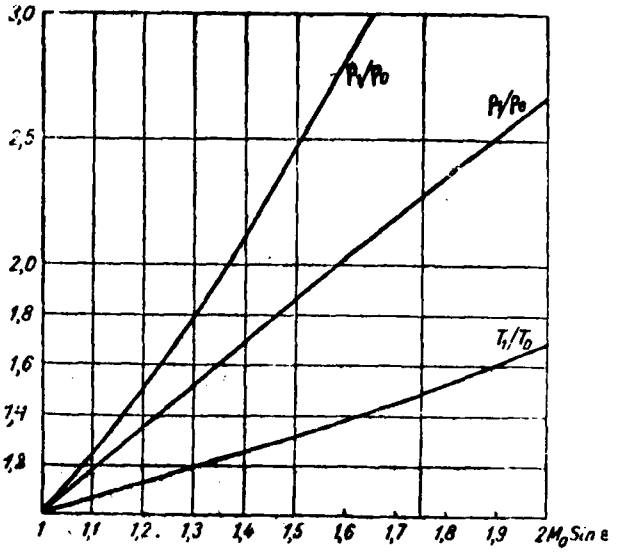

Fig. 30.

Page 95.

Thus, to point A (Fig. 29) drop moves rectilinearly together with flow. At the moment of output from shock wave the drop has entire the same speed $\vec{v_0}$ while flow already has another speed, equal to $\vec{v_1}$, i.e., the speed of potash with respect to flow is equal to $\vec{u_0}=\vec{v_0}-\vec{v_1}$. Consequently, the task of the determination of the trajectory of drop is reduced to the determination of its motion in still air with an initial velocity of $u_0=|\vec{v_0}-\vec{v_1}|$. Thus, the system of differential equations, which is determining the trajectory of the

motion of drop (chapter I, formula 1.6) actually is replaced by one equation of motion of drop relative to the flow

$$m\frac{du}{dt} = F, \tag{5.1}$$

where $m=4/3\pi r_3\rho$ - mass of drop, u - speed of the motion of drop relative to flow, $F=6\pi r\mu_1 \cdot u(1+0.1/Re^{2/3})$ - the resisting force, acting on drop (chapter I, formula 1.4).

The equation of motion of drop considerably is simplified, if we introduce the dimensionless coordinates where as the unit of path λ_0 is accepted the stopping distance of the drop of the given radius r, which obeys the law of Stokes, i.e., $\lambda_0=\frac{2}{9}\frac{u_0 r^2}{\mu}\rho_s$, for time unit τ_0 - transit time of this path at the speed of motion u_0, i.e., $\tau_0=\frac{2r^2}{9\mu}\rho_s$ for the unit of speed - speed u_0. During the introduction of the dimensionless quantities indicated the equation of motion of drop depends only on one dimensionless parameter B [1] and takes the comparatively simple form

$$\frac{d^2\zeta}{d\tau^2}=-\frac{d\zeta}{d\tau}\left[1+B\left(\frac{d\zeta}{d\tau}\right)^{2/3}\right] \tag{5.2}$$

with the initial conditions

$$\zeta(0)=0,\ \zeta'(0)=1. \tag{5.3}$$

FOOTNOTE [1]. Parameter B characterizes the degree of deviation of the

force of viscosity F from that expressed by Stokes' law force F_0, i.e., $B=F-F_0/F_0$ and, as shown in chapter I, $B=0.17RE_0^{2/3}$, where $Re_0=2u_0r/\nu_1$. ENDFOOTNOTE.

Applying consecutively/serially substitutions $\left(\frac{d\zeta}{d\tau}\right)^{3/2}=x$ and $e^{2/3\tau}=z$ equations (5.2) can be integrated to end/lead. The solution of equation (5.2) taking into account initial conditions (5.3) takes in this case the form

$$\zeta=\frac{3}{B^{3/2}}[\operatorname{ctg}\varphi_0-\operatorname{ctg}\varphi-(\varphi-\varphi_0)], \tag{5.4}$$

where

$$\varphi_0=\operatorname{arctg}\frac{1}{\sqrt{B}},$$

$$\varphi=\operatorname{arctg}\sqrt{\left(1+\frac{1}{B}\right)e^{\frac{2}{3}\tau}-1}.$$

Page 96.

The maximum path, which passes the drop, i.e., ζ_m exists

$$\zeta_m=\frac{3}{B^{3/2}}\left[1-B\left(\frac{\pi}{2}-\varphi_0\right)\right]. \tag{5.5}$$

Let us incidentally note that, as one would expect, with $B\to 0$, $\zeta_m\to 1$.

The selected system of dimensionless coordinates ζ and τ is very convenient. The trajectory of drop in this system $\zeta(\tau)$ depends only

on one parameter B and it sufficiently easily yields calculations whose results are represented in Fig. 31. In Fig. 31 along the axis of abscissas is deposited/postponed dimensionless time τ, along the axis of ordinates - the covered path ζ are plotted/applied the corresponding curves of the dependence ζ on τ for the different values of B.

Let us return to Fig. 29 and will note that ζ_m - this is the maximum distance which drop can pass in the direction perpendicular to the surface of shock wave. Consequently, if we conduct normal to shock wave and at a distance ζ_m from the surface of wedge on this standard to conduct the straight/direct, parallel surfaces of wedge, then the intersection with the constructed straight line with oblique shock wave (point A', in Fig. 29) will be critical point. But the drops, which passed the oblique shock between the apex/vertex and point A', will settle on infinite wedge, drop, that passed the jump higher than point A', they will pass past wedge.

From Fig. 29 it is easy to see that $OA' = \zeta_m \cdot \operatorname{ctg}(\varepsilon - \delta)$.

Thus, the wedge of infinite size/dimension recovers only the finite number of drops, determined by impact parameter $\eta_{lim} = \frac{\zeta_m \cdot \sin \varepsilon}{\operatorname{tg}(\varepsilon - \delta)}$, i.e., a complete coefficient of the capture of the wedge of infinite size it is equal to zero. However, the local coefficient of capture

does not depend on the overall sizes of wedge, but it depends only on distance from spout and decreases in proportion to removal/distance from it to zero at infinity. Let us note that during motion with subsonic speeds the complete coefficient of capture as decreases in proportion to the increase in the sizes/dimensions of body and becomes equal to zero, when the size/dimension of body

$$C > C_{кр} = \frac{2 u_{\infty} r^2 \rho_в}{9 \mu p_{кр}}.$$

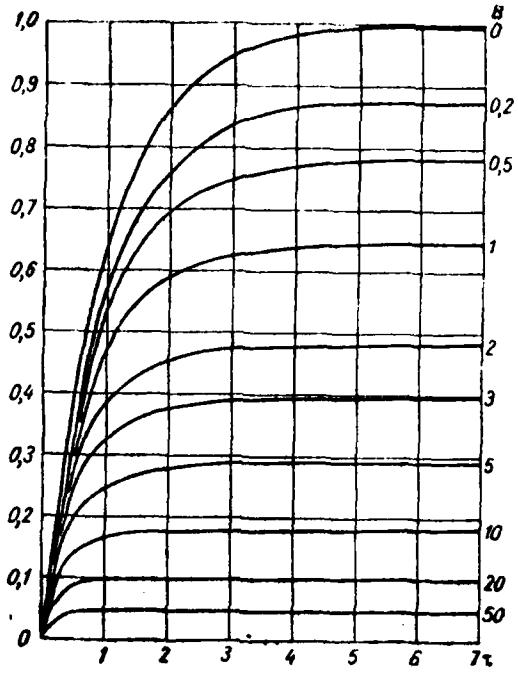

Fig. 31. Stopping distance of drops with the different values of parameter B in dimensionless coordinates (τ, ζ).

Page 97.

In this case, in contrast to supersonic speeds of motion, with increase C decreases the local coefficient of capture, becoming when $C > C_{кр}$ equal to zero even in the spout of profile/airfoil.

Let us pause at the determination of the local and full of

coefficient capture of the wedge of finite length. For this let us turn to schematic Fig. 29. The local coefficient of capture at point P is equal to

$$E_A = \lim_{\Delta S \to 0} \frac{\Delta \tau_1}{\Delta S} = \frac{dS}{d\tau}.$$

If we through ζ designate the path, passable by drop along the normal to shock wave, and through τ - time, calculated from the moment/torque of the passage of this wave, then it is not difficult to show that

$$dS = \frac{d\zeta}{\sin(\varepsilon - \delta)} + \frac{v_1}{u_0} d\tau.$$

From other side $d\eta = d\zeta \cdot \operatorname{ctg}(\varepsilon - \delta)\sin\varepsilon$; thus, the local coefficient of capture E_A it is equal to

$$E_A = \frac{\sin\varepsilon \operatorname{ctg}(\varepsilon - \delta)\frac{d\zeta}{d\tau}}{\frac{1}{\sin(\varepsilon - \delta)}\frac{d\zeta}{d\tau} + \frac{v_1}{u_0}} = \frac{\sin\varepsilon\cos(\varepsilon - \delta)\frac{d\zeta}{d\tau}}{\frac{d\zeta}{d\tau} + \sin(\varepsilon - \delta)\frac{v_1}{u_0}}. \quad (5.6)$$

Substituting in equation (5.6) the value

$$\frac{d\zeta}{d\tau} = \frac{1}{B^{3/2}\left[\left(1 + \frac{1}{B}\right)e^{3/2\tau} - 1\right]^{2/3}}, \quad (5.7)$$

obtained by differentiation of equation (5.4), let us have

$$E_A = \frac{\cos(\varepsilon - \delta)\sin\varepsilon}{B^{3/2}\left[\left(1 + \frac{1}{B}\right)e^{3/2\tau} - 1\right]^{2/3}\sin(\varepsilon - \delta)\frac{v_1}{u_0} + 1}. \quad (5.8)$$

Further, from geometric considerations (Fig. 29) it is apparent that $v_0/u_0 = \frac{\cos\varepsilon}{\sin\delta}$; by substituting this expression in formula (5.8), finally we will obtain

$$E_a = \frac{a_1}{a_2 B^{3/2}\left[\left(1+\frac{1}{B}\right)e^{2/3\,\tau}-1\right]^{3/2}+1} = \frac{a_1}{a_2 f_B(\tau)+1}. \qquad (5.9)$$

Here

$$a_1 = \sin\varepsilon\cdot\cos(\varepsilon-\delta),\ a_2 = \frac{\cos\varepsilon\cdot\sin(\varepsilon-\delta)}{\sin\delta},$$

$$f_B(\tau) = B^{3/2}\left[\left(1+\frac{1}{B}\right)e^{2/3\,\tau}-1\right]^{3/2}. \qquad (5.9')$$

Page 98.

Distance S from the apex/vertex of wedge to the collision point of drop with wedge so can be expressed by τ:

$$S = \frac{z}{\sin(\varepsilon-\delta)} + \frac{v_1}{u_0}\tau,$$

and after the series/row of simple conversions we will obtain

$$S = b_1\left(b_2 - \operatorname{arc\,tg}\sqrt{b_3 e^{2/3\,\tau}-1} - \frac{1}{\sqrt{b_3 e^{2/3\,\tau}-1}}\right) + b_4\tau, \qquad (5.10)$$

where

$$b_1 = \frac{3}{B^{3/2}\sin(\varepsilon-\delta)},$$

$$b_2 = \varphi_0 + \operatorname{ctg}\varphi_0 = \operatorname{arc\,tg}\frac{1}{\sqrt{B}} + \sqrt{B},$$

$$b_3 = 1+\frac{1}{B},$$

$$b_4 = \frac{\cos\varepsilon}{\sin\delta}.$$

It is more expedient to search for the dependence of the local coefficient of capture not on the parameter τ, but on distance of S, measured along the surface of wedge from the spout of profile/airfoil. It is obvious that equations (5.9) and (5.10) together represent this dependence in parametric form. However, it would be the more convenient to connect these two values E_* and S directly in one equation. The series/row of algebraic conversions makes it possible to be freed from the intermediate parameter τ. Equation obtained in this case succeeds in solving relative to S and it takes the form

$$S = C_1 + C_2 \operatorname{arctg} A + \frac{C_2}{A} + C_3 \ln[1 + A^2]. \qquad (5.11)$$

Here C_1, C_2 and C_3 - constants, respectively equal to

$$C_1 = -C_2(\varphi_0 + \operatorname{ctg}\varphi_0) - C_3 \ln\left(1 + \frac{1}{B}\right),$$

$$C_2 = -\frac{3}{B^{3/2}\sin(\varepsilon - \delta)},$$

$$C_3 = \frac{2}{3}\frac{\cos\varepsilon}{\sin\delta}.$$

Value A is connected with E_* the relationship/ratio

$$A=\frac{1}{\sqrt{B}}\sqrt{1+\frac{C_4}{\sin\delta}\left(\frac{\sin\delta}{E_*}-1\right)}=\frac{\sqrt[3]{A'}}{\sqrt{B}}.$$

Here

$$C_4=\sin\delta\,\mathrm{tg}\,\varepsilon\cdot\mathrm{ctg}\,(\varepsilon-\delta).$$

Page 99.

Coefficients, entering equation (5.11) and those connecting E_* and S, depend on three parameters - B, δ and ε. Angle δ, i.e., wedge angle, in real supersonic double wedge airfoils is changed in very insignificant limits. Sc, a change in the thickness ratio of double wedge airfoil from 3.5 to 5o/o corresponds to change δ from 2°00' to 2°52'.

The angle of the slope of oblique shock wave ε oscillates in limits of 45-70° with a change in Mach number of the undisturbed flow from M=1.1 to M=1.5 and of the airflow angle δ from 2 to 3°.

Finally, parameter B in the range of changes δ and ε indicated at real temperatures of air does not exceed value of B=20 [1].

FOOTNOTE [1]. Approximately/exemplarily to these values of B correctly the empirical relationship/ratio $B=0.17\ Re_3^{2/3}$, placed as the basis of

all further calculations. ENDFOOTNOTE.

We produced detailed calculations E_* in dependence on S at the different values of parameter ε for two values δ(2 and 3°) and three values ε (45, 55 and 65°).

The results of calculations are represented in Fig. 32.

In the case of executing Stokes' law (i.e. with B=0) equations (5.8) and (5.0), and consequently also (5.11) substantially they are simplified. so, equation (5.11), takes the form

$$S = \frac{1}{\sin(\varepsilon - \delta)}\left(1 - \frac{1}{A'}\right) + \frac{\cos\varepsilon}{\sin\delta}\ln A'. \qquad (5.12)$$

Each obtained equation (5.12) curves are boundary in Fig. 31, where along the axis of abscissas are deposited/postponed the values of distance from the apex/vertex or wedge S, expressed in unity λ_0^2, and along the axis of ordinates - value E_* in fractions of sin δ.

FOOTNOTE: the stopping distance of drop λ_0, expressed in unity of the significant dimension or body C, i.e., λ_0/C coincides with that introduced on page 18 parameter inertia p, i.e., $p=\lambda_0/C$. ENDFOOTNOTE.

This selection of the scale or the coefficient of capture E_* is determined by the fact that maximum value $E_* = E_0$, attained in the

spout of wedge, is equal to sin δ. Actually/really,

$$E_0 = E_s|_{S=0} = \lim_{\tau \to 0} E_s = \sin\delta.$$

Thus, E_0=sin δ and depends not on what parameters, except the geometry of profile/airfoil itself, i.e., in this case it depends only on angle δ at apex/vertex. This result it was to be expected, also, from simple physical considerations, since in the spout of the trajectory profile of drops they remain rectilinear valid the lack of disturbance of the flow before the wedge, which moves with supersonic speed.

In real profiles/airfoils directly frontal edge has certain rounding, so that actual value E_s at critical point, i.e., E_0 is equal to one and greatly sharply it falls proportional to the sine of the angle between tangent to profile/airfoil and direction of undisturbed flow. Further, at the constant value of this angle falls according to equation (5.11).

With the consideration of that dismantled/selected in section 1 of the present chapter of the mechanism of the icing of high-speed aircraft, frequently so is not essential to know E_s, as it is important to know the average coefficient of settling for an entire surface of profile/airfoil, from spout to the point in question, since, if to this point the temperature of surface is positive, then

because of the possible course of the film of water the coefficient of capture is automatically averaged.

Pages 100-101.

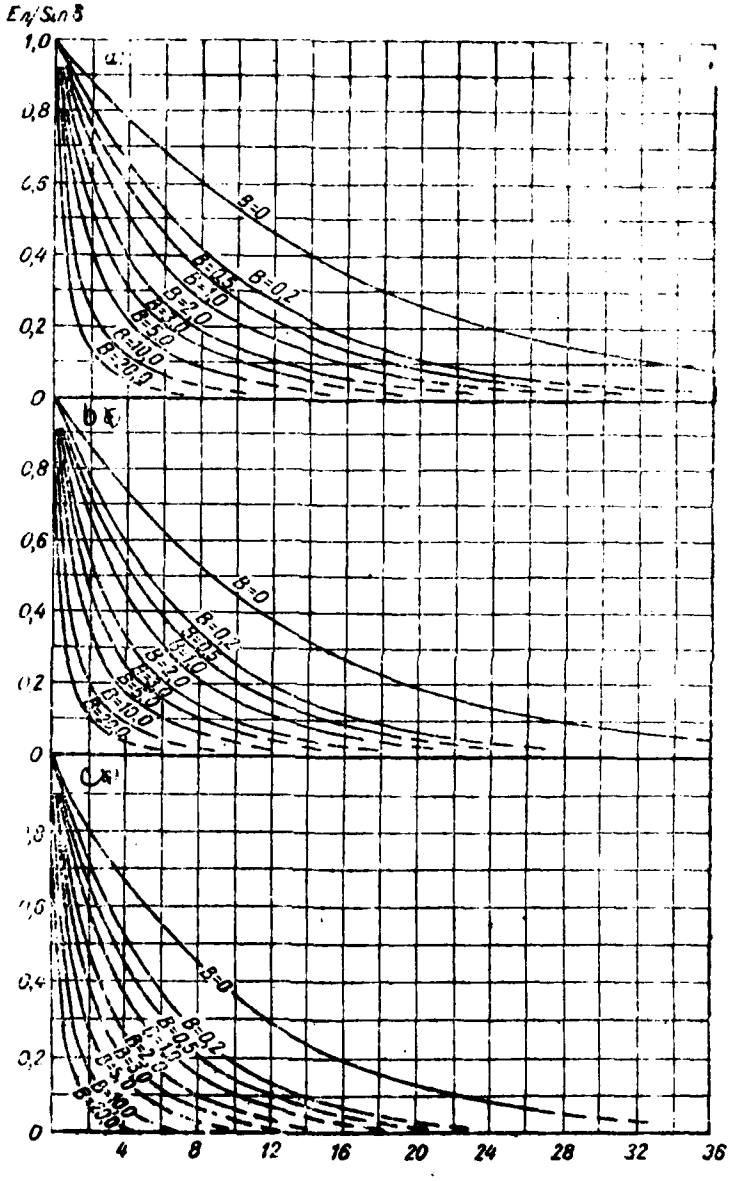

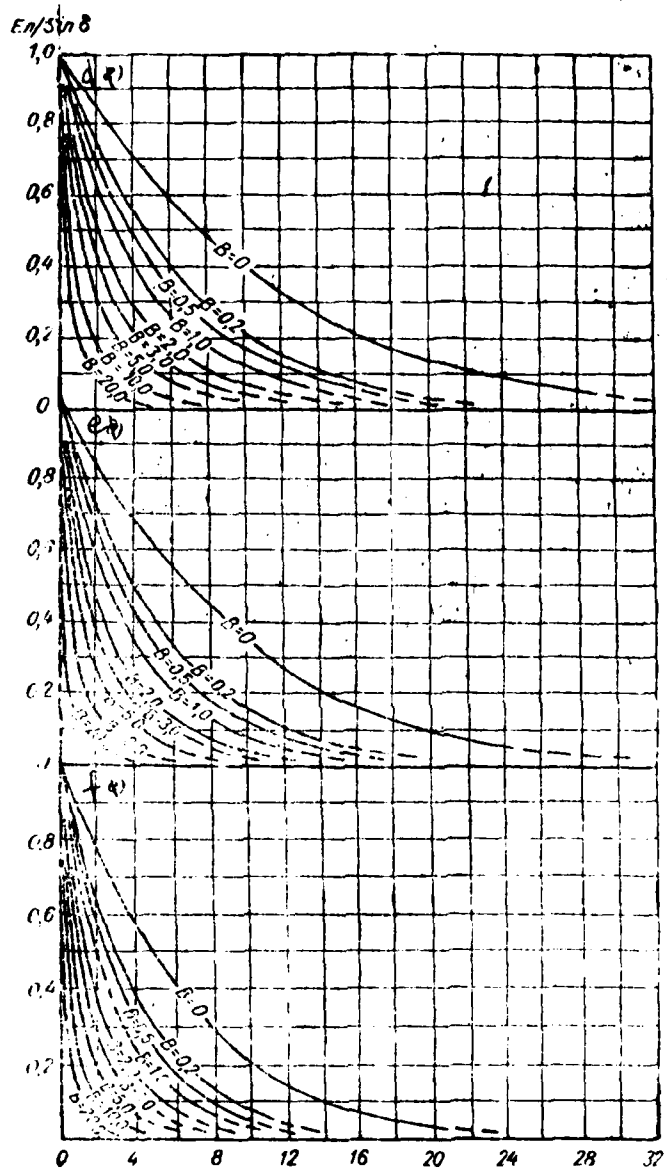

а) δ = 2°, ε = 45°; б) δ = 2°, ε = 55°; в) δ = 2°, ε = 65°; г) δ = 3°, ε = 45°; д) δ = 3°, ε = 57°; е) δ = 3°, ε = 65°.

Fig. 32. Change in the local coefficient of capture l_{λ}, expressed in portions sin δ, with distance from the apex/vertex of wedge, expressed in portions λ_0 at the different values of parameter B. δ - angle between direction of flow and surface of wedge, ε - the angle between direction of flow and shock wave.

Page 102.

From Fig. 29 it is evident that the average coefficient of the capture of surface from apex/vertex to point P, i.e., $E_{S_{cp}}$ is equal to

$$E_{S_{cp}} = \frac{r_1}{S} = \frac{\zeta \operatorname{ctg}(\varepsilon - \delta)\sin\varepsilon}{S} = \cos(\varepsilon - \delta)\sin\varepsilon = \frac{\sin 2\varepsilon \cos(\varepsilon - \delta)}{2\sin\delta} \cdot \frac{r}{S}.$$

For determining the ratio r/S it is possible to use formulas (5.9) and (5.9'), according to which with the given one r is determined E_s and then (on Fig. 31), knowing E_s, it is determined by S.

It does not represent fundamental difficulties to construct the diagrams of dependence S(r) and it is direct according to equation (5.10).

For the series/row of practical tasks is of interest the knowledge of that rate, with which the drops hit the surface of wedge. Let us designate normal to the surface of wedge the component of velocity of drop, expressed in unity u_0 through $\zeta_\perp'$, and the tangential - by $\zeta_\parallel'$. It is not difficult to see that in this case

$$\zeta_\perp' = \zeta' \cos(\varepsilon - \delta),$$

$$\zeta_\parallel' = \zeta' \sin(\varepsilon - \delta) + \frac{\cos\varepsilon}{\sin\delta},$$

where ζ' - rate of the motion of drop relative to air. Dependence $\zeta'=d\zeta/d\tau$ on S can be found from equations (5.7) and (5.10), eliminating of them the intermediate parameter τ. It is interesting to note that in this case the equation, which connects values ζ' and S, can be written completely identically with equation (5.11), i.e.,

$$S = C_1 + C_2 \operatorname{arctg} P + \frac{C_2}{P} + C_3 \ln(1 + P^2), \qquad (5.13)$$

Here C_1, C_2 and C_3 the same as in equation (5.11), but

$$P = \frac{1}{\sqrt{B}(\zeta')^{1/3}}.$$

Thus, the calculations, carried out for the construction of Fig. 32, can be used also for the determination of connection/communication of ζ' with S. In exactly the same manner with B=0, equation (5.13) converts/transfers in equation (5.14), analogous (5.12).

$$S = \frac{1}{\sin(\varepsilon - \delta)}(1 - \zeta') + \frac{\cos\varepsilon}{\sin\delta} \ln\frac{1}{\zeta'}, \qquad (5.14)$$

where ζ' is analog $1/A'$ in equation (5.12).

Connection/communication of normal component of the impact velocity of the drop about the surface of wedge, expressed in values u_0, with distance along surface from the apex/vertex of wedge S, expressed in values λ_0, is given in Fig. 33 for the same conditions as in Fig. 32. tangential component easily can be found on normal

from the relationship/ratio

$$\zeta_{\parallel}' = \zeta_{\perp}' \cdot \operatorname{tg}(\varepsilon - \delta) + \frac{\cos\varepsilon}{\sin\delta}.$$

Page 103.

Thus, the results or calculations, led to the appropriate graphs/curves (Fig. 32 and 33), give the possibility to determine the local coefficient of capture and the rate, with which the drop is hit against any point of the surface of wedge with the assigned apex angle. In this case it is proposed that the wedge moves in cloud with the known rate v_0, which exceeds the speed of sound so, that in its apex/vertex is formed the attached shock wave. The physical parameters of air (P_0, t_0, μ_0, ρ_0) and the sizes/dimensions of drops must be known.

For an example let us dismantle/select one real case.

Wedge with angle δ=arc tg 0.05 flies at the altitude of of 5 km (P_0=500) at velocity, determined by number M_0=1.2. The temperature of air is equal to -30°. Let us find the local coefficient of capture E_a and the impact velocity of the drop of a radius 5μ about the surface of wedge at a distance of 10 cm from apex/vertex.

Let us find the parameters of disturbed flow and the angle of oblique shock wave ε.

On Fig. 336 in [30] we find that with $\delta=2°52'$ and $M_0=1,2$; $\varepsilon\approx64°$ and $M_1=1.07$. Consequently, $M_0\sin\varepsilon=1,168$ and through Fig. 30 we find $T_1/T_0=1.11$, $\rho_1/\rho_0=1.29$ and $p_1/P_0=1.42$. From relationship/ratio $v=M\sqrt{\gamma RT}$ we find v_0 and v_1.

Thus, the parameters of the undisturbed medium, i.e., to oblique shock (upstream), are

$t_0=-30°$,
$T_0=243°$,
$P_0=500$ мб, (1)
$\rho_0=0,712\cdot10^{-3}$ г/см^3, (2)
$M=1,2$,
$v_0=3,75\cdot10^4$ см/сек. (3)

Key: (1). mb. (2). g/cm^3. (3). cm/s.

The parameters of the disturbed medium, i.e., after shock (downstream), are

$T_1=270°$,
$t_1=-3°$,
$P_1=710$ мб. (4) (1)
$\rho_1=0,914\cdot10^{-3}$ г/см^3, (2)
$M_1=1,07$,
$v_1=3,52\cdot10^4$ см/сек. (3)
$\mu_1=1,705\cdot10^{-4}$ г/см. сек.

Key: (1). g/cm^3. (2). cm/s. (3). g/cm s.

Initial relative rate of drop in the disturbed medium

$$u_0 = \frac{\sin\delta}{\cos\varepsilon} v_1 \quad 4{,}01 \cdot 10^3 \text{ см/сек.}$$ (1)

Key: (1). cm/s.

Let us finally find parameters Re_0 and λ_0, after accepting as significant dimension the distance from the apex/vertex of wedge (10 cm), on which to us it is necessary to determine value E_x:

$$Re_0 = \frac{2ru_0}{\nu_1} = 21{,}4$$

$$B = 0{,}17\,Re_0^{1/3} = 1{,}3$$

$$\lambda_0 = \frac{2u_0 r^2}{0{,}3\nu_1} = 1{,}305 \text{ см.}$$

Page 104.

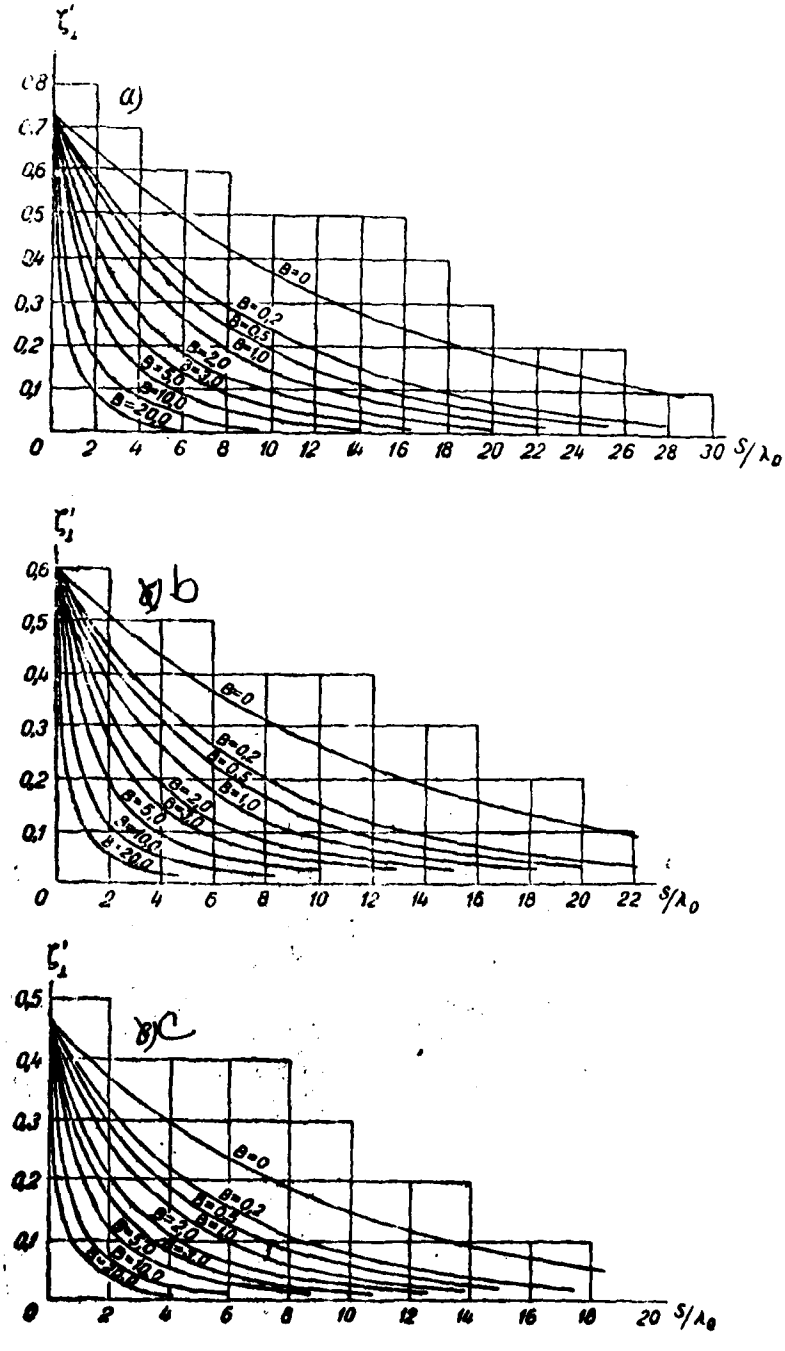

Fig 22a, b, c.

Page 105.

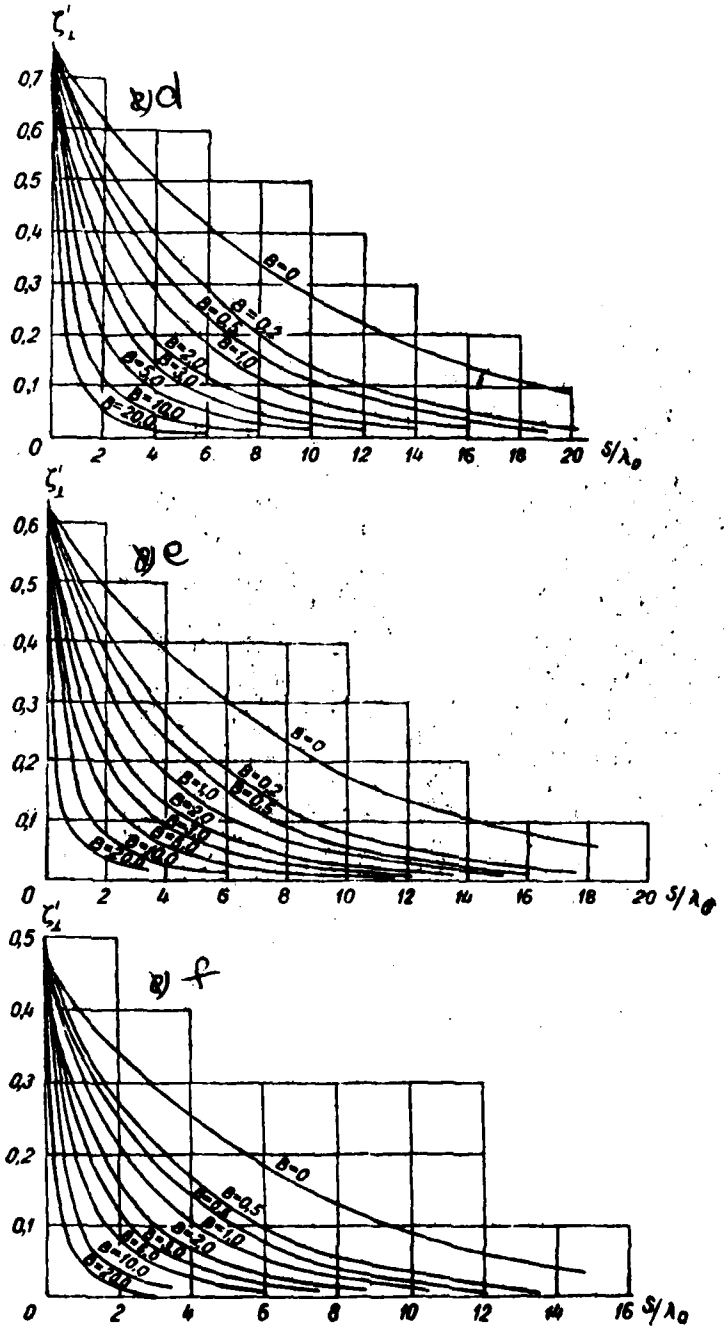
ζ'1
0,7
0,6
0,5
0,4
0,3
0,2
0,1
0
2
4
6
8
10
12
14
16
18
20
S/λ0
в)d
β=0
β=0,2
β=0,5
β=1,0
β=2,0
β=3,0
β=5,0
β=10,0
β=20,0
ζ'1
0,6
0,5
0,4
0,3
0,2
0,1
0
2
4
6
8
10
12
14
16
18
20
S/λ0
в)e
β=0
β=0,2
β=0,5
β=1,0
β=2,0
β=3,0
β=5,0
β=10,0
β=20,0
ζ'1
0,5
0,4
0,3
0,2
0,1
0
2
4
6
8
10
12
14
16
S/λ0
в)f
β=0
β=0,5
β=1,0
β=2,0
β=3,0
β=5,0
β=10,0
β=20,0

Fig. 33. Change in normal component of impact velocity of drop about surface of wedge ζ_1', expressed in portions difference in rates of flow before and after shock wave u_0, with distance from apex/vertex of wedge, at different values of parameter B.

d a) $\delta=2°$, $\varepsilon=45°$; b) $\delta=2°$, $\varepsilon=55°$; c) $\delta=2°$, $\varepsilon=65°$; e) $\delta=3°$, $\varepsilon=45°$; f) $\delta=3°$, $\varepsilon=55°$; g) $\delta=3°$, $\varepsilon=65°$.

Page 106.

Distance S from apex/vertex, equal to 10 cm, expressed in units λ_0, i.e., S/λ_0 will be equal 10/1.305=7.67.

Thus, we found entire necessary and sufficient in order with the aid of Fig. 32 and 33 to find response/answer to the question interesting us. on the basis of Fig. 32 (b, c, e, f) we compose the table of 14 values $E_S/\sin\alpha$ with B=1.3 and S=7.67.

From table 14 by dual interpolation we find that with $\delta=2°52'$ and $\varepsilon=64°$, E_s accepts the value 0.075x$\sin\delta$=0.00375.

Analogously, on Fig. 33 (b, c, e, f), we compose the table of the values of normal to the surface of wedge components of the rate drop at the moment of the shock, expressed in unity u_0. With $\delta=2°52'$ and $\varepsilon=64°$ value $\zeta_\perp'$, found from table 15 with dual interpolation, is equal to 0.037. peripheral component of velocity of drop $\zeta_\parallel'$ is

respectively equal to

$$\zeta_{\parallel}' = \zeta_{\perp}' \operatorname{tg}(\varepsilon - \delta) + \frac{\cos\varepsilon}{\sin\delta} = 8{,}85.$$

Finally, expressing $\zeta_{\perp}'$ and $\zeta_{\parallel}'$ in dimensional unity, we will obtain that normal component of the rate of drop $u_{k\perp} = 148$ m/s, and is tangential $u_{k\parallel} = 3{,}55 \cdot 10^4$ cm/s.

For a comparison let us find values E_*, $u_{k\perp}$ and $u_{k\parallel}$ for a drop with a radius of r=40μ. It is easy to see that in this case of B=5.2; P=8.32, and distance S in units λ_0 is equal to 0.12. Corresponding values $E_*/\sin\delta$ are given in Table 10.

In the case in question up to the distance of 10 cm from the apex/vertex of wedge the bending trajectory of drops with a radius of r=40μ is very small and therefore the local coefficient of capture is close to maximum value, namely $E_* \approx 0{,}9 \sin\delta = 0{,}045$. Without giving here calculations themselves, let us point out that for drops with a radius of $r = 40\mu$, $\zeta_{\perp}' = 0{,}4$ and $\zeta_{\parallel}' = 9{,}5$.

In the beginning of present paragraph it was mentioned, that the solution, obtained for a wedge, can be common for double wedge airfoil. In this case at angle δ should be understood the angle between the surface of rhombus and flow direction. If rhomb flies with certain nonzero angle of attack, then angle $\delta_в$ for its upper surface is not equal to angle $\delta_н$ for a lower surface. It is possible

that the range of changes in values δ_1 and δ_2 is wider than examined in calculations by 2-3°. In this case it is expedient to supplement Fig. 31 and 32 new, which expand the range of changes δ and ε. This expansion does not present fundamental difficulties and can be comparatively easily carried out on the basis of formulas (5.11) and (5/13).

Table 14.

δ \ ε	55°	65°
2°	0,20	0,13
3°	0.115	0,06

Table 15.

δ \ ε	55°	65°
2°	0,11	0,055
3°	0.065	0,030

Table 16.

δ \ ε	55°	65°
2°	0,93	0,90
3°	0.88	0,85

Page 107.

3. Icing index at supersonic flight speeds.

In 1 section of this chapter it was shown that for the final representations about the possibility of aircraft icing during supersonic flights, it is necessary to rate/estimate the value of the integral coefficients of capture $\tilde{E}$.

The integral coefficient of capture $\tilde{E}$ for the assigned body and flight conditions depends substantially on the distribution of cloud drops according to sizes/dimensions, and in its value it approaches a coefficient of the capture of the drops, which give the maximum contribution to liquid-water content. At present we do not have sufficient data about the spectral distribution of drops according to the sizes/dimensions in the strongly supercooled clouds with the temperature of lower than -30°. However, existing knowledges give grounds to assume that in the such strongly supercooled clouds the overwhelming majority of drops has a diameter not more 10 μ. As shows the example, considered at the end of the preceding/previous section the local coefficient of capture for such drops it is changed from values $\sin\delta \sim 0.05$ in the apex/vertex of profile/airfoil to 0.004 already at a distance of 10 cm from apex/vertex. Consequently and value of $\tilde{E}$ actually must not exceed these value. With small corrections this estimation can be attributed also to ice clouds. Although for them effective radius $r_{эф}$[1] can be somewhat more.

FOOTNOTE [1]. By $r_{эф}$ is understood a radius of such drops which are subordinated to approximately/exemplarily the same law of motion, as the crystal of the assigned geometric structure (size/dimension and form). ENDFOOTNOTE.

Actually $\tilde{E}$ fast enough decreases (in proportion to removal/distance from end connections of the profile/airfoil) from the maximum value at apex/vertex, equal to several hundredths, to very low values already at a distance of 10-15 cm from apex/vertex. The character of decrease is similar/such to decrease E in Fig. 31.

If flight occurs at lower speed, then, as has already been mentioned, the values of coefficient of E become still less. Thus, it is possible with confidence to say that at a distance of 5-10 cm from the apex/vertex of the value of the integral coefficient of capture for high-speed/velocity profiles/airfoils actually do not exceed 0.004, if the flight speed of less than the sonic or insignificantly exceeds the speed of sound.

Let us examine the case of flight with M=1.2. In this case, as can be seen from Fig. 17, the temperature of surface even in the recovery factor, equal to 0.7, it is heated more than on 35°. Therefore let us assume that in flight it occurs at temperature t_0=-40° and surface is heated to temperature t_c = -5. Let us estimate, which must be in this case liquid-water content w_l, necessary for the compensation surface evaporation. From nomogram (Fig. 18) it follows that in this case value $K_3 > 1.5 \cdot 10^{-2}$. Accepting $\tilde{E}$ equal to $4 \cdot 10^{-3}$, as

it takes place with the small or removal from the apex/vertex of profile/airfoil, we see that

$$\omega_i = \frac{\pi}{E u_\infty} K_3(t_\infty, t_0, P_0) > 1 \cdot 10^{-3} \text{ г/см}^3 = 0{,}1 \text{ г/м}^3 \quad (1)$$

Key: (1). g/m³.

Page 108.

We do not have any sufficient reliable statistical evidence about water content of clouds at very low temperatures, however, all available data attest to the fact that at temperature of droplet cloud its below -30 liquid-water content must be considerably less than 0.1 g/m³.

Thus, at small supersonic rates (M_0=1.2-1.3), when, as shown in the section of 1 present chapter, still it is possible to expect minus temperature in one or the other sections of the surface of profile/airfoil, $\omega_i > 0{,}1$ g/m³, which, in turn, considerably exceeds real water content of clouds at such low temperatures.

The obtained results of theoretical calculations with sufficient certainty indicate that in flights at the rates, which exceed the speeds of sound, in the first place, the icing of the frontal surfaces of profiles/airfoils is impossible, if there is no heat withdrawal from the internal wing surface, and, in the second place,

is very highly improbable the realization of the mechanism of icing due to a temperature decrease along profile/airfoil upon its transfer through 0°, since a quantity of depositing moisture in this case virtually will not be able to compensate surface evaporation.

However, among specialists' series/row there is an opinion that the icing due to the freezing of the depositing supercooled cloud drops can occur even at supersonic flight speeds. So, Tribus and and Gober [24], on one hand, and Serafini [75], on the other, consider that with the icing of the protruding parts of the aircraft (we emphasize this fact, since still possibly and the icing of engines) it is necessary to collide to the rates, which exceed the speed of sound by 40o/o (to M=1.4) according to Serafini, to 80o/o (to M=1.8) according to Tribus and Gober.

To us it seems that Tribus and Serafini did not pay proper attention to the examination of the processes of heat exchange in the surface of wedge with icing, or to that fact that the low local coefficients of capture for the profiles/airfoils, used in high-speed/velocity aviation, and the large overheatings of surface with respect to flow, acting together, they can lead to the fact that the evaporation from the unit of surface exceeds quantity of moisture depositing on it for the same time.

Besides the considerations indicated, to conclusion/output about the practical impossibility of icing at supersonic speeds due to settling of the supercooled cloud drops, contributes the fact that the large statistical material, assembled in TsAO, gives sufficiently foundations for considering virtually impossible the presence of supercooled clouds of lower than -40° and to unlikely ones the presence of such clouds of lower than -35°.

In press/printing there are several communications/reports [40, 60] about icing at very low temperatures; however, icing in these cases bears specific character. In one case the observed different coating reflects the presence of water vapors and drops in exhaust [40], while in other - plotted ice was clearly caused by the sublimation, which occurred above the tropopause at temperature of -55°. Unfortunately, the absence of the information about the rate of aircraft makes impossible the comparison of these cases with theory.

As to known to us material with certainty attests to the fact that the icing of high-speed aircraft occurs, as a rule, in lower and cloud amount of middle level during takeoff or landing when the rates reach 300-400 km/h, i.e., when to high-speed aircraft is added the theory, developed in the preceding/previous chapters.

It should be noted that the theory, presented in present

chapter, is not absolutely precise, since at its basis lies/rests essential assumption about the absence of heat withdrawal from the internal surface of profile/airfoil. We do not have at our disposal of any data about order of magnitude, which characterize possible heat withdrawal and therefore not in state to rate/estimate the degree of probable deviation from developed theory.

Page 109.

It is possible that if the heat withdrawal is sufficiently great, then can arise the conditions, favorable for ice accumulation.

In connection with this, in spite of the validity of conclusion/output about the extremely small probability of aircraft icing during flights under actual conditions with the speeds higher than speed of sound, a question about the possibility in principle of icing under such conditions must be solved in special experimental flights. In such flights it would be interesting to trace rate of evaporation of ice from one or the other part. This would make it possible to check theoretical relationships/ratios and, possibly, it would be the method of evaluating the heat-transfer coefficient α. Finally, in these flights it would be possible to check considerations about the effectiveness of "speed maneuver" for dealing with icing.

REFERENCES

1. Современное состояние гидроаэродинамики вязкой жидкости. Под ред. С. Гольдштейна, т. т. I и II, М., ИИЛ, 1948.
2. Современное состояние аэродинамики больших скоростей. Под ред. Хауэрта, т. т. I и II, М., ИИЛ, 1955—1956.
3. Боровиков А. М. Некоторые результаты изучения облачных элементов. Труды ЦАО, вып. 3, 1948.
   Боровиков А. М., Мазин И. П. Некоторые новые данные о микроструктуре облаков над ЕТС. Труды ЦАО, 1956.
4. Гухман А. А. и Илюхин П. В. Основы учения о теплообмене при течении газа с большой скоростью. Машгиз, 1951.
5. Дьяченко П. В. Опыт применения методов математической статистики к изучению структуры естественных туманов и облаков. Диссертация, ЛГУ, Л. 1954.
6. Зайцев В. А. Размеры и распределение капель в кучевых облаках. Труды ГГО, вып. 13, 1948.
7. Зайцев В. А. Новый метод определения водности облаков. Труды ГГО, вып. 13, 1948.
8. Клячко Л. Уравнения движения пылевых частиц в пылеприемных устройствах. Отопление и вентиляция, № 4, 1934.
9. Кравченко И. В. Обледенение самолета. Вестник воздушного флота, № 10 1953.
10. Лебедев Н. В. Борьба с обледенением самолетов. Оборонгиз, М., 1939.
11. Левин Л. М. Об осаждении частиц из потока аэрозоля на препятствия. ДАН СССР, т. 91, № 6, 1953.
12. Левин Л. М. О функциях распределения облачных и дождевых капель по размерам. ДАН СССР, т. 94, № 6, 1954.
13. Левин Л. М. О коагуляции заряженных облачных капель. ДАН СССР, XCIV, № 3, 1954.
14. Мазин И. П. Расчет отложения капель на круглых цилиндрических поверхностях. Труды ЦАО, вып. 7, 1952.
15. Минервин В. Е. Об измерениях водности и обледенения в переохлажденных облаках и некоторые ошибки этих измерений. Труды ЦАО, вып. 17, 1956.
16. Милликен Р. И. Коэффициенты скольжения в газах и закон отражения молекул от поверхности твердых тел и жидкостей. Газовая динамика. Сборник статей под ред. С. Г. Попова и С. В. Фальковича., ИЛ. М., 1950. (Перевод из Phys. Revew, 21, 1923).
    Милликен Р. И. Электроны (+ и −), протоны, фотоны, нейтроны и космические лучи. ГОНТИ, М., 1939.
17. Михеев М. А. Основы теплопередачи. Госэнергоиздат, М.—Л., 1949.
18. Научный отчет об оборудовании летающей лаборатории (А. М. Боровиков и Ю. А. Гальперн) Архив ЦАО, М., 1950.
19. Научный совместный отчет Гос. НИИ ГВФ и ЦАО по летным исследованиям в условиях обледенения на самолете ИЛ-14. Архив ЦАО, М., 1955.
20. Научный совместный отчет Гос. НИИ ГВФ и ЦАО по исследованию влияния обледенения на характеристики посадки (ухода на второй круг) одномоторного полета на самолете ИЛ-14 и по изучению зависимости интенсивности обледенения от физико-метеорологических параметров облака и условий полета. Архив ЦАО, М., 1956.
21. Обледенение воздушных судов. Под ред. В. Ф. Бончковского. Ред. изд. отд. ГВФ, М., 1938.

Page 110.

22. Стрижевский С. Е. Реферат докладов Е. Брюн, Карон, М. Пети и М. Вассер на II авиационном конгрессе во Франции в 1946 г. Военно-воздушная академия им. Жуковского. Технические заметки, 22/5, 1947.
23. Пчелкин Ю. Г. Аэрологические условия полетов на больших высотах. Гидрометеоиздат, Л., 1957.
24. Трайбус М. и Гибер А. Влияние сферических водяных капель, содержащихся в атмосфере, на клин, летящий со сверхзвуковой скоростью. Механика № 2 (18), ИИЛ, М., 1953. (перевод из Journal of the aeronautical sciences 19, № 6, 1952).
25. Трунов О. К. и Хариков А. А. К вопросу обледенения самолета. Ред. изд. отд. ГВФ, М., 1954.
26. Фигуровский Н. А. Седиментометрический анализ. АН СССР, М., 1948.
27. Фомин Н. П. Экспериментальные исследования условий обледенения воздушных судов и способов борьбы с ним. «Обледенение воздушных судов». Ред. изд. отд. ГВФ, М., 1938.
28. Фукс Н. А. Механика аэрозолей. АН СССР, М., 1956.
29. Хальд А. Математическая статистика с техническими приложениями ИИЛ. М. 1956.
30. Хилтон У. Ф. Аэродинамика больших скоростей ИИЛ. М., 1955.
31. Хргиан А. Х. и Мазин И. П. О распределении капель по размерам в облаках. Труды ЦАО, вып. 7, 1952.
32. Хргиан А. Х. и Мазин И. П. Расчет ошибок самолетного заборника капель. Труды ЦАО, вып. 12, 1953.
33. Хргиан А. Х. Физика атмосферы ГОНТИ. М., 1953.
34. Хргиан А. Х. и Мазин И. П. Анализ способов характеристики спектров распределения облачных капель. Труды ЦАО, вып. 17, 1956.
35. Чен Г. И. Фильтрация аэрозолей волокнистыми материалами. Успехи химии. т. XXV, вып. 3, 1956. (перевод из Chemical Reviews, № 55, p. 595, 1955).
36. Шифрин К. С. Рассеяние света в мутной среде. ГИТТЛ, 1951.
37. Шишкин Н. С. Облака, осадки и грозовое электричество. ГТТИ, 1953.
38. Шметер С. М. О содержании хлора в воде облаков в связи с их микроструктурой. Труды ЦАО, вып. 9, 1952.
39. Эйгенсон Л. С. Моделирование. Советская наука, 1950.
40. Aanensen C. J. M. Unusual condensation trans. Meteorological Magasin 77, p. 17—18, 1948.
41. Aesignificant accident. Aeroplane. V. 87, N 2253, sept. 24, 1954.
42. Albrecht F. Theoretische Untersuchungen über die Ablagerung von Staub aus stromender Luft und ihre Anwendung auf die Theorie der Staubfilter. Fhysikalische Zeitschrift, № 32, S. 48, 1931.
43. Andreasen. Kolloid Zeitsch. № 48, p. 175, 1929.
44. Bergran N. R. An ampirical method permitting rapid determination of the area, rate and distribution of water drop impingement on an airfoil of arbitrary section at subsonic speeds. NACA. TN 2476, 1951.
45. Bergran N. R. An ampirically derived basis for calculating the area, rate and distribution of water-drop impingement an airfoils. NACA. Report 1107, 1952.
46. Best A. C. The size of cloud droplets in layer-tipe cloud. Quarterly Journal of the Royal Meteorological Society. 77 N 332, 1951.
47. Blacker W. Einige Bemerkungen über Eisansatz an Flugzeugen. Meteorologische Zeitschrift. Bd. 49, н. 9, 1932.
48. Bran R. J., Serafini J. S. and Gallagher. Helen M. Impingement of cloud droplet on aerodynamic bodies as affected by compressibility of air flow around the body. NACA. TN 2903, 1953.
49. Devies C. И., Peetz P. V. Impingement of particles on a transverse cylinder. Proceedings of the Royal Society. A. Mathem. and Phys. sciences. Vol. 234, N 1197, 7 febr. 1956.
50. Dorsey N. E. The freezing of supercooled water. Transections of the American Philosofical Society. Vol. 38, 1948.
51. Flight. Vol. 66, N 2383, p. 502, 24 sept. 1954.
52. Freser D. Rush C. K. and Boxter D. Thermodinamic limitations of ice accreation instruments. Bulletin of the American Meteorological Society. Vol. 34, N 4, april, 1953.
53. Frith R. The icing of aircraft at temperatures below −41°C. Quarterly Journal of the Royal Meteorological Society. Vol. 78, N 336, april, 1952.
54. Gunn R. In flihgt icing of highly electrified aircraft. Journal Aeronautical Sciences 14, N 9, p. 527, 1947.
55. Glauert Muriel. A method of constructing the pathe of raindrops of different diameters moving in the neighbourhood of (1) a circular cylinder, (2) an aerofoil, placed in a uniform stream of air, and determination of the rate of deposit of the drops on the surfice and the percentage of drops cought. Aeronautical Research Commitee LHMSO, N 2025, 1940.

56. Hardy J. K. Kinetic temperature of wet surfaces, a method of calculating the amount of alcohol required to prevent ice, and the derivation of the psychrometric equition. NACA ARR, N 5013, september, 1945.
Hardy J. K. An analysis of the dissipation of heat in conditions of icing from a section of the wing of the C 46 airoplane. NACA TR, N 831, 1945.
57. Hardy J. K. Protection of aircraft against ice. Royal Aircraft Establishment. Report N. S.M.E., 3380, july, 1946.
58. Hardy J. K., Brown C. D. Kinetic temperature of propeller blades in conditions of icing. Aeronautical Research council. R and M. N, 2806, LHMSO, 1954.
59. Houghton H. G. On the physics of clouds and precipitation. Compendium of Meteorology. Amer. Meteor. Soc., p. 165, 1951.
60. Harst G. W. Aircraft icing at very low temperatures. Meteorological Magazine, Vol. 83, N 987, p. 280, 1954.
61. Ice accreation on aircraft. Meteorological Reports, N 9, LHMSO, 1951.
62. Lengmuir I., Blodgett Katherine B. A mathematical investigation of water droplet trajectories. General Electric Company report, july, 1945.
63. Langmuir I. The production of rain by a chain reaction in cumulus clouds at temperatures above freezing. Journal of Meteorology. Vol. 5, N 5, october, 1948.
64. Lacey I. K. A study of meteorological and physical factors affecting the formation of ice on airplanes. Bulletin of the American Meteorological Society 21, 357—367, november, 1940.
65. Lewis W. Meteorological aspects of aircraft icing. Compendium of Meteorology. Amer. Meteor. Soc., p. 1197, 1951.
66. Lewis A. R. Physical and operational aspects of aircraft icing. Compendium of Meteorology. Amer. Meteor. Soc., p. 1190, 1951.
67. Ludlam F. H. The heat economy of rimed cylinder. Quart. Journal of the Royal Meteorological Society. Vol. 77, N 334, october, 1951.
68. Messinger R. L. Equilibrium temperature of an unheated icing surface as a function of air speed. Journal of the Aeronautical Sciences. Vol. 20, N 1, 1953.
69. Meteorological aspects of aircraft icing. Paris, 1950.
70. Neel C. B., Bergran N. R., Jukoff D. and Schaff B. A. The calculation of the heat required for wing thermal ice prevention in specified icing conditions. NACA TN 1472, 1947.
71. Patterson D. M. A simplified procedure for the determination of heat requirements for ice protection of fixed areas of aircraft. Central Air Documents Office, Technical Data Digest. Vol. 14, N 4, february, 15, 1949.
72. Peppler W. Reif und Eisbildung in der freien Atmosphäre. Beiträge zur Physik der freien Atmosphäre. 10, 38—50, 1922—1923.
73. Robinson A. On the motion of small particles in a potential field of flow. Communications on pure and applied mathematics. Vol. 9, N 1, 1956.
74. Squire H. B. Heat transfer calculations for aerofoils aeronautical Research. Council reports and memoranda, № 1986, 1942.
75. Seratini J. S. Impingement of water droplets on wedges and double wedge airfoils at supersonic speeds. NACA Report, N 1159, 1954.
76. Taylor F. R. S. Notes on possible equipment and technique for experiments on icing on aircraft. Aeronautical Research Committee. R M N 2024, LHMSO, 15-th january, 1940.
77. Tribus M., Young C. B. W. and Boelter L. M. K. Limitations and mathematical basis for predicting aircraft icing characteristics from scall-model studes Transactions of the ASME. Vol. 70, N 8, november, 1948.
78. Tribus M. Intermittent heating for protection in aircraft icing. Transactions of the ASME. Vol. 73, N 8, november, 1951.
79. Weiner F. Further remarks on intermitten heating for aircraft ice protection. Transactions of the ASME. Vol. 73, N 8, november, 1951.
80. Vonnegut B. A. A cappilary collector for measuring the deposition of water drops on a surface moving through clouds. The Review of scientific instruments. Vol. 20, N 2, 1949.

Appendices.

I. Fig. 34, taken from Bergran's work [45], makes it possible to determine the value of critical parameter $p_{кр}$ depending on the lift coefficient c_{max} and thickness ratio - for the Zhukovskiy profile of elliptical profile.

Tables 1, 2, 3, 4 and 5 give the results, obtained by Bergran [45] during determination with the aid of the differential analyzers of the trajectories of drops, weighed in air flow during flow of this flow about different aircraft profiles/airfoils. Data in the graphs/counts of 1, 2, 4, 5, 6, 7 and 8 all tables are borrowed directly from [45]. data in graphs/counts 3, 9 and 10 have designed we.

II. In 1, 2 and by the 3rd graphs/counts are given the values of parameters φ, Re_0 and p (see conventional designations, page 8). In the 4th graph/count it is indicated: is located the place of the collision of drop with the profile/airfoil of higher than the face grinding (upper surface) or lower than it (lower surface). Index 1 marked tangential trajectories at these values of p and Re_0. In the

5th graph/count is given the distance from the point of the collision of drop with profile/airfoil to face grinding (referred to airfoil chord) in the 6th - value ξ' - drop in component of speed parallel to chord, at the moment of its collision with the profile/airfoil (rate is related to the rate of the undisturbed flow). In the 7th graph/count are represented the values of composing the rates drop normal in chord in the same dimensionless unity. In the 8th graph/count are given impact parameters of drops i.e., distance from drop to centerline in the undisturbed part of the flow. In 9th given distance $\Delta\eta$ between tangential trajectories of drops in the undisturbed region and finally in the 10th graph/count is given the complete coefficient of capture E, equal to relation $\Delta\eta$ to midship profile cross section.

In Tables 4 and 5 is midsection the section accept by conditionally equal to with respect 0.15 and 0.157.

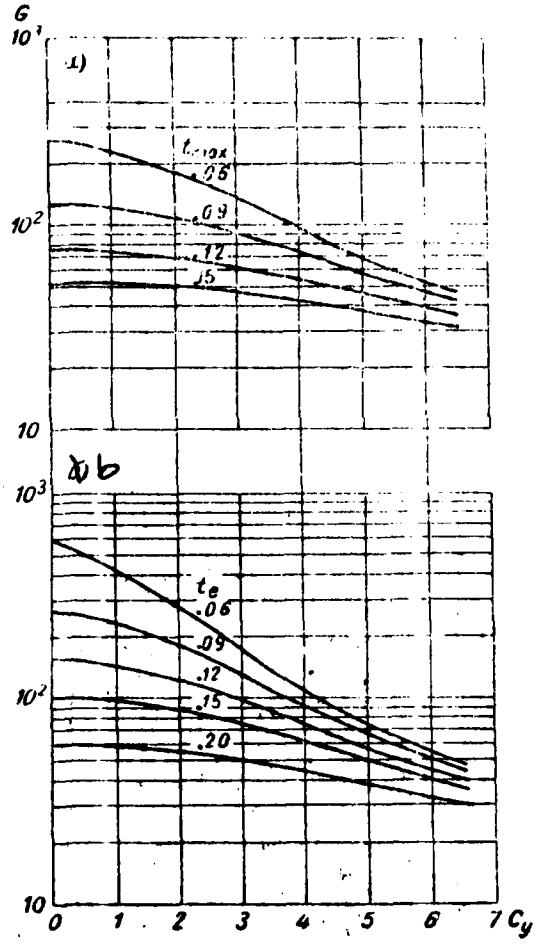

Fig. 34. Gradient of velocity of flow in the vicinity of the critical point G depending on thickness ratio and lift coefficient c_y: a) the Zhukovskiy profile, b) ellipse.

Page 113.

Table 1. 15% symmetrical Zhukovskiy profile (c_y=0; α=0°).

Key: (1). Surface. (2). upper. (3). lower.

ψ	Re_0	$p = \frac{Re_0}{\psi}$	(1) Поверхность	s, C	ξ_s'	v_{is}'	v_{i0}	$\Delta\eta$	$E = \frac{\Delta\eta}{0,15}$
1	2	3	4	5	6	7	8	9	10
2	128	64	(2) верхняя	0,265	1,0	0	0,074	—	—
2	128	64	(3) нижняя	−0,265	1,0	0	−0,074	0,148	0,99
8	512	64	(2) верхняя	0,273	0,997	0,004	0,074	—	—
8	512	64	(3) нижняя	−0,273	0,997	−0,004	−0,074	0,148	0,99
32	2048	64	(2) верхняя	0,262	0,997	0,013	0,072	—	—
32	2048	64	(3) нижняя	−0,262	0,997	−0,013	−0,072	0,144	0,96
4	32	8	(2) верхняя	0,273	1,0	0,012	0,073	—	—
4	32	8	(3) нижняя	−0,273	1,0	−0,012	−0,073	0,146	0,98
16	128	8	(2) верхняя	0,244	1,005	0,023	0,070	—	—
16	128	8	(2) верхняя	0,068	0,99	0,013	0,045	—	—
16	128	8	(2) верхняя	0,021	0,982	0,009	0,020	—	—
16	128	8	(3) нижняя	−0,021	0,982	−0,009	−0,020	—	—
16	128	8	(3) нижняя	−0,068	0,99	−0,013	−0,045	—	—
16	128	8	(3) нижняя	−0,244	1,005	−0,023	−0,070	0,140	0,94
64	512	8	(2) верхняя	0,225	1,004	0,043	0,0655	—	—
64	512	8	(3) нижняя	−0,225	1,004	−0,013	−0,0665	0,130	0,87
256	2048	8	(2) верхняя	0,188	1,007	0,092	0,058	—	—
256	2048	8	(2) верхняя	0,058	0,949	0,069	0,040	—	—
256	2048	8	—	0,023	0,931	0,029	0,020	—	—
256	2048	8	(3) нижняя	−0,023	0,931	−0,029	−0,020	—	—
256	2048	8	—	−0,058	0,949	−0,069	−0,040	—	—
256	2048	8	(3) нижняя	−0,188	1,007	−0,092	−0,058	0,116	0,78
8	8	1	(2) верхняя	0,197	0,994	0,078	0,059	—	—
8	8	1	(3) нижняя	−0,197	0,994	−0,078	−0,059	0,118	0,79
32	32	1	(2) верхняя	0,185	0,992	0,089	0,056	—	—
32	32	1	(3) нижняя	−0,185	0,992	−0,089	−0,056	0,112	0,74
128	128	1	(2) верхняя	0,150	0,989	0,149	0,0485	—	—
128	128	1	(3) нижняя	−0,150	0,989	−0,149	−0,0485	0,097	0,64
512	512	1	(2) верхняя	0,108	0,941	0,225	0,038	—	—
512	512	1	(3) верхняя	−0,108	0,941	−0,225	−0,038	0,076	0,51
2048	2048	1	(2) верхняя	0,072	0,856	0,349	0,025	—	—
2048	2048	1	(3) нижняя	−0,072	0,856	−0,349	−0,025	0,050	0,33
64	8	0,125	(2) верхняя	0,078	0,870	0,321	0,0255	—	—
64	8	0,125	—	0,031	0,693	0,192	0,018	—	—
64	8	0,125	—	0,010	0,698	0,061	0,008	—	—
64	8	0,125	(3) нижняя	−0,010	0,698	−0,061	−0,008	—	—
64	8	0,125	—	−0,031	0,693	−0,192	−0,018	—	—
64	8	0,125	(3) нижняя	−0,078	0,870	−0,321	−0,0255	0,050	0,33
256	32	0,125	(2) верхняя	0,073	0,828	0,359	0,021	—	—
256	32	0,125	(3) нижняя	−0,073	0,828	−0,359	−0,021	0,042	0,28
1024	128	0,125	(2) верхняя	0,052	0,741	0,451	0,015	—	—
1024	128	0,125	(2) верхняя	0,020	0,572	0,198	0,010	—	—
1024	128	0,125	—	0,009	0,563	0,109	0,005	—	—
1024	128	0,125	(3) нижняя	−0,009	0,563	−0,109	−0,005	—	—
1024	128	0,125	—	−0,020	0,572	−0,198	−0,010	—	—
1024	128	0,125	—	−0,052	0,741	−0,451	−0,015	0,030	0,20
4096	512	0,125	(2) верхняя	0,038	0,584	0,452	0,0110	—	—
4096	512	0,125	(3) нижняя	−0,038	0,584	−0,452	−0,0110	0,0220	0,147
16384	2048	0,125	(2) верхняя	0,022	0,329	0,469	0,004	—	—
16384	2048	0,125	(3) нижняя	−0,022	0,329	−0,469	−0,004	0,008	0,053
512	8	0,015	(2) верхняя	0,023	0,355	0,514	0,0035	—	—
512	8	0,015	(3) нижняя	−0,023	0,355	−0,514	−0,0035	0,007	0,047
8192	128	0,015	(2) верхняя	0,015	0,251	0,401	0,0020	—	—
8192	128	0,015	(3) нижняя	−0,015	0,251	−0,401	−0,0020	0,004	0,027
32768	512	0,015	(2) верхняя	0,016	0,187	0,459	0,0005	—	—
32768	512	0,015	(3) нижняя	−0,016	0,187	−0,459	−0,0005	0,0010	0,015

Page 114-115.

Table 2. 15o/o symmetrical Zhukovskiy profile ($c_y' = 0{,}22$; $\alpha = 2°$)

ψ	Re_0	$p = \frac{Re_0}{c}$	(1) Поверхность	s/C	ξ_s'	τ_0'	τ_0	$\Delta\eta$	$E = \frac{\Delta\eta}{0{,}153}$
1	2	3	4	5	6	7	8	9	10
4	256	64	верхняя$_1$	0,236	1,001	0,011	−0,0016	—	—
4	256	64	нижняя$_1$	−0,316	0,996	0,015	−0,1518	0,1502	0,98
16	1024	64	верхняя$_1$	0,223	1,003	0,041	−0,0055	—	—
16	1024	64	нижняя$_1$	−0,310	0,998	0,030	−0,1539	0,1484	0,97
2	16	8	верхняя$_1$	0,226	1,009	0,053	−0,0081	—	—
2	16	8	нижняя$_1$	−0,311	0,997	0,027	−0,1533	0,1452	0,95
8	64	8	верхняя$_1$	0,212	1,011	0,062	−0,0095	—	—
8	64	8	верхняя$_1$	0,045	0,983	0,051	−0,0381	—	—
8	64	8	верхняя$_1$	0,005	0,984	0,044	−0,0667	—	—
8	64	8	нижняя	−0,026	0,974	0,033	−0,0956	—	—
8	64	8	нижняя	−0,082	0,972	0,033	−0,1243	—	—
8	64	8	нижняя$_1$	−0,308	0,997	0,022	−0,1532	0,1437	0,94
32	256	8	верхняя$_1$	0,156	1,015	0,083	−0,0140	—	—
32	256	8	верхняя$_1$	0,041	0,980	0,066	−0,0410	—	—
32	256	8	верхняя$_1$	0,003	0,969	0,052	−0,0683	—	—
32	256	8	нижняя	−0,026	0,970	0,038	−0,0958	—	—
32	256	8	нижняя	−0,078	0,975	0,024	−0,1232	—	—
32	256	8	нижняя$_1$	−0,295	0,995	0,013	−0,1508	0,1368	0,895
128	1024	8	верхняя$_1$	−0,168	1,021	0,126	−0,0214	—	—
128	1024	8	верхняя$_1$	0,034	0,958	0,100	−0,0464	—	—
128	1024	8	верхняя$_1$	0,002	0,941	0,063	−0,0721	—	—
128	1024	8	нижняя	−0,027	0,939	0,032	−0,0977	—	—
128	1024	8	нижняя	−0,079	0,955	0,004	−0,1231	—	—
128	1024	8	нижняя	−0,265	0,992	−0,008	−0,1488	0,1274	0,83
16	16	1	верхняя$_1$	0,149	1,010	0,160	−0,0435	—	—
16	16	1	нижняя$_1$	−0,245	0,984	−0,023	−0,1598	0,1165	0,76
64	64	1	верхняя$_1$	0,128	1,012	0,202	−0,0493	—	—
64	64	1	верхняя$_1$	0,027	0,908	0,140	−0,0705	—	—
64	64	1	нижняя	−0,001	0,881	0,083	−0,0902	—	—
64	64	1	нижняя	−0,027	0,881	0,033	−0,1130	—	—
64	64	1	нижняя	−0,071	0,921	−0,013	−0,1345	—	—
64	64	1	нижняя$_1$	−0,225	0,983	−0,052	−0,1558	0,1065	0,66
256	256	1	верхняя$_1$	0,100	0,999	0,283	−0,0587	—	—
256	256	1	верхняя$_1$	0,022	0,852	0,189	−0,0763	—	—
256	256	1	нижняя	−0,002	0,827	0,103	−0,0940	—	—
256	256	1	нижняя	−0,023	0,815	0,015	−0,1118	—	—
256	256	1	нижняя	−0,058	0,863	−0,050	−0,1298	—	—
256	256	1	нижняя$_1$	−0,177	0,963	−0,105	−0,1475	0,0988	0,58
1024	1024	1	верхняя$_1$	0,063	0,914	0,424	−0,0743	—	—
1024	1024	1	нижняя$_1$	−0,118	0,902	−0,195	−0,1360	0,0617	0,42
128	16	0,125	верхняя$_1$	0,055	0,881	0,472	−0,0955	—	—
128	16	0,125	верхняя$_1$	0,009	0,640	0,235	−0,1065	—	—
128	16	0,125	нижняя	−0,004	0,637	0,113	−0,1260	—	—
128	16	0,125	нижняя	−0,017	0,642	−0,006	−0,1290	—	—
128	16	0,125	нижняя	−0,036	0,685	−0,109	−0,1335	—	—
128	16	0,125	нижняя$_1$	−0,098	0,854	−0,246	−0,1430	0,0475	0,31
512	64	0,125	верхняя$_1$	0,038	0,767	0,528	−0,1005	—	—
512	64	0,125	верхняя$_1$	0,007	0,560	0,270	−0,1080	—	—
512	64	0,125	нижняя	−0,004	0,542	0,132	−0,1155	—	—
512	64	0,125	нижняя	−0,016	0,535	−0,011	−0,1230	—	—
512	64	0,125	нижняя	−0,03	0,611	−0,140	−0,1310	—	—
512	64	0,125	нижняя$_1$	−0,079	0,813	−0,300	−0,1382	0,0377	0,25
2048	256	0,125	верхняя$_1$	0,028	0,562	0,611	−0,1085	—	—
2048	256	0,125	верхняя$_1$	0,004	0,394	0,255	−0,1130	—	—
2048	256	0,125	нижняя	−0,005	0,379	0,118	−0,1182	—	—
2048	256	0,125	нижняя	−0,014	0,377	−0,050	−0,1228	—	—
2048	256	0,125	нижняя	−0,029	0,500	−0,235	−0,1275	—	—
2048	256	0,125	нижняя$_1$	−0,055	0,688	−0,356	−0,1325	0,0240	0,16

8192	1042	0,125	(2) верхняя,	0,015	0,210	0,514	-0,1165	—	—
8192	1024	0,125	—	0	0,270	0,230	-0,1190	—	—
8192	1024	0,125	нижняя	−0,004	0,260	0,085	−0,1218	—	—
8192	1024	0,125	нижняя	−0,012	0,273	−0,110	−0,1250	—	—
8192	1024	0,125	нижняя,	−0,031	0,520	−0,390	−0,1275	0,0110	0,072
1024	16	0,015	(2) верхняя,	0,008	0,186	0,610	−0,1232	—	—
1024	16	0,015	(3) нижняя,	−0,015	0,100	−0,243	−0,1262	0,0030	0,020
4096	64	0,015	(2) верхняя,	0,003	0,090	0,434	−0,1243	—	—
4096	64	0,015	(3) нижняя,	−0,015	0,246	−0,235	-0,1278	0,0035	0,022
16384	256	0,015	(2) верхняя,	0,002	0,103	0,506	−0,1254	—	—
16384	256	0,015	(3) нижняя,	−0,014	0,175	0,295	−0,1275	0,0021	0,014

Key: (1). Surface. (2). upper. (3). lower.

Page 116-117.

Table 3. 15o/o symmetrical Zhukovskiy profile($c_y = 0,11$; $\varepsilon = 4°$)

$\bar{\nu}$	Re_0	$Re_0 \cdot \frac{p}{\nu}$	(1) Поверхность	s/C	ξ'_s	η'_s	η_0	$\Delta\eta_s$	$E = \frac{\Delta\eta}{0,157}$
1	2	3	4	5	6	7	8	9	10
4	256	64	верхняя$_1$	0,204	0,9996	0,0785	−0,1682	—	—
4	256	64	нижняя$_1$	−0,108	0,9946	0,0705	−0,3215	0,1533	0,98
16	1024	64	верхняя$_1$	0,194	1,0086	0,1005	−0,1692	—	—
16	1024	64	нижняя$_1$	−0,400	0,9976	0,0705	−0,3223	0,1531	0,98
2	16	8	верхняя$_1$	0,192	1,0031	0,0962	−0,1818	—	—
2	16	8	нижняя$_1$	−0,409	0,9891	0,0688	−0,3330	0,1512	0,96
8	64	8	верхняя$_1$	0,170	1,0055	0,1032	−0,1837	—	—
8	64	8	нижняя	−0,135	0,9802	0,0728	−0,3073	—	—
8	64	8	нижняя	−0,064	0,9782	0,0789	−0,2824	—	—
8	64	8	нижняя	−0,024	0,9663	0,1120	−0,2577	—	—
8	64	8	верхняя	0,004	0,9793	0,0940	−0,2330	—	—
8	64	8	верхняя	0,037	0,9854	0,1011	−0,2083	—	—
8	64	8	нижняя$_1$	−0,400	0,9930	0,0638	−0,3320	0,1483	0,94
32	256	8	верхняя$_1$	0,148	1,0174	0,1381	−0,1881	—	—
32	256	8	верхняя$_1$	0,034	0,9764	0,1221	−0,2121	—	—
32	256	8	верхняя$_1$	0,002	0,9653	0,1050	−0,2358	—	—
32	256	8	нижняя	−0,024	—	—	−0,2594	—	—
32	256	8	нижняя	−0,062	—	—	−0,2832	—	—
32	256	8	нижняя	−0,124	0,9652	0,0628	−0,3068	—	—
32	256	8	нижняя	−0,379	0,9831	0,0618	−0,3316	0,1435	0,92
128	1024	8	верхняя$_1$	0,127	1,0294	0,2031	−0,1994	—	—
128	1024	8	верхняя$_1$	0,062	0,9804	0,0931	−0,2074	—	—
128	1024	8	верхняя$_1$	0,028	0,9514	0,1670	−0,2205	—	—
128	1024	8	верхняя$_1$	0,004	0,9304	0,1410	−0,2386	—	—
128	1024	8	нижняя	−0,041	0,9273	0,0869	−0,2748	—	—
128	1024	8	нижняя	−0,125	0,9433	0,0519	−0,3077	—	—
128	1024	8	нижняя	−0,350	1,0200	0,0468	−0,3316	0,1322	0,84
16	16	1	верхняя$_1$	0,121	1,0116	0,2241	−0,2403	—	—
16	16	1	нижняя$_1$	−0,336	0,9628	0,0415	−0,3665	0,1262	0,80
64	64	1	верхняя$_1$	0,100	1,0133	0,2881	−0,2472	—	—
64	64	1	нижняя	−0,113	0,8940	0,0448	−0,3422	—	—
64	64	1	нижняя	−0,060	0,8712	0,0731	−0,3231	—	—
64	64	1	нижняя	−0,028	0,8694	0,1147	−0,3043	—	—
64	64	1	нижняя	−0,004	0,8638	0,1675	−0,2853	—	—
64	64	1	верхняя	0,018	0,8990	0,2148	−0,2665	0,1134	0,72
64	64	1	нижняя$_1$	−0,286	0,9578	0,0135	−0,3606	—	—
256	256	1	верхняя$_1$	0,068	1,0121	0,4088	−0,2622	—	—
256	256	1	верхняя$_1$	0,012	0,8138	0,2746	−0,2775	—	—
256	256	1	нижняя	−0,008	0,7827	0,1843	−0,2925	—	—
256	256	1	нижняя	−0,028	0,7864	0,1092	−0,3078	—	—
256	256	1	нижняя	−0,084	0,8281	0,0149	−0,3353	—	—
256	256	1	нижняя	−0,125	0,8660	0,0142	−0,3444	—	—
256	256	1	нижняя$_1$	−0,247	0,9558	−0,0313	−0,3537	0,0915	0,59
1024	1024	1	верхняя$_1$	0,043	0,8758	0,5817	−0,2782	—	—
1024	1024	1	нижняя$_1$	−0,155	0,8780	−0,1212	−0,3440	0,0658	0,42
128	16	0,125	верхняя$_1$	0,042	0,8255	0,5550	−0,3126	—	—
128	16	0,125	нижняя	−0,067	0,7143	0,0364	−0,3598	—	—
128	16	0,125	нижняя	−0,040	0,6586	0,0228	−0,3500	—	—
128	16	0,125	нижняя	−0,022	0,6048	0,1031	−0,3406	—	—
128	16	0,125	нижняя	−0,006	0,615	0,2444	−0,3313	—	—
128	16	0,125	верхняя	−0,006	0,6562	0,3437	−0,3220	—	—
128	16	0,125	нижняя$_1$	−0,145	0,8632	0,1358	−0,3688	0,0562	0,36
512	64	0,125	верхняя$_1$	0,026	0,6392	0,7017	−0,3216	—	—
512	64	0,125	нижняя	−0,004	0,5021	0,3024	−0,3303	—	—
512	64	0,125	нижняя	−0,015	0,4678	0,1513	−0,3388	—	—
512	64	0,125	нижняя	−0,027	0,5197	0,0390	−0,3411	—	—
512	64	0,125	нижняя	−0,042	0,5566	0,0782	−0,3500	—	—
512	64	0,125	нижняя	−0,062	0,6465	−0,1363	−0,3558	—	—
512	61	0,125	нижняя$_1$	−0,112	0,8133	−0,2045	−0,3605	0,0389	0,25

2048	256	0,125	верхняя[1]	0,015	0,4240	−0,7513	−0,3293	—	—
2048	256	0,125	верхняя[1]	0,002	0,3300	0,4553	−0,3324	—	—
2048	256	0,125	нижняя	−0,008	0,2858	0,2442	−0,3373	—	—
2048	256	0,125	нижняя	−0,022	0,3548	0,0060	−0,3432	—	—
2048	256	0,125	нижняя	−0,032	0,4137	−0,1191	−0,3471	—	—
2048	256	0,125	нижняя	−0,045	0,1956	−0,1923	−0,3501	—	—
2048	256	0,125	нижняя[1]	−0,072	0,0575	−0,2912	−0,3529	0,0236	0,15
8192	1024	0,125	верхняя[1]	0,004	0,0918	0,7521	−0,3382	—	—
8192	1024	0,125	нижняя	−0,005	0,1918	0,4371	−0,3405	—	—
8192	1024	0,125	нижняя	−0,012	0,1787	0,1520	−0,3441	—	—
8192	1024	0,125	нижняя	−0,020	0,2767	0,0669	−0,3458	—	—
8192	1024	0,125	нижняя	−0,031	0,2867	−0,2011	−0,3474	—	—
8192	1024	0,125	нижняя[1]	−0,041	0,4186	−0,2832	−0,3480	0,0098	0,06
1024	16	0,015	верхняя[1]	0,001	0,1147	0,6545	−0,3495	—	—
1024	16	0,015	верхняя[1]	−0,03	0,3496	−0,2808	−0,3544	0,0049	0,031
4096	64	0,015	верхняя[1]	0,002	0,1047	0,6945	−0,3495	—	—
4096	64	0,015	нижняя[1]	−0,026	0,2146	−0,2157	−0,3530	0,0035	0,022
16384	256	0,015	верхняя[1]	0,002	0,1597	0,8494	−0,3504	—	—
16384	256	0,015	нижняя[1]	0,025	0,2746	−0,2256	−0,3535	0,0031	0,020

Key: (1). Surface. (2). upper. (3). lower.

Page 118.

Table 4. 15o/o bent Zhukovskiy profile ($c_y = 0{,}41$; $\alpha = 0°$)

ψ	Re_0	$p=\frac{Re_0}{\tau}$	Поверхность	s, C	ξ_s'	v_{is}'	v_{i0}	Δv_i	$E=\frac{\Delta\eta}{0{,}150}$
1	2	3	4	5	6	7	8	9	10
4	256	64	верхняя$_1$	0,317	1,003	0,007	0,0935	—	—
4	256	64	нижняя$_1$	−0,216	0,998	−0,002	−0,0565	0,1500	1,00
16	1024	64	верхняя$_1$	0,310	1,008	0,013	0,0915	—	—
16	1024	64	нижняя$_1$	−0,213	0,999	−0,006	−0,0565	0,1480	0,99
2	16	8	верхняя$_1$	0,305	1,009	0,022	0,0855	—	—
2	16	8	нижняя$_1$	−0,215	0,994	−0,001	−0,0600	0,1455	0,97
8	64	8	верхняя$_1$	0,294	1,012	0,031	0,0818	—	—
8	64	8	верхняя$_1$	0,096	0,992	0,022	0,0536	—	—
8	64	8	нижняя	0,038	0,998	0,020	0,0253	—	—
8	64	8	нижняя	0,002	0,985	0,011	−0,038	—	—
8	64	8	нижняя	−0,033	0,984	0,003	−0,0318	—	—
8	64	8	нижняя	−0,212	0,999	−0,008	−0,0610	0,1428	0,95
32	256	8	верхняя$_1$	0,275	1,022	0,050	0,0775	—	—
32	256	8	верхняя$_1$	0,092	0,989	0,042	0,0503	—	—
32	256	8	верхняя$_1$	0,034	0,976	0,030	0,0225	—	—
32	256	8	верхняя$_1$	0,001	0,972	0,017	−0,0045	—	—
32	256	8	нижняя$_1$	−0,033	0,973	0,002	−0,0325	—	—
32	256	8	нижняя$_1$	−0,199	0,990	−0,016	−0,0800	0,1375	0,92
128	1024	8	верхняя$_1$	0,243	1,033	0,090	0,0660	—	—
128	1024	8	верхняя$_1$	0,077	0,976	0,075	0,0420	—	—
128	1024	8	верхняя$_1$	0,030	0,954	0,054	0,0160	—	—
128	1024	8	верхняя$_1$	0,000	0,943	0,024	0,0085	—	—
128	1024	8	нижняя	−0,032	0,946	−0,006	−0,0335	—	—
128	1024	8	нижняя$_1$	−0,183	0,984	−0,036	−0,0585	0,1245	0,83
16	16	1	верхняя$_1$	0,211	1,028	0,128	0,0377	—	—
16	16	1	нижняя$_1$	−0,180	0,978	−0,042	−0,0770	0,1147	0,76
64	64	1	верхняя$_1$	0,192	1,038	0,168	+0,0312	—	—
64	64	1	верхняя$_1$	0,061	0,936	0,131	0,0100	—	—
64	64	1	верхняя$_1$	0,022	0,898	0,095	−0,0110	—	—
64	64	1	нижняя	−0,003	0,884	0,048	−0,0315	—	—
64	64	1	нижняя	−0,031	0,891	−0,007	−0,0525	—	—
64	64	1	нижняя$_1$	−0,157	0,971	−0,078	−0,0731	0,1043	0,70
256	256	1	верхняя$_1$	0,158	1,038	0,238	0,0180	—	—
256	256	1	верхняя$_1$	0,050	0,893	0,188	0,0010	—	—
256	256	1	верхняя$_1$	0,018	0,839	0,127	−0,0165	—	—
256	256	1	нижняя	−0,004	0,820	0,054	−0,0340	—	—
256	256	1	нижняя	−0,028	0,838	−0,017	−0,0510	—	—
256	256	1	нижняя	−0,120	0,940	−0,129	−0,0680	0,0860	0,57
1024	1024	1	верхняя$_1$	0,109	1,000	0,357	0,0000	—	—
1024	1024	1	нижняя$_1$	−0,085	0,883	−0,220	−0,0620	0,0620	0,41
128	16	0,125	верхняя$_1$	0,092	0,958	0,405	−0,028	—	—
128	16	0,125	верхняя$_1$	0,032	0,727	0,288	−0,0382	—	—
128	16	0,125	верхняя$_1$	0,012	0,638	0,189	−0,0480	—	—
128	16	0,125	нижняя	−0,004	0,649	0,060	−0,0575	—	—
128	16	0,125	нижняя	−0,019	0,644	−0,046	−0,0670	—	—
128	16	0,125	нижняя$_1$	−0,068	0,838	−0,264	−0,0772	0,0492	0,33
512	64	0,125	верхняя$_1$	0,072	0,911	0,487	−0,0347	—	—
512	64	0,125	верхняя$_1$	0,025	0,634	0,350	−0,0425	—	—
512	64	0,125	верхняя$_1$	0,010	0,535	0,208	0,150	—	—
512	64	0,125	нижняя	−0,005	0,485	0,631	−0,0582	—	—
512	64	0,125	нижняя	−0,018	0,544	−0,124	−0,066	—	—
512	64	0,125	нижняя$_1$	−0,053	0,754	−0,319	−0,0725	0,0378	0,25
2048	256	0,125	верхняя$_1$	0,046	0,686	0,576	−0,0440	—	—
2048	256	0,125	верхняя$_1$	0,015	0,448	0,360	−0,050	—	—
2048	256	0,125	нижняя	0,005	0,381	0,192	−0,0548	—	—
2048	256	0,125	верхняя$_1$	0,004	0,368	0,048	−0,0594	—	—
2048	256	0,125	нижняя	−0,013	0,407	−0,103	−0,0638	—	—
2048	256	0,125	нижняя$_1$	−0,038	0,604	−0,384	−0,0685	0,0215	0,163

8192	1024	0,125	верхняя[1]	0,025	0,471	0,650	−0,0548	—	—
8192	1024	0,125	верхняя[1]	0,007	0,258	0,308	−0,0569	—	—
8192	1024	0,125	нижняя	−0,001	0,178	0,082	−0,0590	—	—
8192	1024	0,125	нижняя	−0,008	0,184	−0,079	−0,0610	—	—
8192	1024	0,125	нижняя	−0,012	0,211	−0,163	−0,0630	—	—
8192	1024	0,125	нижняя[1]	−0,025	0,464	−0,428	−0,0650	0,0102	0,07
1024	16	0,015	верхняя[1]	0,022	0,346	0,561	−0,0604	—	—
1024	16	0,015	нижняя[1]	−0,018	0,317	−0,368	−0,0700	0,0096	0,06
4096	64	0,015	верхняя[1]	0,015	0,285	0,527	−0,0650	—	—
4096	64	0,015	нижняя[1]	−0,012	0,143	−0,253	−0,0675	0,0025	0,17
16384	256	0,015	верхняя[1]	0,006	0,113	0,391	−0,0655	—	—
16384	256	0,015	нижняя[1]	−0,008	0,046	−0,118	−0,0670	0,0015	0,0100

Key: (1). Surface. (2). upper. (3). lower.

Page 119-120.

Table 5. 15o/o profile/airfoil NACA 65_2-015.

ψ	Re_0	$p=\frac{Re_0}{\psi}$	(1) Поверхность	s/C	ξ'_s	η'_s	η_a	$\Delta\eta$	$E=\frac{\Delta\eta}{0,157}$
1	2	3	4	5	6	7	8	9	10
4	256	64	верхняя$_1$	0,281	1,0023	0,0814	−0,1281	—	—
4	256	64	нижняя$_1$	−0,523	0,9973	0,0704	−0,2817	0,1536	0,98
16	1024	64	верхняя$_1$	0,267	1,0073	0,0864	−0,1298	—	—
16	1024	64	нижняя$_1$	−0,514	0,9973	0,0704	−0,2818	0,1520	0,97
2	16	8	верхняя$_1$	0,259	1,0047	0,0945	−0,1395	—	—
2	16	8	верхняя$_1$	0,031	0,9881	0,0875	−0,1646	—	—
2	16	8	нижняя	−0,022	0,9847	0,0825	−0,2026	—	—
2	16	8	нижняя	−0,074	0,9867	0,0793	−0,2246	—	—
2	16	8	нижняя	−0,150	0,9857	0,0753	−0,2467	—	—
2	16	8	нижняя	−0,256	0,9847	0,0742	−0,2687	—	—
2	16	8	нижняя$_1$	−0,514	0,9927	0,0711	−0,2909	0,1514	0,96
8	64	8	верхняя$_1$	0,240	1,0107	0,1065	−0,1424	—	—
8	64	8	верхняя$_1$	0,016	0,9847	0,0935	−0,1719	—	—
8	64	8	нижняя	−0,050	0,9757	0,0824	−0,2163	—	—
8	64	8	нижняя	−0,125	0,9807	0,0743	−0,2409	—	—
8	64	8	нижняя	−0,236	0,9797	0,0712	−0,2655	—	—
8	64	8	нижняя$_1$	−0,512	0,0907	0,0641	−0,2899	0,1475	0,95
32	256	8	верхняя$_1$	0,209	1,0187	0,1326	−0,1403	—	—
32	256	8	верхняя$_1$	0,023	0,9761	0,1155	−0,1702	—	—
32	256	8	нижняя	−0,052	0,9617	0,0874	−0,2193	—	—
32	256	8	нижняя	−0,131	0,9647	0,0743	−0,2437	—	—
32	256	8	нижняя	−0,249	0,9717	0,0632	−0,2685	—	—
32	256	8	нижняя$_1$	−0,506	1,0057	0,0531	−0,2894	0,1401	0,89
128	1024	8	верхняя$_1$	0,150	1,0207	0,1805	−0,1603	—	—
128	1024	8	верхняя$_1$	0,008	0,9517	5,1375	−0,1826	—	—
128	1024	8	нижняя	−0,068	0,9427	0,0853	−0,2282	—	—
128	1024	8	нижняя	−0,145	0,9407	0,0642	−0,2505	—	—
128	1024	8	нижняя	−0,267	0,9557	0,0462	−0,2726	—	—
128	1024	8	нижняя$_1$	−0,485	0,9837	0,0382	−0,2878	0,1275	0,82
16	16	1	верхняя$_1$	0,128	1,0015	0,2008	−0,1951	—	—
16	16	1	нижняя$_1$	−0,481	0,9776	0,0383	−0,3202	0,1251	0,80
64	64	1	верхняя$_1$	0,092	0,9956	0,2507	−0,2030	—	—
64	64	1	верхняя$_1$	0,012	0,9155	0,2055	−0,2136	—	—
64	64	1	нижняя	−0,048	0,8795	0,1092	−0,2535	—	—
64	64	1	нижняя	−0,127	0,8975	0,0609	−0,2787	—	—

64	64	1	(3) нижняя	−0,247	0,9255	0,0227	−0,3013	—	
64	64	1	нижняя$_1$	−0,417	0,9756	0,0074	−0,3111	0,1081	0,89
256	256	1	(2) верхняя$_1$	0,047	0,9116	0,3416	−0,2143	—	—
256	256	1	нижняя	−0,007	0,8256	0,1961	−0,2543	—	—
256	256	1	нижняя	−0,040	0,8086	0,1102	−0,2543	—	—
256	256	1	(3) нижняя	−0,093	0,8316	0,0410	−0,2717	—	—
256	256	1	нижняя	0,184	—	—	−0,2892	—	—
256	256	1	нижняя$_1$	−0,355	0,9686	0,0443	−0,2983	0,0840	0,53
1024	1024	1	(2) верхняя$_1$	0,026	0,8575	0,4614	−0,2267	—	—
1024	1024	1	(2) верхняя$_1$	0,010	0,7726	0,3935	−0,2313	—	—
1024	1024	1	нижняя	−0,015	0,6715	0,1972	−0,2492	—	—
1024	1024	1	(3) нижняя	−0,060	0,6295	0,0300	−0,2692	—	—
1024	1424	1	нижняя	0,104	0,7875	−0,0251	−0,2782	—	—
1024	1024	1	нижняя	−0,166	0,7495	−0,0692	−0,2853	—	—
1024	1024	1	нижняя$_1$	0,245	0,9175	−0,0942	−0,2883	0,0616	0,40
128	16	0,125	(2) верхняя$_1$	0,021	0,7926	0,4950	−0,2633	—	—
128	16	0,125	нижняя	−0,012	0,6436	0,2336	−0,2798	—	—
128	16	0,125	(3) нижняя	−0,042	0,6395	0,1003	−0,2945	—	—
128	16	0,125	нижняя	−0,080	0,7194	−0,0500	−0,3028	—	—
128	16	0,125	нижняя	−0,104	0,7634	−0,0860	−0,3059	—	—
128	16	0,125	нижняя$_1$	−0,185	0,8804	−0,1302	−0,3091	0,0458	0,29
512	64	0,125	(2) верхняя$_1$	0,018	0,7536	0,5779	−0,2676	—	—
512	64	0,125	(2) верхняя$_1$	0,005	0,6496	0,4378	−0,2719	—	—
512	64	0,125	(3) нижняя	−0,020	0,4935	0,1605	−0,2857	—	—
512	64	0,125	(3) нижняя	−0,034	0,5504	0,0403	−0,2926	—	—
512	64	0,125	(3) нижняя	−0,079	0,6954	−0,0989	−0,3015	—	—
512	64	0,125	(3) нижняя$_1$	−0,145	0,8284	−0,1540	−0,3035	0,0359	0,22
2048	256	0,125	(2) верхняя$_1$	0,014	0,6606	0,6718	−0,2737	—	—
2048	256	0,125	(2) верхняя$_1$	0,007	0,5986	0,5868	−0,2748	—	—
2048	256	0,125	—	0,000	0,5216	0,4106	−0,2781	—	—
2048	256	0,125	нижняя	−0,012	0,4085	0,2245	−0,2861	—	—
2048	256	0,125	(3) нижняя	0,022	0,3905	0,0604	−0,2906	—	—
2048	256	0,125	нижняя	−0,048	0,5485	−0,0967	−0,2965	—	—
2048	256	0,125	нижняя$_1$	−0,100	0,7584	−0,1768	−0,2989	0,0255	0,17
8192	1024	0,125	(2) верхняя$_1$	0,010	0,5976	0,7847	−0,2798	—	—
8192	1024	0,125	(2) верхняя$_1$	0,005	—	—	−0,2801	—	—
8192	1024	0,125	нижняя	−0,004	—	—	−0,2850	—	—
8192	1024	0,125	(3) нижняя	−0,010	0,3035	0,2454	−0,2886	—	—
8192	1024	0,125	нижняя	−0,022	0,2124	0,0033	−0,2932	—	—
8192	1024	0,125	нижняя	−0,030	0,3423	−0,0868	−0,2945	—	—
8192	1024	0,125	нижняя	−0,033	0,3983	−0,1068	−0,2958	—	—
8192	1024	0,125	нижняя$_1$	−0,065	0,6765	−0,1867	−0,2971	0,0173	0,11
1024	16	0,015	(2) верхняя$_1$	0,008	0,4372	0,8238	−0,2933	—	—
1024	16	0,015	(3) нижняя$_1$	−0,040	0,4891	−0,1997	−0,3037	0,0104	0,07
4096	64	0,015	(2) верхняя$_1$	0,008	0,5712	0,8627	−0,2947	—	—
4096	64	0,015	(3) нижняя$_1$	−0,024	0,2221	−0,1126	−0,3026	0,0079	0,050
16384	256	0,015	(2) верхняя$_1$	0,008	0,5730	0,9007	−0,2952	—	—
16384	256	0,015	(3) нижняя$_1$	−0,019	0,1099	−0,0525	−0,3028	0,0076	0,048

Key: (1). Surface. (2). upper. (3). lower.

DISTRIBUTION LIST

DISTRIBUTION DIRECT TO RECIPIENT

ORGANIZATION		MICROFICHE
A205	DMATC	1
A210	DMAAC	2
B344	DIA/RDS-3C	9
C043	USAMIIA	1
C509	BALLISTIC RES LABS	1
C510	AIR MOBILITY R&D LAB/FIO	1
C513	PICATINNY ARSENAL	1
C535	AVIATION SYS COMD	1
C591	FSTC	5
C619	MIA REDSTONE	1
D008	NISC	1
H300	USAICE (USAREUR)	1
P005	DOE	1
P050	CIA/CRB/ADD/SD	2
NAVORDSTA (50L)		1
NASA/NST-44		1
AFIT/LD		1
LLL/Code L-389		1
NSA/1213/TDL		2

ORGANIZATION		MICROFICHE
E053	AF/INAKA	1
E017	AF/RDXTR-W	1
E403	AFSC/INA	1
E404	AEDC	1
E408	AFWL	1
E410	ADTC	1
	FTD	
	CCN	1
	ASD/FTD/NIIS	3
	NIA/PHS	1
	NIIS	2